



*Ministero dell'Istruzione
dell'Università e Ricerca*



**Università
degli Studi
di Palermo**

PhD in Molecular and Clinical Medicine
Department of Health Promotion, Mother and Child Care, Internal Medicine and Medical
Specialties
SSD MED/46

The role of driver mutations in the initiation and progression of thyroid cancer

CANDIDATE
FRANCESCO VERONA

COORDINATOR
PROF. ANTONINO TUTTOLOMONDO

TUTOR
PROF. GIORGIO STASSI

CO-TUTOR
PROF. VERONICA VESCHI

CYCLE: XXXVI
2023/2024

INDEX

Introduction

Thyroid gland: cells and hormones
Thyroid carcinomas and histotypes
Genetic mutations and rearrangements in thyroid carcinomas
Therapeutic strategies for thyroid carcinoma patients
Thyroid cancer stem cells vs Thyroid normal stem cells
Thyroid carcinogenesis models

Aim of the work

Chapter 1: Cancer Stem Cells in Thyroid Tumors: From the Origin to Metastasis

Chapter 2: Recapitulating thyroid cancer histotypes through engineering embryonic stem cells

Conclusions

Bibliography

Publications

Acknowledgements

Introduction

Thyroid gland: cells and hormones

The thyroid gland is structured into two lobes, which are separated by partitions originating from its capsule. The thyroid lobules structural and functional units are represented by the thyroid follicles which consisting of follicular cells.

In particular, follicular cells origin from endoderm and they produce and secrete thyroid hormones. The inactive form of thyroid hormone that circulates through the bloodstream is called thyroxine, which is also recognized as tetraiodothyronine (T4), that can be converted in the activated form triiodothyronine (T3). Briefly, T3 governates the regulation of the Basal Metabolic Rate of the body (i.e. induction of lipolysis or lipid synthesis, metabolism of carbohydrates, anabolism and catabolism of proteins) [1]. Of note, in thyroid metabolism, the Sodium/Iodide Symporter (NIS) is a transmembrane protein which play a crucial role in active iodide (I⁻) trafficking into the thyroid. This marks the initial stage in the production of thyroid hormones thanks to the binding of oxidated iodide, via Thyroid peroxidase (TPO), and its incorporation in tyrosines residues on thyreoglobulin (TG) [2]. Between or inside the thyroid follicles are present another cell population: the small C cells, or parafollicular cells. Parafollicular cells origin from ectodermal neural crest cells and secrete calcitonin hormone. This hormone helps in the deposition of calcium and phosphate in skeletal and other tissues, ensuring a balanced level of calcium in the blood (preventing hypocalcemia) [3]. The thyroid follicles act as storage for T3-T4 hormones thanks to a specific substance called the colloid. Colloid is mainly composed by a protein

named thyroglobulin, an iodide glycoprotein which is able to bind and keep T3-T4 (**Fig.1**).

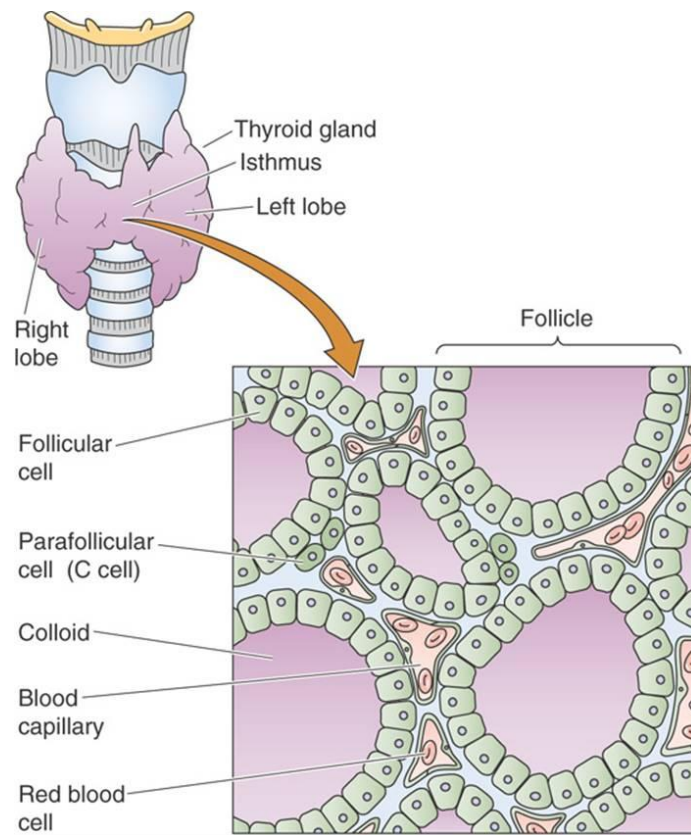


Fig.1 Figure showing thyroid anatomy and cell populations. Adapted from *Medical Physiology a Cellular and Molecular Approach, Updated 2nd Ed. THE THYROID GLAND Eugene J. Barrett.*

Thyroid carcinomas and histotypes

Thyroid cancers (TCs) display considerable heterogeneity and are the most common tumors among endocrine neoplasms. Based on their specific histopathological characteristics, four subtypes of TC are classified: papillary thyroid carcinoma (PTC), follicular thyroid carcinoma (FTC), anaplastic thyroid carcinoma (ATC) and medullary thyroid carcinoma (MTC). While ATC, FTC and PTC originate from the transformation of thyroid follicular cells of endodermal origin, MTC originate from the transformation of thyroid parafollicular cells of ectodermal origin [4, 5].

Papillary Thyroid Carcinoma (PTC)

PTC is an high grade differentiated, typically enclosed within a capsule, thyroid adenocarcinoma representing 80-85% of the total amount of TCs, it originates from a pathological papillary proliferation. In 90% of patients diagnosed with PTC have a positive prognosis, typically achieving a 5-year overall survival rate of approximately 95% while the remaining 10% undergo a malignant transformation with lymph nodes and lung metastasis. Despite PTC have a low mutational burden, in most cases they show activating mutations of genes involved in MAPK signaling pathway (mitogen-activated protein kinase), such as RAS (rat sarcoma) and BRAF^{V600E} (rapidly accelerated fibrosarcoma type-B), and rearrangements of RET (Proto-Oncogene Tyrosine-Protein Kinase Receptor Ret), NTRK (neurotrophic receptor tyrosine kinase) and ALK (anaplastic lymphoma kinase) (**Fig.2**) [6-9].

Follicular Thyroid Carcinoma (FTC)

FTCs represent 10-15% of TCs. They are encapsulated tumors with follicular differentiation. Patients diagnosed with FTC generally exhibit a favorable prognosis, often achieving a 5-year overall survival rate of 91%. While the remaining 9% of FTC patients have a worst prognosis because of hematological spread within bone and lung metastasis. They are characterized by a low mutational burden and the main driver mutations include RAS mutations and PAX8/PPAR γ rearrangements. Particularly, RAS mutations involve both MAPK and PI3K activation (**Fig.2**) [10, 11].

Anaplastic Thyroid Carcinoma (ATC)

ATC represents 2% of all TCs. It is a very aggressive TC characterized by undifferentiated phenotype, worst prognosis and 100% mortality with an overall survival from diagnosis approximately of 6 months [12, 13]. ATCs are able to invade surrounding tissues and to give rise to metastases. They are refractory to radioiodine therapy because of lack of NIS expression and unresectable [14]. ATC displays high mutational burden and activating mutations on MAPK and PI3K pathways. Moreover, mutations in genes that confer aggressiveness in ATC involve mutations in TP53 and EIF1AX, changes in epigenetic modifiers, or mutations in the promoter of the TERT gene (**Fig.2**) [15, 16].

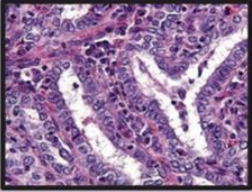
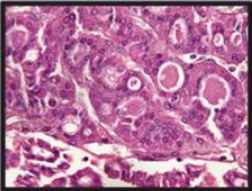
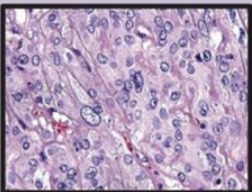
	Histology	Incidence	Driver genes	Survival rate	Other features
PTC		80%	BRAF ^{V600E} RET/PTC	95%	<ul style="list-style-type: none"> · Local spreading · Lymph node metastases · Low mutational burden
FTC		10-15%	NRAS ^{Q61D/R} PAX8/PPAR γ	91%	<ul style="list-style-type: none"> · Haematological spreading · Bone and lung metastases · Low mutational burden
ATC		1-2%	BRAF ^{V600E} NRAS ^{Q61D/R} PIK3CA PTEN	1-7%	<ul style="list-style-type: none"> · Locoregional invasion · Bone and lung metastases · High mutational burden

Fig.2 Histological and other features of thyroid carcinomas follicular cell derived.

Adapted from Zaballos MA et al. *J Endocrinol.* 2017.

Genetic mutations and rearrangements in thyroid carcinomas

Several multiple genetic mutations and rearrangements are responsible for TC development, occurring in genes crucial for survival, proliferation, invasive capacity and metastatic potential of thyroid cancer cells.

In summary 90% of all TCs are characterized by mutually exclusive activating oncogenic mutations in BRAF or RAS genes. Additionally, they show rearrangements in RET, ALK and NTRK genes. The 10% of TCs display loss-of-function mutations on oncosuppressor genes such as phosphatase and tensin homologue (PTEN), PPAR γ and Tumor suppressor protein 53 (TP53). Moreover, in the last decade The Cancer Genome Atlas (TCGA) revealed also the mutations of phosphoinositide 3-kinase (PI3K) pathway members such as Eukaryotic translation initiation factor 1A X-linked (EIF1AX) [6]. Moreover, carcinogenesis of TCs is characterized by dysregulation of cell signaling pathways mitogen-activated protein kinase (MAPK) and phosphatidylinositol-3 kinase (PI3K)/Akt strain transforming (AKT)/mammalian target of rapamycin (mTOR) signaling pathways. Particularly, the aberrant activation of MAPK and PI3K/AKT signaling pathways depend on RAS, BRAF and PIK3CA point mutations and on RET/PTC rearrangements which drive tumorigenesis in thyroid organ [17, 18].

MAPK Pathway

MAPK signaling is responsible for crucial cellular functions such as proliferation and differentiation. The aberrant activation of MAPK signaling pathway is based on mutations in the following genes coding for receptor tyrosine kinases (RET, ALK, vascular endothelial growth factor receptor [VEGFR] and NTRK1/3, RAS, rapidly accelerated fibrosarcoma (RAF), mitogen-activated protein kinase (MEK) and extracellular signal regulated kinase (ERK) [19]. These genes result mutated in PTC and in ATC patients (**Fig.3**) [20-22].

PI3K/ AKT/mTOR Pathway

The PI3K/AKT pathway is composed by several key components such as PIK3CA, PIK3C2G, PIK3CGM, PIK3C3, PIK3R1, PIK3R2, AKT1, AKT3, TSC1, TSC2, PTEN, and the mTOR signaling complex proteins. Activation of the PI3K/AKT signaling occurs when RAS binds to the p110 catalytic subunits of PI3K. Notably, PIK3CA (α -type) and PIK3CB (β -type) are among the most expressed subunits. Alternatively, this pathway can be triggered by the binding of receptor tyrosine kinases to various growth factors, leading to the activation of the p110 catalytic subunits and the production of phosphatidylinositol-3, 4, 5-triphosphate (PIP3). This, in turn, initiates a downstream cascade, including the phosphorylation of AKT, which activates a series of effectors, mTOR [23]. PTEN acts as an inhibitor further down the signaling pathway. The role of the PI3K/AKT pathway in promoting tumorigenesis in thyroid cancers is confirmed by the existence of PTEN germline mutations. These mutations are particularly evident in conditions like Cowden disease, which is known to be linked with the development of various cancers, including those affecting the thyroid [24]. Furthermore, mutations in PIK3CA are present in 5–25% of ATCs and in 0–11% of poorly differentiated thyroid cancers (PDTCs). AKT1 mutations occur in 0–8% of ATCs and

0–13% of PDTCs, while PTEN mutations are identified in 10–15% of ATCs. These mutations are uncommon in differentiated thyroid cancers (DTCs), with 11% of follicular thyroid cancers (FTCs) exhibiting PIK3CA mutations, and 3% displaying PIK3CA mutations and 2% showing PTEN mutations in PTCs (**Fig.3**) [25].

RAS Mutation

The rat sarcoma viral oncogene homolog (RAS) proto-oncogene encodes various protein isoforms—NRAS, HRAS, and KRAS. These isoforms, classified as oncogenes, are frequently mutated in numerous types of cancers. These proteins are molecular activators of MAPK and PI3K/AKT/mTOR signaling cascades. RAS protooncogenes encode for p21RAS GTPases, a 21kDa G-proteins, that interacts with guanosine diphosphate (GDP) and guanosine triphosphate (GTP in their inactivated and activated state respectively. Specifically, RAS is implicated in the signal transmission from tyrosine kinase membrane receptors (RTKs), via downstream effectors, to transcription factors. Mutations in RAS impede apoptosis, encouraging the rapid growth of cancer cells in the presence of TSH. On the other hand, aberrant RAS expression in the absence or low levels of TSH triggers cell growth independently of TSH, illustrating how thyrocytes harboring oncogenic RAS rely on TSH levels for their growth. Moreover, RAS mutation is able to cause DNA damage and subsequently de-differentiation by inhibiting the expression of differentiation genes such as TTF-1 and PAX8 [26-28]. Among the different isoforms such as NRAS, HRAS, and KRAS, the NRAS exon 2 mutation (codon 61) is extensively studied and linked with an increased risk of metastasis. RAS mutations are present in both low- and high-grade cancerous thyroid follicular cells, occurring more frequently in follicular thyroid cancer (FTC) and less frequently in PTC (**Fig.3**) [29-31].

BRAF Mutation

The RAF proteins group, is a serine-threonine kinase family, composed of different isoforms called ARAF, BRAF and CRAF (RAF1). They are induced via RAS interaction, initiating MAPK activation downstream pathway [32]. BRAF mutation is an early stage mutation in TCs, particularly BRAF^{V600E} is a prevalent substitution from valine to glutamate at position 600 is observed in 60% of PTCs, 12–33% PDTCs and 25–29% ATCs (**Fig.3**) [33-36].

TP53 Mutation

In TCs p53 mutation is particularly common in 8–35% PDTCs and 73% ATCs, especially in association with BRAF^{V600E} mutation [37]. Whereas, TP53 alterations have low frequency in metastatic PTCs (13%) or FTC (8%) [38]. This led to the consideration that p53 suppression in association with other oncogenes mutations, for example BRAF^{V600E}, drives cancer transformation in thyrocyte, especially in ATCs. Interestingly, studies in transgenic mice demonstrated BRAF^{V600E} and TP53 mutations give rise to PTCs with iperproliferative phenotype and worst prognosis leading to the progression into less differentiated PTDCs and ATCs, considering TP53 as a late-stage mutation (**Fig.3**) [39].

RET/PTC Rearrangements

RET is a proto-oncogene located on chromosome 10q11.2. It encodes a transmembrane tyrosine kinase receptor expressed in both thyroid parafollicular and follicular cells. When the 3' part of the RET gene combines with the 5' section of various genes, this results in the constitutive activation of RET. Consequently, the tyrosine kinase domain of the receptor is expressed, leading to the creation of an

oncogenic form of the RET receptor. Nowadays 10 rearrangements have been identified between RET and potential fusion genes. The most common include RET/PTC1, originated by a paracentric inversion of chromosome 10's long arm that merges with the CCDC6/H4 gene; RET/PTC2, derived from a reciprocal translocation between chromosomes 10 and 17, resulting in the fusion of the c-RET tyrosine kinase domain with a regulatory subunit of the cAMP-dependent protein kinase A; and RET/PTC3, arising from fusion with the NCOA4/RFG/ELE1 genes [40-42]. RET/PTC rearrangements trigger the activation of both the MAPK and PI3K/AKT pathways, leading to cellular dedifferentiation and promoting TSH-independent growth. These rearrangements have been identified in thyroiditis, indicating their role in the early stages of tumorigenesis through proinflammatory activation pathways. Additionally, the presence of RET/PTC rearrangements in benign lesions suggests that this genetic alteration marks an early phase in the development of thyroid cancers. These rearrangements are commonly found in PTCs but are less prevalent in PDTC (**Fig.3**) [43].

PAX8/PPAR γ , ALK and NTRK Rearrangements

The PAX8/PPAR γ rearrangement arises from the fusion of the PAX8 gene, a thyroid-specific transcription factor located on chromosome 3p25, and the PPAR γ gene, a transcription factor expressed in adipocytes, found on chromosome 2q13. PPAR γ typically regulates lipid metabolism and plays a crucial role in the differentiation of adipocytes [44, 45]. In TCs, PAX8/PPAR γ rearrangement has a prevalence of in 4–33% of follicular adenomas, 30–58% of FTC and 37.5% of PTCs [44-47]. ALK rearrangements show a frequency of 16% in PDTCs [48, 49]. Moreover, NTRK fusion oncogenes are mainly identified in 26% of PTCs (**Fig.3**) [50].

Telomerase Reverse Transcriptase (TERT) Promoter Mutations

TERT induces carcinogenesis by enabling replicative immortality in cancer cells. Specifically, the catalytic subunit of telomerase, results mutated (C250T and C228T) on its promoter region. TERT-promoter mutations are relatively rare, occurring in approximately 9-10.6% of non-metastatic PTCs. However, their prevalence significantly rises to 60% in cases of metastatic PTCs[51]. TERT mutations co-exist in presence of BRAF^{V600E} and RAS mutation generating aggressive TCs histotypes, with metastatic capabilities, poor prognosis and refractory to current therapies (**Fig.3**) [52-55].

Eukaryotic translation initiation factor 1A X-linked (EIF1AX) Mutations

EIF1AX was recognized originally in uveal melanomas showing change-of-function or gain-of-function mutations (in exons 2, 5 and 6). These mutations occur in both low and high grade TCs with a prevalence of 17% in FTCs, 1–2% in PTCs, 11% in PDTCs and 9–30% in ATC, mutually exclusive with other driver mutations [6, 37, 56]. Interestingly, EIF1AX mutations cooperate in thyroid carcinogenesis with RAS, BRAF, TERT promoter or TP53 mutations [57, 58].

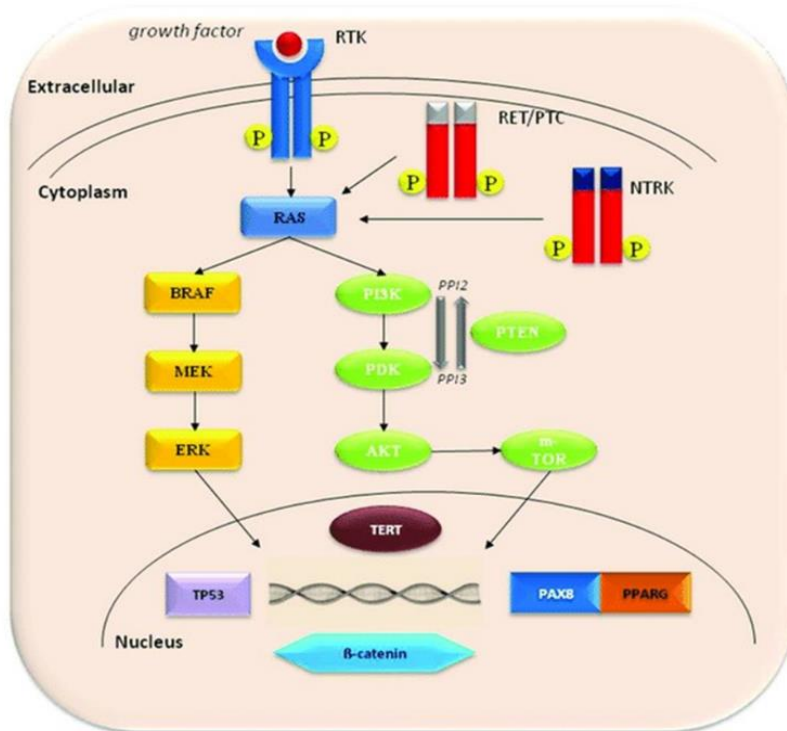


Fig.3 Scheme showing the main signaling pathways involved in thyroid carcinogenesis. Adapted from *Prete A et al. Fundamental Mechanisms of Thyroid Cancer. Front Endocrinol (Lausanne) 2020.*

Therapeutic strategies for thyroid carcinoma patients

Therapies for DTC patients

Radioiodine therapy (RAI) is the gold standard treatment for differentiated thyroid cancers (DTC) which include both PTC and FTC (**Fig.4**) [59]. Conceptually, this therapeutic approach is based on its relative specific affinity for thyroid cells. Accordingly, incorporation of radioiodine inside thyroid cells is carried out via NIS, physiologically expressed on these cells [60].

RAI therapy is a crucial therapeutic approach also for metastatic DTC [61]. Traditionally, it has been a longstanding post-surgery treatment for thyroid cancer patients which show lymph node metastatization [62, 63]. Nevertheless, the efficacy of RAI treatment needs to be evaluated within the scenario of the genetic characteristics and mutations present DTC.

In most instances, DTC is primarily driven by the BRAF^{V600E} mutation, a genetic alteration associated with hyperactivation of the MAPK pathway, which results in reduced responsiveness to RAI [53]. In contrast, DTC patients with metastatic disease characterized by RAS mutations tend to be more responsive to RAI due to a less active MAPK pathway [64]. However, promising findings from open-label phase II studies have shown that the use of MEK inhibitors can potentially restore RAI responsiveness in approximately 30% of patients with RAI-refractory metastatic BRAF^{V600E}-driven thyroid cancer [65]. This information underscores the importance of tailoring RAI therapy based on the specific genetic alterations driving thyroid cancer, and the potential for targeted therapies like MEK inhibitors to improve treatment outcomes in certain cases.

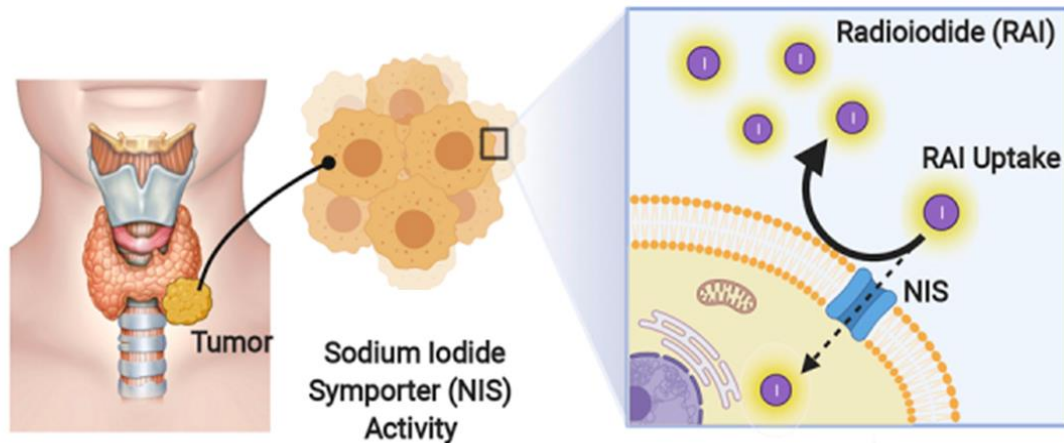


Fig.4 Figure showing the radioiodine (RAI) treatment uptake in DTCs via NIS transporter. Adapted and modified from *Targeting non-canonical pathways as a strategy to modulate the sodium iodide symporter*, *Read Cell Chem Biol*, 2022.

Therapies for ATC patients

Surgery, when possible, followed by chemoradiotherapy is the current approach in ATC patients [66]. The prognosis for ATC patients with distant metastases results worse because of the highly aggressive nature of these tumors.

Particularly, 45% of ATCs show BRAF^{V600E} mutation [51]. Fortunately, ATC BRAF mutated patients respond to the RAF kinase inhibitor vemurafenib [67]. In contrast, usually ATC develops RAF Kinase inhibitor resistance, for this reason a combination of MEK/RAF inhibitors is a potential therapeutic choice to inhibit MAPK pathway and to overcome resistance [68]. Accordingly, an innovative open-label phase II study of ATC BRAF^{V600E}-mutant patients undergoing a combinatorial treatment of BRAF inhibitor dabrafenib and the MEK inhibitor trametinib highlighted a significant response (**Fig.5**) [69, 70].

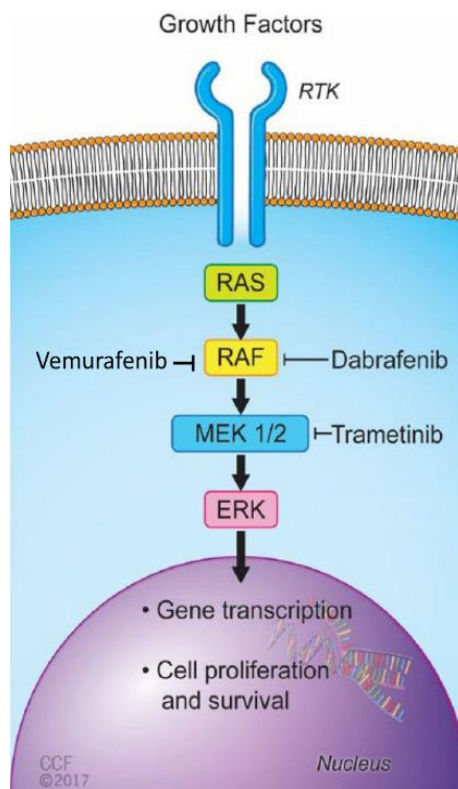


Fig.5 Vemurafenib alone or in combination with Dabrafenib and Trametinib block key proteins involved in MAPK pathway in ATC cells. Adapted and modified from *Ther Adv Respir Dis.* 2018 Jan-Dec. doi: 10.1177/1753466618767611.

Furthermore, ATCs are characterized by an enriched immune cell infiltration including macrophages, NK cells, CD4+ and CD8+ T cells, these latter cell types expressing markers of exhaustion [71-73]. How MAPK inhibitors could modulate this robust antitumor immune response is still unclear. However, encouraging evidence showed PD1 inhibitor spartalizumab reduces T cells suppression by increasing therapeutic responses in patients with ATC expressing high levels of PDL1 (**Fig.6**) [74].

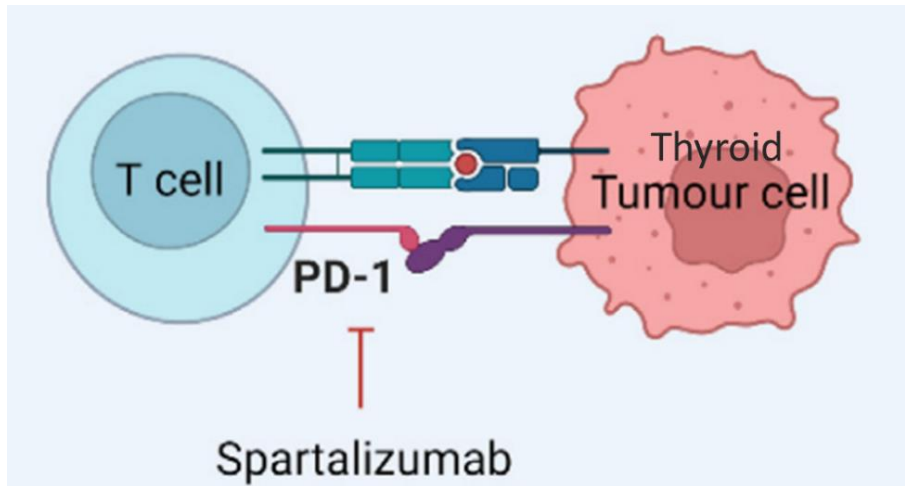


Fig.6 Spartalizumab reduces T cells suppression by increasing immunity activity against ATC cells. Adapted and modified from *Genomic landscape of anaplastic thyroid cancer and implications on therapy, Current Opinion in Endocrine and Metabolic Research, Cheng 2023.*

Other therapeutic targets and strategies in TCs

TC cell survival depend on driver mutations and chromosomal rearrangements in genes crucially involved in survival/proliferation signaling pathways, which can be targeted via innovative small molecules [75, 76]. Accordingly, RET and NTRK inhibitors showed effective response in metastatic TC patients harboring RET and NTRK rearrangements, respectively [43, 77]. Moreover, innovative small molecules targeting KRAS mutant 251 and HRAS mutant 252 have been designed, whereas drugs targeting NRAS^{Q61R} are currently still unavailable [78, 79].

Thyroid cancer stem cells vs Thyroid normal stem cells

Cancer Stem Cells (CSCs) are a small subpopulation that represent a reservoir of self-sustaining cells within tumor bulk. However, increasing evidence has shown that CSCs and normal SCs share features in common but they can present difference in characteristics and properties. Similarly to normal stem cells (SCs), CSCs are not specialized, they can divide asymmetrically giving rise to specialized/differentiated cells recapitulating tumor bulk heterogeneity [80]. Particularly, the maintenance of SCs pool is ensured thanks to the cellular asymmetrical division and population asymmetrical renewal. In asymmetrical division, one SC generates both a SC and a differentiated cell, while in population asymmetry, one SC produces either two SCs or two differentiated cells. These mechanisms remain in a comparable balance, ultimately maintaining a consistent number of both SCs and differentiated cells [81]. In a general context, SCs exhibit various degrees of differentiation, including totipotency, pluripotency, multipotency, oligopotency, and ultimately unipotency or monopotency [82]. Conversely, CSCs stand out as multipotent cells capable of upholding a heterogeneous hierarchy within the tumor mass [83]. An important difference among SCs and CSCs is that SCs are usually slow cycling dormant-cells during adulthood until regeneration tissues are necessary, whereas CSCs are usually in a high-cycling status. This led to detect CSC basing on markers found specifically in high proliferative cells [84]. Furthermore, SCs and CSCs exhibit varying levels of dependency on the stem cell niche, which is a specialized microenvironment where SCs are located. CSCs can drive deregulation or alteration of the niche via proliferation-inducing signals whereas normal SCs are totally supported by niche which guarantee homeostasis maintenance [85]. Another pivotal feature of CSCs is their ability to exert influence on the surrounding stromal environment through the secretion of proteins and molecular components, including

those associated with the extracellular matrix (ECM). This mechanism shares similarities with the behavior of SCs in various mammalian systems. This remodeling of the niche can also regulate the biochemical state of CSCs, potentially maintaining them in a state of dormancy. This concept is intricately connected to the destiny and adaptability of CSCs, as well as their resilience to conventional therapeutic approaches [86].

The existence of thyroid cancer stem cells (TCSCs) has been substantiated through the generation of thyrospheres in vitro and their tumorigenic potential in in vivo mouse models. The identification of this specific cellular subpopulation has been facilitated through the identification of markers such as CD133, CD44, and the aldehyde dehydrogenase gene (ALDH) [87, 88]. A great number of studies highlighted that TCSCs can be distinguished from normal thyroid stem cells (TSCs). The two cytotypes are characterized by differences in phenotype, clonogenic and differentiative potential. Accordingly, thyrospheres derived from CSCs PTCs showed distinct characteristics. These thyrospheres were larger, irregularly shaped, exhibited elevated levels of specific markers related to stemness (such as Oct-4, Sox-2, ABCG2) and epithelial-mesenchymal transition (EMT) (e.g., vimentin) in comparison to normal TSCs. Conversely, TCSCs displayed reduced levels of differentiation markers like Pax-8 and TTF-1, and their capacity for differentiation was notably lower than that of normal TSCs [89].

Thyroid carcinogenesis models

Various models of carcinogenesis have been proposed to explain the origins of TCs. According to the multistep carcinogenesis model, TCs develop from multiple genetic mutation accumulation in thyrocyte follicular cells derived. Particularly ATC originates from a dedifferentiation process of PTC or FTC after acquiring PT53 and CTNNB1 mutations. This event is characterized by high expression of transition epithelial mesenchymal markers (EMT) which drives the transformation of well differentiated phenotypes to undifferentiated ones. Whereas PTC derive from thyrocytes following RAS and BRAF mutations or RET/PTC rearrangements while FTC depend on RAS mutation and PAX8/PPAR γ rearrangement [90, 91]. The Fetal cell carcinogenesis model affirm that TCs emerge from the alteration of three distinct cell types within the thyroid lineage: thyroid stem cells, thyroblasts, and prothyrocytes. These transformations lead to the development of ATC, PTC and FTC, respectively [92]. Considering that TCs emerge from various cell types; they also display distinct mutational profiles dictated by their histopathological characteristics. ATC originates from SCs expressing onco-fetal fibronectin and lacks differentiation markers. On the other hand, PTC arises from thyroblasts expressing onco-fetal fibronectin as well as differentiation markers such as TG. FTC originates from prothyrocytes, which exhibit a more differentiated phenotype [93]. Of note, it has been postulated the cancer stem cells model to explain TC initiation [87]. Accordingly, within the tumor mass, CSCs represent a minority population that can propel the process of carcinogenesis by acquiring genetic mutations and undergoing epigenetic alterations [94-96]. Nowadays, the dynamic cancer stem cell model represents an evolution of the traditional CSC concept. Here, CSCs are recognized for their flexible and changeable nature, capable of transitioning between a stem cell state and a non-

stem cell state influenced by tumor microenvironment stimuli or spontaneously in different cancer histotypes (**Fig.7**) [97, 98].

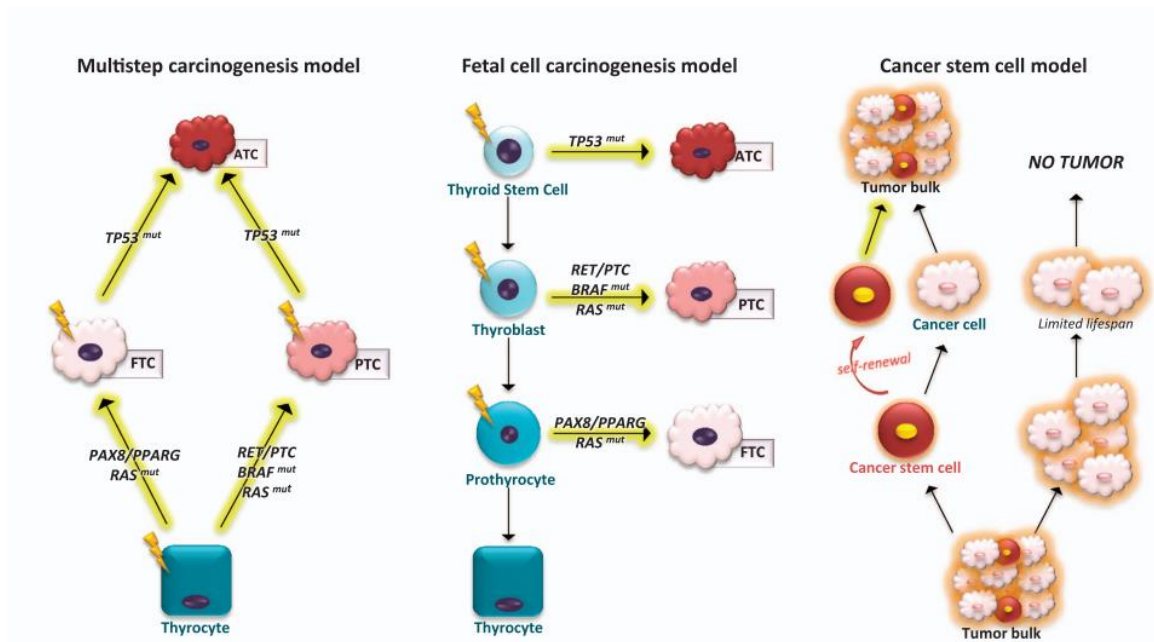


Fig.7 Thyroid carcinogenesis models. Adapted from Zane M, Scavo E, Catalano V, Bonanno M, Todaro M, De Maria R, Stassi G. *Oncogene*. 2016.

Since the existing models fail to fully elucidate the multifaceted phenotypic and genetic diversity within the tumor mass of TCs, a more recent proposal is the genetic mutation model. This model aims to underscore the molecular mechanisms driving the different histotypes of TCs. In the genetic mutation model, it is suggested that multiple genetic mutations may take place within a single CSC, giving rise to various tumor phenotypes. Accordingly, it can be termed as the CSC genetic mutation model in TCs (**Fig.8**) [99].

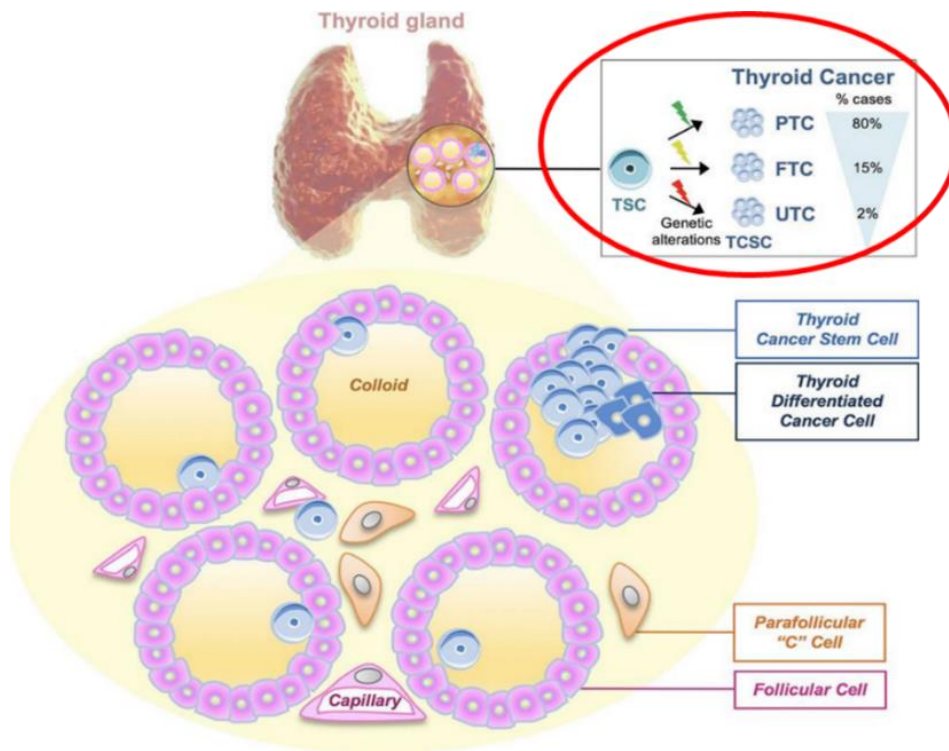


Fig.8 The genetic mutation model. *Adapted and modified from Veschi, Verona et al. Front Endocrinol (Lausanne). 2020 Aug.*

Aim of the work

TCs represent a highly frequent and heterogeneous group among endocrine cancers [4, 5]. Global morbidity due to thyroid cancers has increased dramatically over the past three decades [100]. In 2020, approximately 586,202 incident cases of thyroid cancer and 43,646 deaths from thyroid cancer occurred showing a certain urgency in discovering and defining the molecular basis for a better understanding of the disease and identification of new therapeutic targets and effective therapies [101]. As discussed above, different carcinogenesis models have been proposed to explain the origin of TCs. According to the “multistep model”, ATCs derive from FTC or PTC through a process of cellular dedifferentiation following the accumulation of further mutations in TP53 [90, 92]. The “fetal cell carcinogenesis model” or “cell of origin model” instead affirmed that thyroid cancer cells originate from fetal thyroid cells and underwent different mutagenesis events at different maturation stages (stem cells, thyroblasts, prothyrocytes and thyrocytes). A growing number of scientific studies support the “cancer stem cell model”, indicating CSCs as the cause of the origin and propagation of TC [87]. CSCs represent a subpopulation of tumor cells present within the tumor mass capable of driving tumor initiation and progression following the acquisition of gene mutations and epigenetic alterations, characterized by self-renewal capacity, metastatic potential and chemoresistance [94, 102]. However the previous models do not recapitulate the complex phenotypic and intratumoral heterogeneity of TCs, for this reason, we proposed the “genetic mutation model”, according to which multiple mutations would affect the same cell in thyroid lineage generating the different TC phenotypes. Specifically, this work aims to investigate the role of the most common driver mutations in the carcinogenesis and progression of TCs. Particularly, we aim to identify the specific cellular subpopulation from which the different follicular cells derived

histotypes TCs originate. Moreover, unveiling the underlying molecular mechanisms, which determine the fate and behavior of TC cells could identify potential biomarkers for the development and design of innovative and effective therapeutic strategies, particularly in metastatic TCs.

Chapter 1

Cancer Stem Cells in Thyroid Tumors: From the Origin to Metastasis

Veschi V, **Verona F**, Lo Iacono M, D'Accardo C, Porcelli G, Turdo A,
Gaggianesi M, Forte S, Giuffrida D, Memeo L, Todaro M.

Published in Frontiers in endocrinology, 2020



Cancer Stem Cells in Thyroid Tumors: From the Origin to Metastasis

Veronica Veschi^{1†}, Francesco Verona^{1†}, Melania Lo Iacono^{1†}, Caterina D'Accardo², Gaetana Porcelli¹, Alice Turdo², Miriam Gaggianesi¹, Stefano Forte³, Dario Giuffrida³, Lorenzo Memeo³ and Matilde Todaro^{2*}

¹ Department of Surgical, Oncological and Stomatological Sciences (DICHIRONS), University of Palermo, Palermo, Italy,

² Department of Health Promotion, Mother and Child Care, Internal Medicine and Medical Specialties (PROMISE), University of Palermo, Palermo, Italy, ³ Department of Experimental Oncology, Mediterranean Institute of Oncology (IOM), Catania, Italy

OPEN ACCESS

Edited by:

Natalia Simona Pellegata,
Helmholtz Zentrum
München, Germany

Reviewed by:

Giovanni Vitale,
University of Milan, Italy
Marcello Maggolini,
University of Calabria, Italy

*Correspondence:

Matilde Todaro
matilde.todaro@unipa.it

[†]These authors have contributed
equally to this work

Specialty section:

This article was submitted to
Cancer Endocrinology,
a section of the journal
Frontiers in Endocrinology

Received: 29 May 2020

Accepted: 10 July 2020

Published: 25 August 2020

Citation:

Veschi V, Verona F, Lo Iacono M,
D'Accardo C, Porcelli G, Turdo A,
Gaggianesi M, Forte S, Giuffrida D,
Memeo L and Todaro M (2020)
Cancer Stem Cells in Thyroid Tumors:
From the Origin to Metastasis.
Front. Endocrinol. 11:566.
doi: 10.3389/fendo.2020.00566

Thyroid tumors are extremely heterogeneous varying from almost benign tumors with good prognosis as papillary or follicular tumors, to the undifferentiated ones with severe prognosis. Recently, several models of thyroid carcinogenesis have been described, mostly hypothesizing a major role of the thyroid cancer stem cell (TCSC) population in both cancer initiation and metastasis formation. However, the cellular origin of TCSC is still incompletely understood. Here, we review the principal epigenetic mechanisms relevant to TCSC origin and maintenance in both well-differentiated and anaplastic thyroid tumors. Specifically, we describe the alterations in DNA methylation, histone modifiers, and microRNAs (miRNAs) involved in TCSC survival, focusing on the potential of targeting aberrant epigenetic modifications for developing novel therapeutic approaches. Moreover, we discuss the bidirectional relationship between TCSCs and immune cells. The cells of innate and adaptive response can promote the TCSC-driven tumorigenesis, and conversely, TCSCs may favor the expansion of immune cells with protumorigenic functions. Finally, we evaluate the role of the tumor microenvironment and the complex cross-talk of chemokines, hormones, and cytokines in regulating thyroid tumor initiation, progression, and therapy refractoriness. The re-education of the stromal cells can be an effective strategy to fight thyroid cancer. Dissecting the genetic and epigenetic landscape of TCSCs and their interactions with tumor microenvironment cells is urgently needed to select more appropriate treatment and improve the outcome of patients affected by advanced differentiated and undifferentiated thyroid cancers.

Keywords: cancer stem cells, thyroid tumors, epigenetic alterations, microenvironment, immune system

THYROID TUMORS AND CANCER STEM CELLS

Thyroid cancers (TCs) are highly heterogeneous and represent the most frequent tumors among the endocrine neoplasms (1, 2). In the past years, TC incidence increased worldwide, and the gender disparity became more pronounced, especially considering women at age 40–49 with a female/male ratio of about three times higher (3). The molecular basis of these gender differences in TC is still unclear. However, it has been postulated that female steroid hormones play a critical role in TC development mediated by the differential expression of the nuclear α - and β -estrogen receptors in various TC histological subtypes (4). Moreover, estrogens increase adherence, invasion, and migration capability of thyroid cancer cell lines (5). Recently, it has been demonstrated that estradiol regulates a higher production of reactive oxygen species (ROS) in adult female rats

compared with male counterparts (6, 7). Overall, the risk of thyroid proliferative diseases is increased during pregnancy, while the specific risk for TC is decreased after menopause.

According to their histopathological features, it is possible to distinguish four subtypes of thyroid carcinoma: papillary thyroid carcinoma (PTC), follicular thyroid carcinoma (FTC), anaplastic thyroid carcinoma (ATC), and medullary thyroid carcinoma (MTC). PTC, FTC, and ATC derive from malignant transformation of follicular cells, while MTC derives from calcitonin-producing parafollicular C cells. PTCs and FTCs represent the majority of differentiated TCs with good prognosis, accounting for 80–85 and 10–15% of all TCs, respectively. On the contrary, ATC is a rare and undifferentiated TC (UTC), characterized by an aggressive phenotype and poor prognosis. Although current therapeutic strategies including surgery, radioiodine therapy, and chemotherapy are able to eradicate the majority of primary TCs, the management of advanced and undifferentiated TCs is still a clinical hurdle. The existence of cancer stem cell (CSC) population explains the aggressiveness of TCs and their resistance to the clinical treatments. Scientific advances in stem cell biology have paved the way to a better understanding of the molecular mechanisms driving tumorigenesis in many types of cancers, including TCs (8) (**Figure 1**). CSCs are a small subset of cancer cells within tumors that exhibit exclusive self-renewal ability, clonogenic, and metastatic potential. They show a key role during the initiation, progression, drug resistance, and cancer recurrence or metastasis (9, 10). The isolation and characterization of thyroid cancer stem cell (TCSC) population in different thyroid tumors improved the knowledge about TC initiation. Nevertheless, there are still many questions to elucidate: (i) how TCSCs influence the initiation, progression, and metastasis within the four subtypes of TCs; (ii) how the tumor microenvironment (TME) affects TCSCs; (iii) which are the interactions between TCSCs and tumor bulk population; and (iv) which is the broad genetic/epigenetic landscape of TCs. Here, we provide an overview of the principal markers and pathways sustaining TCSC survival, their epigenetic alterations and interactions with immune cells, and TME cell components. We summarize the potential and innovative therapeutic approaches targeting TCSCs. Nowadays, dissecting the role of TCSCs in TC initiation, progression, and invasiveness may lead to the development of more effective therapies in advanced TCs.

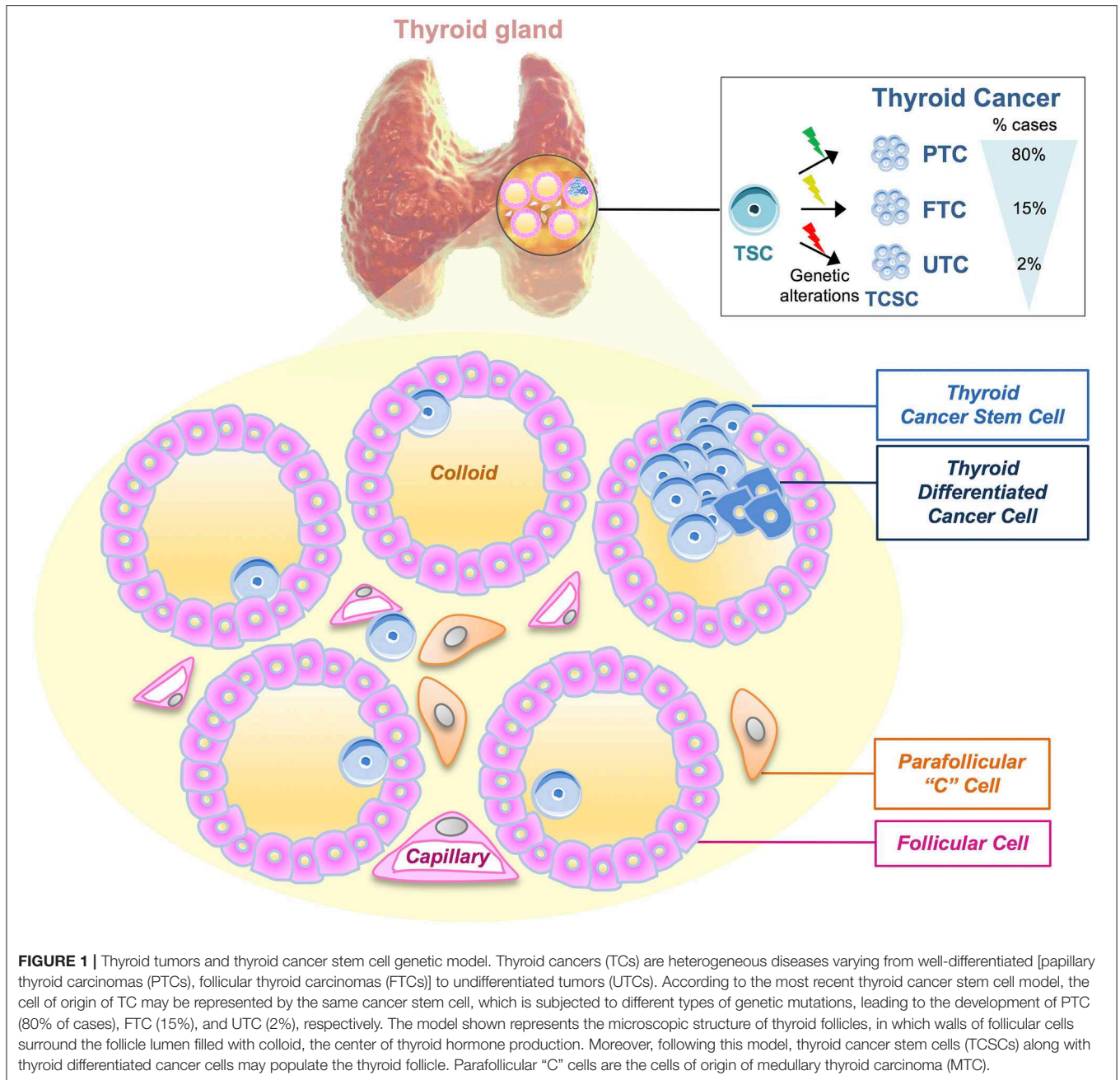
Thyroid Cancer Model of Origin

Different carcinogenesis models have been proposed to describe TC origin. According to the multistep carcinogenesis model, ATC cells derive from FTC or PTC cells following a dedifferentiation process and the accumulation of different mutations, particularly the inactivating mutations of *TP53* and *CTNNB1* (11, 12). This model is supported by scientific evidence, such as the presence of *TP53* and *BRAF* mutations in differentiated and undifferentiated carcinomas, including ATCs (13), but it cannot explain the presence of specific *RET/PTC* rearrangements and *PAX8/PPAR γ* gene fusion that may occur in ATCs (14). Moreover, the slow cell cycle of follicular thyroid cells reduces the potential accumulation of mutations, which sustain cancer progression

(15). Thus, according to the multistep carcinogenesis model, TCSCs can derive from thyrocytes upon genetic alterations and the epithelial–mesenchymal transition (EMT) process, which induces in TCSCs a more aggressive phenotype able to give rise to metastasis (16). During EMT, TCSCs lose polarity and adhesion, thus acquiring an invasive phenotype through Snail upregulation, which impairs E-cadherin expression (17). The fetal cell carcinogenesis model foresees that thyroid cancer cells derive from thyroid fetal cells upon the acquisition of specific mutations. The term thyroid fetal cells refers to TCSCs or thyroid precursor cells such as thyroblasts or prothyrocytes (18). TCs present a different cell of origin as well as a different mutational profile based on their distinct histopathological features. Specifically, ATC originates from fetal TCSCs expressing onco-fetal fibronectin without the expression of any differentiation markers, while PTC originates from thyroblasts expressing onco-fetal fibronectin and differentiation markers as thyroglobulin (Tg). Finally, FTC originates from the prothyrocytes, representing a more differentiated thyroid cell (19). Interestingly, to date, many evidence support the CSC model also for TC origin and initiation (20). CSCs represent a small population in the tumor bulk. They are placed at the apex of the hierarchical pyramid that includes also progenitors and differentiated cells. CSCs are able to drive cancer initiation and progression by acquiring genetic mutations and epigenetic alterations (21). Nowadays, the dynamic CSC model superseded the CSC model. Indeed, CSC phenotype has been considered plastic and dynamic, able to interchange between a CSC state and a non-CSC state, spontaneously or in response to microenvironment stimuli (EMT or IL-6) in various cancer types (22–24). An extensive description of the thyroid carcinogenesis models can be found in (25). Given that all the above-described models do not completely explain the phenotypic and genetic heterogeneity of tumor bulk, it has been recently postulated the genetic mutation model to elucidate the molecular mechanisms underlying the distinct TC histopathology and behavior. Specifically, according to this model, a variety of genetic mutations may occur in the same CSC by leading to different tumor phenotypes. This can be termed as the CSC genetic mutation model in TC (**Figure 1**).

Normal vs. Thyroid Cancer Stem Cells

To date the origin of TCSC population is still incompletely understood. Specifically, whether TCSCs originate from precursors or mature cells and whether TC cells are the result of genetic mutations or epigenetic alterations occurring in thyroid stem cells (TSCs) are issues to be clarified. Nevertheless, the existence of TCSCs is confirmed by *in vitro* thyrosphere generation and by the development of *in vivo* mouse models. To date, several markers have been proposed to identify TCSCs, such as CD133, CD44, and aldehyde dehydrogenase gene (ALDH) (20, 26). Several studies highlighted that TCSCs present specific features that distinguish them from normal TSCs. Both CSCs and stem cells (SCs) undergo symmetric division, but their clonogenic and differentiative potential is different. Giani et al. observed that thyrospheres generated from PTC-derived CSCs (PTC-CSCs) were larger and irregular compared with



normal TSCs. The clonogenic potential and expression levels of stemness markers (Oct-4, Sox-2, ABCG2) and EMT markers, as vimentin, were higher in PTC-CSCs compared with normal TSCs. Moreover, TCSCs showed lower expression levels of differentiation markers such as Pax-8 and TTF-1, and their differentiation efficiency was poorer than normal TSCs (27). Malguarnera et al. dissected the differences between CSCs derived from PTC and thyroid normal stem/progenitor cells. Both cellular types are able to generate thyrospheres in culture. However, only thyrospheres derived from normal thyroid stem progenitor cells could differentiate when plated in adhesion

in presence of thyroid-stimulating hormone (TSH). Stemness markers as CD133, CD44, Oct-4, Sox-2, and Nanog were revealed in both normal and cancer thyrospheres; conversely, thyroid differentiation markers [thyroperoxidase (TPO), thyroglobulin (Tg), thyroid-stimulating hormone receptor (TSH-R)] were detected at low levels in both cellular types. In addition, the authors showed that insulin receptors (IR-A and IR-B), insulin growth factors (IGF-I and IGF II), and the IGF receptor (IGF-IR) were expressed at higher levels in CSCs compared to the differentiated cells. These findings confirm that insulin resistance is related to an enhanced susceptibility to develop TC, and

therefore, insulin and/or IGFs should be considered as novel potential targets for TC treatment (28).

Markers Identifying TCSCs and Pathways Sustaining Their Maintenance

Many studies have been carried out to identify specific biomarkers of TCSCs in the four histopathological TC variants, but their combination and/or association needs to be further investigated. Friedman et al. demonstrated that cell lines derived from ATCs are CD133⁺, and when transplanted in immunodeficient non-obese diabetic (NOD)/severe combined Immunodeficiency (SCID) mice, they are able to develop tumor (29). Todaro and coworkers were the first to isolate TCSCs from primary thyroid tumors using ALDH activity. The authors highlighted the ability of TCSCs to form thyrospheres and recapitulate the parental tumor behavior when transplanted in murine thyroid gland. They found that a higher activity of ALDH in ATCs compared with FTCs and PTCs is correlated to the migration ability of TCSCs. ALDH⁺ TCSCs derived from ATC showed an enhanced migratory ability compared to ALDH⁺ cells derived from FTC and PTC. This phenotype is associated with an increase in c-MET and AKT activation. Silencing of these genes completely blocks the ALDH⁺ TCSCs metastatic capacity. Thus, c-MET and AKT have been proposed as potential therapeutic targets (20). Controversial data have been shown on cells derived from ATCs expressing stem cell markers, as Nanog and POU class 5 homeobox 1 (POU5F1) but lacking the expression of CD133 (30). Ahn et al. demonstrated that TCSCs present in PTCs express high levels of CD44, but no expression was revealed for CD24. The frequency of CD44⁺CD24⁻ CSC population was higher in recurrent PTCs than primary PTCs. POU5F1 was almost exclusively expressed by CD44⁺CD24⁻ cells compared with CD44⁺CD24⁺ cells (31). Shimamura et al. performed a comprehensive analysis of multiple markers (CD13, CD15, CD24, CD44, CD90, CD117, CD133, CD166, CD326, and ALDH activity) on eight cell lines derived from TCs and evaluated their ability to generate thyrospheres *in vitro* and tumor *in vivo*. This study identified ALDH activity and CD326 expression as reliable candidates to mark TCSCs (32).

Distinct signaling pathways are implicated in tumor initiation and progression by sustaining TCSC survival. In FTCs, the activation of mitogen-activated protein kinase (MAPK) and phosphatidylinositol 3-kinase (PI3K) pathways has been extensively described. In PTCs, the genetic alterations activate only MAPK pathway, while in ATCs, the MAPK, PI3K, and β -catenin pathways are activated. It has been widely demonstrated that *BRAF* and *RAS* mutations, *RET/PTC* rearrangements, and also *ALK* mutations activate MAPK pathway, which has a key role in thyroid tumorigenesis (33). The pathogenesis of TC, including angiogenesis, invasion, and metastasis process, is dictated by aberrant MAPK signaling pathway, altered production of chemokines, growth factors, matrix-metalloproteinases (MMPs), hypoxia-inducible factor 1 α (HIF-1 α), and tissue inhibitor of metalloproteinases-1 (TIMP-1). In particular, in *BRAF*^{V600E} PTC, TIMP-1 is upregulated by nuclear factor kappa B (NF- κ B) activation, leading to

invasiveness, inhibition of apoptosis, increase in proliferation rate, and resistance to chemotherapy (34). Despite its role as MMP inhibitor, TIMP-1 exerts also its function in promoting tumor proliferation and regulating metastatic potential through hepatocyte growth factor (HGF) induced by HIF-1 α . Thus, TIMP-1 could be used as a predictive biomarker and therapeutic target in advanced PTCs (35). PI3K-AKT pathway plays an important role in tumor progression and vascular intravasation in FTCs. In particular, elevated levels of AKT1 and its nuclear localization promote the invasiveness and the metastatic potential of FTC (36). This finding is supported by the presence of *AKT1* mutations in metastatic TCs (37).

Recently, it has been demonstrated that NF- κ B regulates the proliferative and antiapoptotic signaling pathways in TCSCs. In ATC, the administration of NF- κ B inhibitors in combination with radio- or chemotherapy exerts antiproliferative effects and induces massive apoptosis (38). Moreover, NF- κ B is also upregulated by the MAPK pathway, suggesting a direct coupling with the presence of *BRAF*^{V600E} mutations as described above. In poorly differentiated TCs and ATCs, WNT- β -catenin signaling pathway is upregulated. This pathway has a role in the proliferation and differentiation of SCs, and its aberrant activation is a consequence of the activation of PI3K-AKT pathway by glycogen synthase kinase 3 β (GSK3 β) (39). Aberrant activation of the all above described signaling pathways represents the first step of TC tumorigenesis and can be considered as a target for novel therapeutic approaches.

EPIGENETIC ALTERATIONS SUSTAINING TCSCs ORIGIN AND MAINTENANCE

Epigenetic regulation of gene expression and chromatin compactness is a reversible and dynamic process crucial in developmental biology and in many diseases, including cancer (40). The impaired differentiation of normal stem cells into tissue subtypes and their acquisition of CSC capabilities as self-renewal, chemoresistance, and metastatic potential are finely governed by epigenetic modulators (9). Epigenetic alterations fundamental in the tumorigenesis of many cancer types, including TC, are mainly related to the following mechanisms and/or modulators summarized in **Figure 2**: (1) DNA methylation, inducing the silencing of many tumor suppressor gene transcription through the DNA methyltransferases (DNMTs); (2) histone modifiers, which regulate gene expression by adding or removing mostly acetyl or methyl groups to the histone tails; (3) Chromatin remodelers that control the structural organization of chromatin by modulating its degree of condensation; (4) non-coding RNAs, including microRNAs (miRNAs) and long non-coding RNAs (lncRNAs), which may exert their role in both inhibiting or aberrantly inducing gene transcription. In thyroid tumors many epigenetic modifiers are altered, but further studies are needed to better elucidate how the complex regulation of histone modifying enzymes and chromatin remodelers could interfere with or facilitate the tumor growth of the CSC subset. Here, we highlight the key points related to the most relevant epigenetic mechanisms altered in the different subtypes of

TCs: (i) Thyroid-specific differentiation and tumor suppressor genes aberrantly methylated in their promoter regions along with altered expression of miRNAs represent the most frequent epigenetic features in well-differentiated thyroid tumors, as PTC and FTC, while the amount of reports regarding the histone modifications are very limited. (ii) The most common altered epigenetic mechanisms that contribute to well-differentiated TC initiation and progression, lead to the activation of MAPK and PI3K/AKT survival pathways, which sustain TCSCs origin and maintenance. (iii) In UTCs in addition to MAPK and PI3K/AKT pathways, other signaling pathways, as Wnt/ β -catenin and Notch, crucial for the survival of TCSCs are epigenetically compromised. Unlike the well-differentiated thyroid tumors, the DNA methylation profiling in the undifferentiated subtypes reveals more often the aberrant promoter hypomethylation compared with hypermethylation.

DNA Methylation in Thyroid Tumors

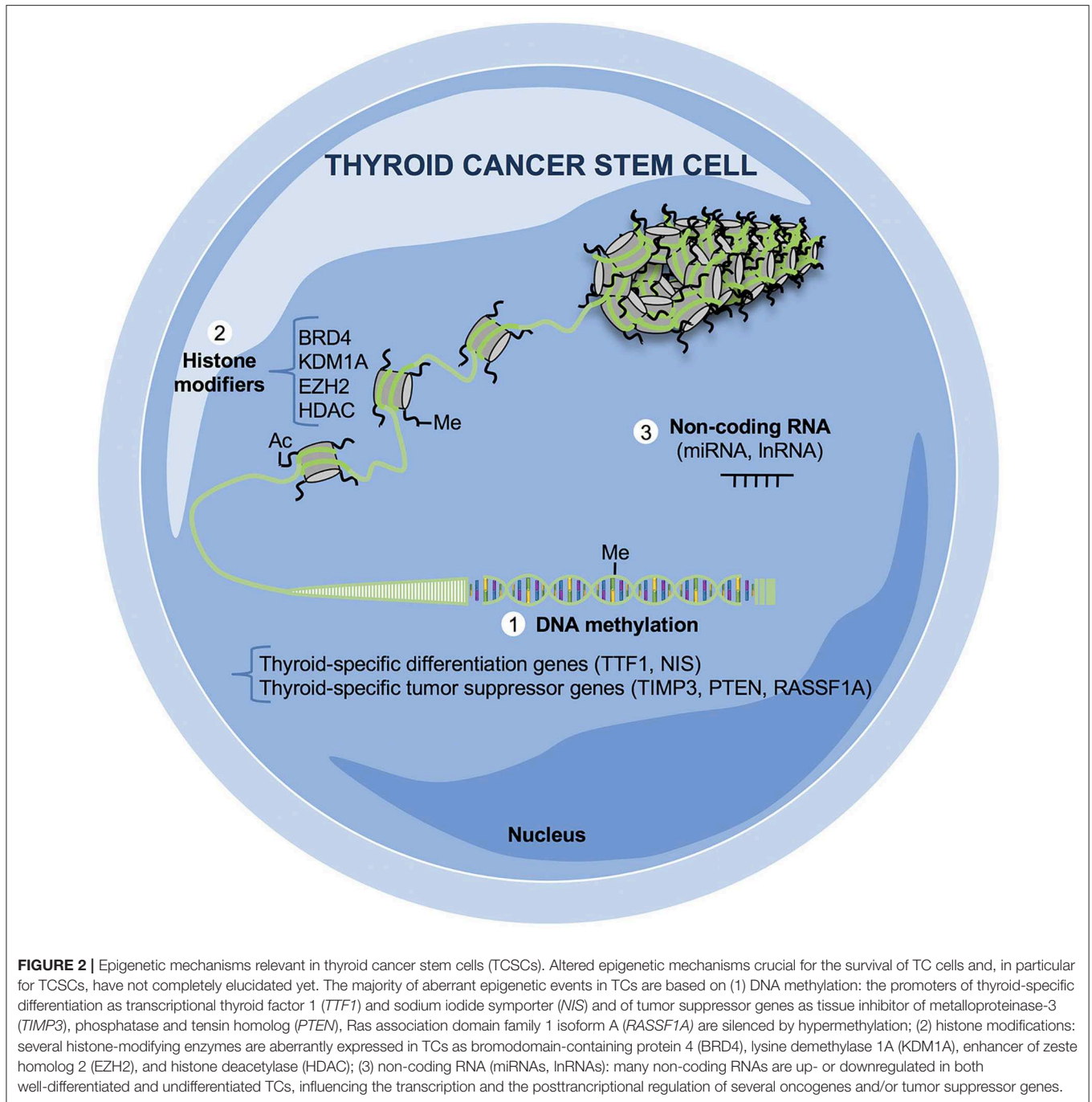
Global DNA methylation studies utilizing next generation sequencing (NGS) platforms (41–43) have identified different DNA methylation patterns associated with TC histological variants and their distinct mutational status. Specifically, the hypermethylation has been associated with the well-differentiated TCs while the hypomethylation with the undifferentiated ones. DNA methylation status has been correlated with *BRAF* mutation, tumor progression, and aggressive behavior in PTCs (44). Thus, genome-wide approach shed new lights on the methylome profiles of TC subtypes; nevertheless, novel potential biomarkers for early diagnosis, prognosis, and therapy resistance have not been identified yet. The majority of the thyroid-specific tumor suppressor genes, which have been found aberrantly methylated in their promoter regions, exert their role as antagonists or modulators of PI3K pathway, RAS signaling, and EMT process. Of note, *PTEN* (phosphatase and tensin homolog) acts as an inhibitor of PI3K pathway (45); RAS association domain family 1A (*RASSF1A*) (46) and *RASAL* (RAS protein activator like-1) (47) are both involved in RAS signaling, cell cycle regulation, and mitotic progression; *TIMP3* (tissue inhibitor of metalloproteinase 3), is an inhibitor of metastasis, angiogenesis, and invasion; and others are known as tumor suppressors as the death associated protein kinase (*DAPK*) and the retinoic acid receptor beta2 (*RAR β 2*) (44). Silencing of E-cadherin (*CDH1*) by its promoter methylation has been hypothesized as a potential mechanism of enhanced EMT in FTC cells, whereas in PTC cells, *CDH1* expression levels are maintained (48, 49). Moreover, thyroid differentiation specific genes, as thyroid transcription factor-1 (*TTF1*) and sodium-iodide symporter (*NIS*), are also hypermethylated particularly in undifferentiated tumors (50). High expression levels of DNMT1 have been associated with silencing of *NIS* (51). The role of *KISS1/KISS1R* signaling is controversial in various types of cancers, as it has been associated with both roles in metastatic promotion and suppression (52–54). Savvidis et al. found increased levels of *KISS1* in extrathyroidal tissues of advanced differentiated TCs while an inverse correlation between *KISS1R* and tumor size (55). Interestingly, it has been demonstrated that *KISS1R* promoter is hypermethylated particularly in FTCs (42).

Therefore, further studies are needed to define the methylome profile in TCSC population in an attempt to find specific targets in this cell compartment. However, the fact that components of the principal pathways involved in TCSC survival are silenced by hypermethylation strongly suggests that this could be a mechanism specific also of this subset.

Histone Modifications and miRNAs Role in Thyroid Tumors

Aberrant alterations in the histone modifier epigenetic enzymes as well as in the chromatin remodeling complexes have not been completely studied in TCs and in the subset of TCSCs. Nowadays, there are few reports about the histone modifications in TCs. Histone deacetylase (HDAC) enzymes modulate the levels of histone tail residues acetylated. It is now widely accepted that treatment with HDAC inhibitors is very effective in TCs subtypes, as they impair cell growth and induce apoptosis of TC cells while increasing the radioiodine uptake. Of note, the global acetylation levels in TCs are higher than in healthy tissues (56). Moreover, UTCs express lower levels of acetylated H3 on lysine 18 compared with well-differentiated TCs, suggesting that the deacetylation is a step required for the acquisition of a more aggressive phenotype. Interestingly, in cells with reduced levels of *TTF1* because of hypermethylation, levels of acetyl H3K9 are reduced and dimethyl H3K9 are increased. BRD4 is a bromodomain protein, which binds the acetylated histones facilitating the recruitment of transcription factors and ultimately the transcription. The role of BRD4 as a potential oncogene in TCs has been recently elucidated. Levels of BRD4 are higher in ATCs compared to healthy tissues. The BRD4 inhibition, by JQ1, which also inhibits c-Myc and induce *TTF1*, or by AZD5153, impairs TC cell growth, suggesting that it is critical for thyroid proliferation (57, 58). KDM1A is a H3K9 demethylase frequently overexpressed in PTCs and required for migratory and invasive capabilities of PTC cells (59). TIMP1 has been described as a KDM1A target. KDM1A epigenetically silences TIMP1 and subsequently activates MMP9 promoting metastasis and migration (59). Finally, the enzymatically active component of the PRC complex, EZH2, involved in the regulation of embryonic development and responsible for the trimethylation of lysine 27 on H3 (H3K27me3), leading to silencing of gene transcription, is overexpressed in ATCs (60). Future studies are needed to better characterize the epigenetic modifications and their use as potential therapeutic targets in TCs.

miRNAs are short molecules of 19–23 nucleotides involved in blocking transcription or degradation of messenger RNA (mRNA), which have been associated with critical roles in TC initiation and progression because they can downregulate tumor suppressor genes or upregulate oncogene transcription. Their expression is also specific for each TC subtype. An extensive overview about the principal aberrant epigenetic events and, in particular, the most differentially up- or downregulated miRNAs involved in both well-differentiated or undifferentiated TCs is reported in (61, 62).



Epigenetic Therapy in Thyroid Tumors

Epigenetic drugs can be used to revert the chemoresistance of TCs. Given that epigenetic modifications are reversible, these may be approached differently than genetic mutations, which are irreversible. HDAC and DNMT inhibitors represent the first Food and Drugs (FDA)-approved epigenetic drugs and are currently used in several clinical trials showing promising results for TC treatment (63). Recently, many *in vitro* and *in vivo* studies have reported that treatment with HDAC inhibitors alone or in combination with chemotherapy or other biological

agent induces apoptosis and cell cycle arrest, impairing the growth while incrementing the radioiodine uptake of TC cells (64). Moreover, HDAC inhibitors, as Trichostatin A (TSA), and Valproic acid (VA) combined with DNMT inhibitors as azacitidine, exerts an antitumoral effect by reducing MMP2 and MMP9 levels in PTC and FTC. Unfortunately, some clinical limitations have been associated with the use of the epigenetic inhibitors in many solid tumors, including TC, as remethylation, the lack of specificity and general toxicity. Although the use of DNMT inhibitors was expected to revert the silencing of

many tumor suppressor genes involved in TC tumorigenesis, it has been demonstrated that they also promote oncogenes and prometastatic genes transcriptional activation through a global change in gene expression. Currently, only two clinical studies verified the efficacy of demethylating agents in patients affected by recurrent and/or metastatic differentiated TCs, with no partial or complete responses and severe side effects (www.clinicaltrials.gov, NCT00085293 and NCT00004062) (65). Nevertheless, these inhibitors may be potentially translated in clinical settings in combination with HDAC inhibitors and/or other targeted therapies such as mammalian target of rapamycin (mTOR) inhibitors (66). Notably, HDAC inhibitors, although generally well-tolerated, induced cardiac arrhythmias in patients with heart disease. The final data from the ongoing clinical trials are needed to understand their efficacy in treating TC refractory to current therapies (67, 68). The hurdles in the administration of these epigenetic drugs will be overcome with the use of highly specific inhibitors (for instance HDAC inhibitors specific for a single class or a single HDAC) and/ or nanoparticle (liposomes, nanogels, polymeric nanoparticles) to reduce off-target effects and improve the delivery system (69). Overall, so far, the successful preclinical results obtained in TC cells treated with the epigenetic drugs have not been recapitulated in clinical settings mostly due to the epigenetic landscape heterogeneity of thyroid tumors, the influence of immune cells, and the lack of a complete knowledge about the other TC histological subtypes other than PTCs. A better understanding of the epigenetic changes in TCSCs is crucial to design more effective molecular therapies (70).

THE CROSS-TALK BETWEEN IMMUNE SYSTEM AND CSCs IN THYROID CANCER

The first barrier to tumorigenesis is the immune surveillance. CSCs represent a heterogeneous subpopulation able to modulate the host immune response and ultimately escape the attacks mediated by the immune cells. The experts define this phenomenon as cancer immunoediting, a process that includes three different phases: the elimination, the equilibrium, and the escape. The elimination phase consists in the ability of innate and adaptive immune cells to recognize and destroy CSCs (71). In the equilibrium phase, the tumor is not eliminated but contained. In this phase, the immune system eliminates the immunogenic cancer cell clones. In the escape phase, the quiescent state and the low immunogenicity, typical of CSCs, allow them to remain in their niches without being recognized from host immune system. In particular, CSCs can escape immune destruction by reducing their expression of major histocompatibility complex I (MHC I) and by completely eliminating the expression of MHC II and co-stimulatory molecules.

The CSCs can also minimize the host immune response recruiting immunosuppressive cells by secretion of growth factors and interleukins, such as transforming growth factor beta (TGF- β), interleukin (IL)-6, IL-10, and prostaglandin E₂ (PGE₂) (72). Immune cells with pro- and antitumorigenic roles have been detected in thyroid TME (73). Of note, specific classes of immune cells can be related to TC patient outcome.

Unlike the infiltration of natural killer (NK) cells, presence of T regulatory lymphocytes in PTC is positively associated with advanced disease (74). Currently, in TC TME, the role of tumor-associated macrophages (TAMs), tumor-associated neutrophils (TANs), and tumor-associated mast cells (TAMCs) has been extensively described, while few studies have been reported regarding the presence of NKT cells, $\gamma\delta$ T cells, Th9, and Th17 in different TCs (75–77).

In the following paragraphs, we will review in details the bidirectional cross-talk between the TCSCs and immune cells (Figure 3).

Immune Cells and Their Protumorigenic Role

The innate and adaptive immune cells are in charge of the defense against foreign agents. Among the immune cells, NK cells are the first to recognize and kill CSCs, with the resulting apoptotic cell fragments being eliminated by macrophages. Tumor neoantigens are processed and presented to the T cells by dendritic cells (DCs). The release of cytokines by DCs and other immune cells induce the activation of T and B cells promoting an inflammatory environment that further stimulates the innate immunity and supports the expansion of T cells and the production of antibodies toward antigens expressed on CSCs. In TME, immune cells exhibit not only an antitumorigenic role, but they can also induce a protumorigenic and anti-inflammatory condition contributing to CSC subpopulation survival (71). In TC TME, TAMs can exert different functions by dynamically interchanging between M1 (proinflammatory) and M2 (anti-inflammatory) phenotypes (78). TAMs polarize into M1 phenotype in presence of interferon gamma (IFN γ) and lipopolysaccharide (LPS), while acquiring an M2 phenotype for IL-4 and IL-13 action. Typically, TAMs with M2 phenotype play an important role in promoting tumor angiogenesis and progression (79) and are correlated with poor prognosis in several tumors, including TCs (80). In the different subtypes of TCs, the frequency of TAMs is variable and has been correlated with various prognoses. In ATCs, TAMs represent 50% of all immune cells and correlate with poor prognosis (81). In PTCs, the presence of TAMs is associated with large size tumors, presence of lymph node metastasis, and decreased survival (80, 82, 83). In poorly differentiated TCs, TAMs are correlated with negative outcomes as capsular invasion and extrathyroid tumor extension (80). The interaction between TAMs and TCSCs can be directly and indirectly mediated by the release of many cytokines and chemokines. It has been demonstrated that TAM-secreted CXCL8 and CXCL16 can promote the metastatic process in PTCs. Blocking CXCL8 and CXCL16 signaling reduced the invasiveness of PTC cells (83, 84), suggesting their targeting as a possible therapeutic strategy in PTCs. In PTCs, TGF- β produced by TAMs is overexpressed and correlates with the presence of CD68⁺ TAM infiltration and with tumor invasion (85). In BRAF-induced PTC mouse model, Ryder et al. observed an increased expression of two TAM chemoattractants: colony stimulating factor-1 (Csf-1) and CCL-2. The increase in Csf-1 is correlated with a high number of infiltrating TAMs expressing Csf-1r and CCR2 and with PTC

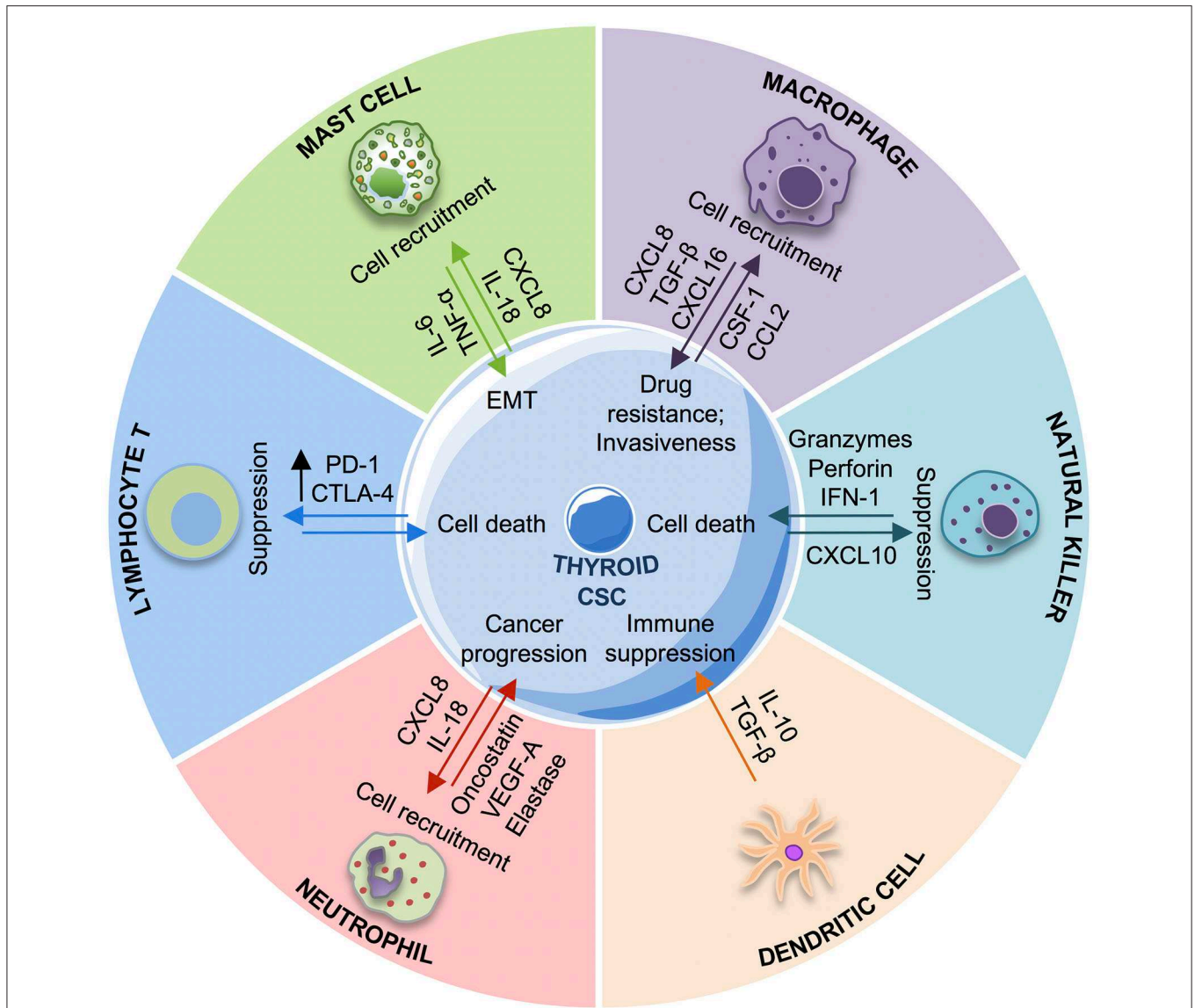


FIGURE 3 | Cross-talk between immune system and thyroid cancer stem cells (TCSCs). The schematic picture describes the interactions between TCSCs and different innate and adaptive immune cells. TCSCs escape from immune response by different mechanisms: recruiting macrophages M2, mast cells, neutrophils with protumorigenic roles promoting the immunosuppressive response through the release of interleukin (IL)-10 by MDSCs and iDCs, suppressing the NK cells cytotoxic activity, EMT, epithelial-to-mesenchymal transition; iDC, immature dendritic cells; IL-6, interleukin-6; IL-10, interleukin-10; CXCL-8, C-X-C motif chemokine ligand-8; CXCL16, C-X-C motif chemokine ligand 16; TGF- β , tumor growth factor- β ; VEGF-A, vascular endothelial growth factor A; TNF- α , tumor necrosis factor- α ; PGE2, prostaglandin-E2; CXCR3, CXC chemokine receptor; CCL-2, C-C motif chemokine ligand-2; csf-1, colony stimulating factor-1; NK cells, natural killer cells.

progression (86). A high number myeloid derived suppressor cells (MDSCs), considered as precursors of monocytes and neutrophils, has been reported in cancer patients as index of poor prognosis. In differentiated TCs, the presence of MDSCs has been correlated with tumor aggressiveness (87). MDSCs can be identified as M-MDSCs or PMN-MDSCs, with a phenotype similar to monocytes or neutrophils, respectively. Both cell types are activated in the TC microenvironment by CCL2, CCL5, and CSF-1 and act as inhibitors of the antitumor response by releasing IL-10 (88). Many studies have suggested that chemotherapy

or other treatments such as tyrosine kinase and nitric oxide inhibitors improve TC patient prognosis by inducing MDSC differentiation or by inhibiting their function (89). Unlike other immune cells, DCs are not usually present in TCs, except for PTCs bearing *BRAF*^{V600E} mutation. In PTCs, DCs are immature cells (CD1a⁺ and S100⁺) able to secrete cytokines as IL-10 and TGF- β , thereby promoting immune suppressive response (90). Similarly to DCs, Tregs are also elevated in PTCs and contribute to immune suppressive TME, favoring tumor cell survival. The mechanisms underlying this function have not been completely

clarified; nonetheless, it has been hypothesized that Tregs induce an anergy state in T effector cells, which become unable to recognize and attack the CSCs (74).

Mast cells are the first immune cells recruited during the inflammatory process, and they can also exert a protumorigenic role (91). The presence of mast cells has been associated with extrathyroidal tumor extension in 95% of PTCs and with invasiveness in poorly differentiated TCs and ATCs (77). Tumor-associated mast cells are more abundant in thyroid follicles of patients affected by PTCs compared with patients with thyroid adenoma (92). By releasing IL-6, TNF- α , and CXCL8/IL-8, mast cells can promote the EMT process in thyroid cells derived from all TC subtypes (FTC, ATC, and PTC). To date, the role of neutrophils in cancer is controversial. An elevated number of neutrophils in cancer patients have been correlated with better clinical outcomes (93–95) or with tumor progression (96, 97). TCSCs recruit the neutrophils by releasing CXCL-8/IL8 and upregulate their proinflammatory roles, thus promoting tumor progression. Galdiero et al. in TCs showed a correlation between the density of neutrophils and the tumor size, suggesting that these immune cells are involved in the tumorigenesis process. It has been demonstrated that TANS favor the tumor proliferation and invasion by the secretion of cytokines as oncostatin M and vascular endothelial growth factor A (VEGF-A) and by elastase action (98). In TC patients, it has been observed that a higher neutrophil/lymphocyte ratio correspond to a larger tumor size and high risk of recurrence (76). NK cells are responsible for the earliest stages of immune defense against microbe infections or the expansion of stressed or transformed cells. NK cells possess a cytotoxic activity, and their activation depend on two factors: they recognize the stimulatory receptors in the target cells and simultaneously their inhibitor receptors fail to link MHC I molecules on foreign cells. It is possible to distinguish two populations of NK cells, with different localization and functions: the CD56^{bright}/CD16^{dim} cells, which predominate in the circulation and the CD56^{dim}/CD16^{bright} cells, which are more cytotoxic and present in the majority of tissues (99). In the tumor, the NK cells CD56^{bright} have a key role to eliminate the nascent tumor cells, identified as stressed and abnormal cells, with a low expression or lack of expression of MHC I class. In TCs, the role of NK cells needs further investigations. In PTC patients, the presence of NK cells is negatively correlated with disease stage (100). In fact, some studies have demonstrated that ATC cell lines are susceptible to NK-mediated immunotherapy (101, 102). However, tumor immunosuppression by NK targeting may also represent an obstacle to the activation of their cytotoxic function (103, 104).

TCSCs and Evasion Mechanisms

CSCs can attenuate the immune surveillance contributing to the tumor development. CSC interaction with immune cells consists in the secretion of immunosuppressive factors or the recruitment of immunosuppressive cells. In particular, CSCs downregulate some key elements for the antigen processing and presentation, contributing to their immune privileged status, thus leading to the inactivation of T cells (105). CSCs can escape NK cell action by different mechanisms: (i) increased expression

of ligands that bind the inhibitor NK receptors; (ii) recruitment of T regs, which can promote the immune evasive state; (iii) NK and T-cells-mediated IL-22 secretion, which promotes CSC phenotype (72). The activation of a T-cell-mediated immune response needs not only the presence of MHC molecules but also of co-stimulatory molecules as CD80 and CD86. Tumor cells downregulate CD80/CD86 expression while upregulates the expression of PD-L1 (B7-H1), which binds to PD-1 on T cells promoting their anergy state (106). Thus, targeting PD-L1 represents a promising immunotherapy approach in many cancers and in advanced differentiated TCs and ATCs (107).

Immunotherapy and TCSCs

CSCs are resistant to different chemotherapeutic agents and radiotherapy due to high expression levels of drug efflux pumps, efficient DNA repair mechanisms, and the support of TME. Immunotherapy approach has been developed as a novel frontier also in targeting CSCs (108). Cancer immunotherapy consists in the administration of recombinant antibodies toward immune molecules defined as immune checkpoint (PD-1, CTLA-4), along with recombinant cytokines, oncolytic viruses, cancer vaccines, or engineered T cells (109). Given that immune cells play a key role in supporting the initiation and progression of TC, the identification of specific immune targets could improve the efficacy of TC therapy. Different immunotherapy strategies have been implemented for the treatment of TC: (i) failure of TAM recruitment, (ii) TAM polarization in M1 phenotype, (iii) identification of tumor antigens for the development of cancer vaccines, and (iv) inhibition of immune checkpoints (110). TAMs are highly represented in ATC TME, as compared to advanced differentiated TCs. High levels of CCL-2 and CSF-1, two TAMs chemoattractants, have been found in human TC tissues (82). In this context, blocking and targeting CCL-2/CCR-2 and CSF-1/CSF1R inhibits the recruitment of TAM with M2 phenotype and the repolarization of these cells into the anti-tumor M1 phenotype (86, 111). To date, clinical trials are ongoing to test the efficacy of the CSF-1R antibody (LY3022855) and CSF-1R inhibitor (PLX3397) (NCT01346358 and NCT01525601, respectively). TAMs represent the half of TME cells in ATC; in this way, the block of CSF-1 and CCL-2 represent a potential target therapy. TC cells express a specific inhibitory receptor membrane, CD47 that binds SIRP α , a ligand expressed on TAMs. The interaction receptor–ligand leads to inhibition of phagocytosis by TAMs and affects the tumor antigen presentation by DCs by supporting TC progression. The block of SIRP α /CD47 interaction in mouse model leads to tumor growth impairment and regression. Use of a specific antibody represents a way through which this pathological pathway re-educated in TAMs (112). Specifically, *in vitro* study using the anti-CD47 on TC cell lines shows the induction of apoptosis (113). Another potential strategy could identify TC-specific antigens to develop a successful vaccine for T cells and dendritic cells in the context of TME. Some studies suggest that potential TC antigens, as the proto-oncogene c-MET, melanoma antigen encoding genes (MAGE), and mucin-1 antigen (MUC-1), are co-expressed with thyroglobulin and thyroid peroxidase in differentiated TCs (114, 115). A promising study demonstrated that dendritic

cells vaccines targeting the carcinoembryonic antigen (CEA), an antigen highly revealed in MTC, induced a complete regression of metastases in lung and liver (116). Further clinical studies are ongoing to test adoptive cytotoxic T cells that target preferentially expressed antigen in melanoma (PRAME), New York esophageal squamous cell carcinoma 1 (NY-ESO-1), MAGE Family member A4 (MAGEA4), synovial sarcoma translocated gene (SSX), and survivin in patients with advanced tumors, including TCs. Currently, the immune checkpoints (PD-1, CTLA-4) inhibition represents a valid strategy for treatment of different types of cancers. Blocking these pathways strengthens T cells and inhibits T reg suppressor cells. In TC histological subtypes, different levels of PD-L1 expression have been detected (7.6% of FTC, in 6.1% of PTCs, and 22.2% of ATCs) (117). Moreover, PDL-1 has been found expressed in more than the half of 126 cases of primary PTCs, and its expression positively correlates with rich tumor-infiltrating lymphocytes (118). Two antibodies targeting PD-1, the receptor of PD-L1 (Pembrolizumab and Nivolumab), have been FDA-approved for treatment of melanoma, renal carcinoma, and non-small cell lung carcinoma, and recently also for PTC patients. Specifically, clinical trials are ongoing to test the efficacy of Pembrolizumab in association with PLX3397 in TCs to better maximize the clinical results in these tumors (NCT02452424). Although the immunotherapy needs further evaluation in TCSC compartment, it may represent a reliable strategy for TC treatment.

INFLUENCE OF THE TUMOR MICROENVIRONMENT ON TCSCs

TME is composed of different cell types (endothelial cells, fibroblasts, immune cells) and extracellular components (cytokines, chemokines, exosomes, growth factors, hormones, extracellular matrix) that support tumor growth. TME exerts an important role not only during tumor initiation, progression, and metastasis but also in drug resistance. Therapy refractoriness is mediated by a continuous crosstalk between tumor and stromal cells (119, 120). In TCs, an inflammatory TME has been involved in thyroid carcinogenesis. Specifically, the molecular interplay between cytokines and chemokines with a protumorigenic role could explain how the inflammation could favor TC initiation (121). TCSCs survival is crucially modulated by TME cells, through a bidirectional complex network of chemokines/cytokines and the induction of an EMT-like phenotype mediated by tumor-associated fibroblasts (CAFs) and by exosomes release (Figure 4).

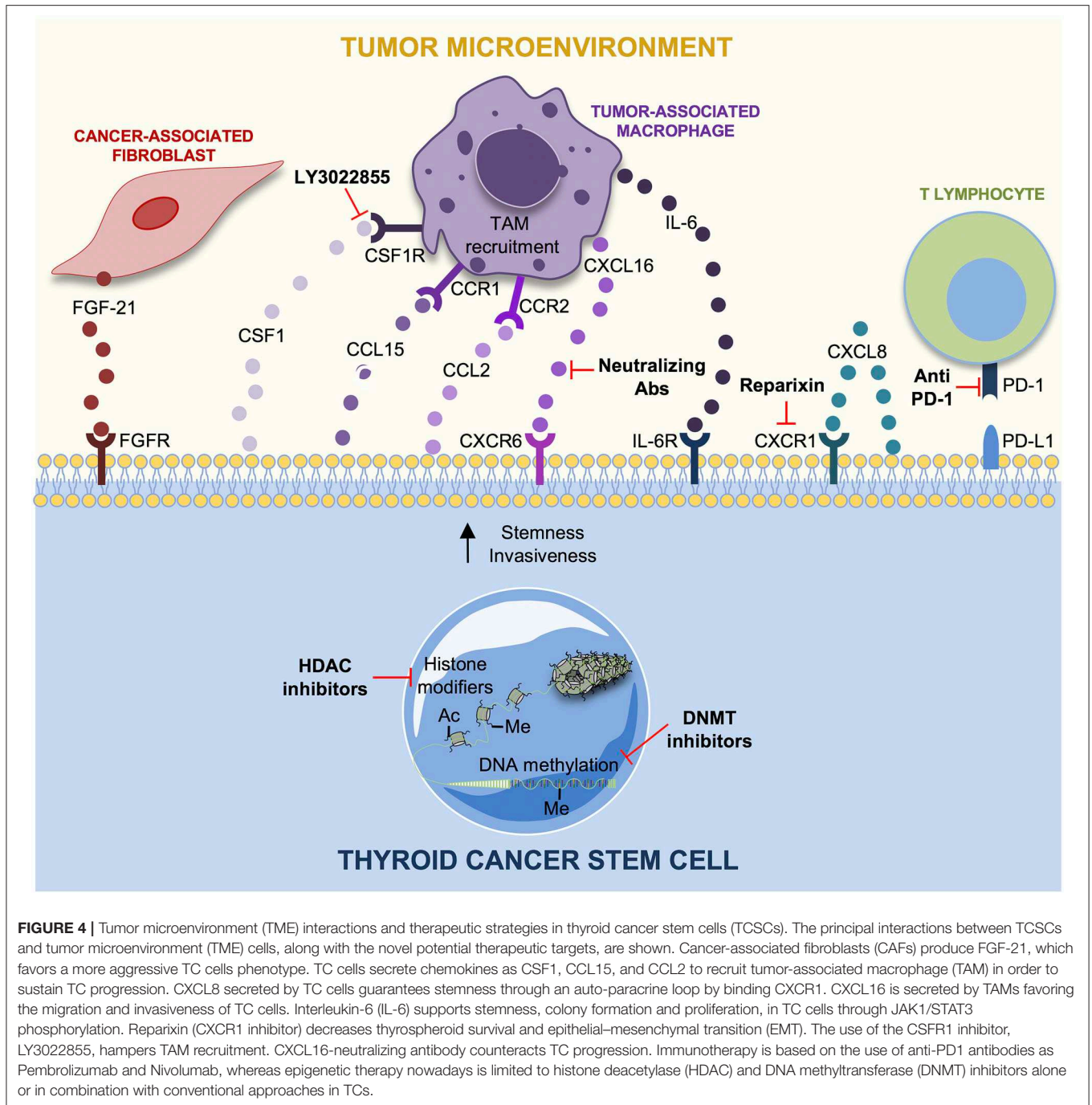
TCSCs and the Interplay With Chemokines/Cytokines

The interplay between TCSCs and stromal cells supports tumor progression by recruiting fibroblasts or macrophages to facilitate metastasis. This crosstalk is mediated by different kinds of chemokines, which are low molecular weight peptides with proangiogenic, cytoproliferative, and prometastatic properties (122). Among the main players of thyroid tumorigenesis, many chemokines and cytokines have been proposed such as CXCL8,

CCL2, CXCL16, CCL15, and IL-6 (123). Of note, FTC cells produce CCL15, which is a chemokine that binds CCR1 receptor expressed by TAMs to facilitate their recruitment and to favor tumor progression and metastasis (124). Studies of co-culture of macrophages and PTC cells showed that CXCL16, abundantly secreted by TAMs, promotes PTC cells migration and invasiveness. It has been demonstrated that TC progression is arrested by using an antihuman CXCL16 neutralizing antibody (84). CCL2, a chemokine secreted by PTC cells, facilitates TAM recruitment in thyroid TME. CCL2 production has been positively correlated with *BRAF*^{V600E} mutations in PTC cells and with TAM infiltration (123). Several studies show how CXCL8, a chemokine secreted by TC cells, plays a protumorigenic activity by enhancing mechanisms such as stemness and EMT in TC cells. In fact, *in vitro* data showed that CXCL8, through an auto-paracrine circuit, binds CXCR1 receptor and induces the tumor sphere formation, typical of CSCs (77). CXCL8's role in carcinogenesis is also confirmed by *in vivo* studies that show as the inoculation of TC cell line, BCPAP, in NOD/SCID mouse model induces metastasis if treated with exogenous recombinant human CXCL8 (83). TAM-derived IL-6 has a pivotal role in tumor initiating, survival, proliferation, and drug resistance in solid tumors (125–128). Similarly, IL-6 drives TC progression even if its molecular mechanism is unknown (129, 130). Zheng et al. studied the effect of IL-6 on ATC-derived CSCs showing that the *in vitro* treatment of HTh74 and HTh74R TC cell lines with exogenous IL-6 leads to increased number of tumor spheres and stemness markers, OCT4 and CD133. IL-6 promotes the colony formation and EMT through the upregulation of vimentin and Snail and the downregulation of E-cadherin in HTh74 and HTh74R TCSCs, contributing to TC progression. In addition, IL-6 increases dramatically TCSCs growth and proliferation through JAK1/STAT3 pathway activation (131).

TCSCs and Tumor-Associated Fibroblasts (CAFs)

Cancer cells establish a complex relationship with the surrounding stromal cells such as cancer-associated fibroblasts (CAFs). During tumor progression, CAFs create a “reactive stroma” by releasing a series of signals inducing phenotypic changes in cancer cells, which reciprocally communicate with CAFs (132). Many studies have shown a positive correlation between specific mutations in TC cells and fibroblast activation. For instance, *BRAF*^{V600E} mutation in TC cells has been involved with a metastatic phenotype by modulating TME and the extracellular matrix (ECM) (133). *BRAF*^{V600E} mutation is associated with upregulation of integrin and fibronectin, which compose the ECM. The upregulation of ECM-associated genes induces the formation of a fibrotic tumor stroma in which an increased number of fibroblasts is recruited to facilitate TC progression (134). Further studies showed that several ATC cell lines are able to reprogram human normal fibroblasts in CAFs to support tumor growth. Treatment of quiescent fibroblasts with conditional medium from ATC cells induces their transformation in CAFs. These findings have been confirmed by the evaluation of fibroblast-specific markers such as platelet-derived growth



factor receptor α (PDGFR- α) and alpha smooth muscle actin (α -SMA). Therefore, the activated CAFs acquire a more intense metabolic and proliferative activity and a secretory phenotype, which improves the invasiveness and aggressiveness of FTC cells (135). Taken together, these findings demonstrated that factors secreted by CAFs, upon activation by ATC cell-derived conditioned media (CM), represent key modulators in TC progression. Fibroblasts are able to secrete fibroblast growth factor 21 (FGF-21) and to release it into blood circulation by

acting at distance on TC cells. High FGF-21 levels increase EMT in PTC through FGFR signaling pathway. Treatment of PTC cell lines with recombinant FGFR1 leads to FGFR pathway signaling activation, leading to ERK and AKT phosphorylation, EMT, and to the development of a more aggressive phenotype of tumor cells. Thus, FGFR1 can promote invasion and migration of PTC cells (136). Parascandolo et al. showed that mesenchymal stem cell (MSC) cultures derived from non-tumorigenic thyroid tissues and from PTCs, exposed to cancer cell-released factors,

are able to differentiate into a multitude of cell types, including CAFs, which eventually support tumor progression. Of note, a subpopulation of PTC cell line, expressing the TCP1 marker, influences the switch from autocrine to paracrine MSC-mediated secretion of superoxide dismutase 3 (SOD3). This leads to MSC activation and differentiation, with the upregulation of fibrotic markers such as FAP, tenascin and Col1 A1, suggesting the presence of CAFs in TC microenvironment. Stromal SOD3 exerts a stimulatory effect on TC cell growth representing a potential target for the treatment of these tumors (137). TIMP family is characterized by a specific structure, with the C-terminal region able to bind specific parts of MMPs in order to form MMP-TIMP complex, which inhibits tumor metastasis and invasion. However, TIMP family components as TIMP-1 and TIMP-2 could play opposite functions as promoting tumor growth, inhibiting apoptosis, and contributing to therapy resistance in different types of cancer, including PTCs (138–140). Consistently, TIMP-1 expression has been detected in fibroblasts of differentiated thyroid carcinoma and thyroid adenoma. Its expression levels are positively correlated to tumor growth, tumor-node-metastasis (TNM) stage, metastasis, and recurrence. In particular, Zhang et al. found that the presurgery peripheral blood levels of TIMP-1 and MMP9 in patients with differentiated TCs are significantly elevated, although TIMP-1 expression levels still remain lower than MMP-9 levels, thus promoting the development of cancer because the balance between the two was broken (141).

TCSCs and Exosomes

Exosomes are a subtype of extracellular vesicles, which originate in the endosomal cell compartment via multivesicular bodies (MVBs). Upon their maturation, exosomes emerge from the extracellular membrane and initiate a cross-talk with bulk tumor cells (142). Cancer cells and cancer-associated cells in TME, as fibroblasts and macrophages, release exosomes through which they transfer specific molecular messages between malignant and non-malignant cells and activate pathways that facilitate tumor initiation and progression (143). Specifically exosomes mediate intercellular communication by the so-called “exosomal cargo,” which includes proteins, miRNAs, and mRNAs (144). In TC, exosomes derived from TCSCs have a central role in supporting metastasis by enhancing EMT through non-coding RNA transfer. Hardin et al. used a subpopulation of the TCP1 TC cell line, expressing adult stemness markers, and isolated exosomes from them. Treatment with exosomes of normal thyroid cell lines NTHY-ori-3 leads to the upregulation of long non-coding RNAs (lncRNAs) (MALAT1 and linc-ROR), whose molecular function is unclear, of the EMT marker SLUG and the stem cell marker SOX2 in normal cells, which acquire and increase their proliferative ability. TCP1-derived exosomes are able to activate EMT program in the same cells contributing to a more aggressive phenotype (145).

TCSCs and EMT

EMT is a clear example of cellular plasticity, through which epithelial cells develop a mesenchymal phenotype that enhances their migratory and invasive features (146). Different studies

underlined the correlation between EMT process and an increased number of TCSCs in TCs (145, 147, 148). Consistently, Yasui et al. by analyzing thyroidectomy specimens, found that ATC regions coexisted with DTC. ATC regions showed absence of E-cadherin and a dramatic upregulation of the stem cell markers CD44, CD133, and of a neuronal marker nestin. Meanwhile, differentiated TCs and non-neoplastic regions showed a decrease in stem markers expression and nestin, but they were positive for E-cadherin (149). Furthermore, Heiden et al. demonstrated that sonic hedgehog pathway promotes the maintenance of a CSCs pool in ATC. They observed that Gli 1-induced Snail upregulation and increase ALDH⁺ CSCs number in ATC cell lines (150). Hardin et al. reported that PTC cell lines acquired stem-cell-like features simultaneously to TGF- β -induced EMT. Interestingly, PTC cells upregulated a novel EMT activator paired-related homeobox protein 1 (Prrx1) (151). Ma et al. confirmed the upregulation of SSEA1 in TSCCs, which were positive also for Nanog, Sox2, and Oct4. They found a correlation between stemness and EMT; indeed, TSCCs showed EMT initiation through the increased expression of vimentin and snail and decreased expression of E-cadherin (152). Mato et al. showed for the first time the correlation between the expression of stem markers ABCG2 and the expression of EMT activator genes. They identified the subpopulation of PTC cells named PTC1, expressing ABCG2. PTC1 cells were characterized by an aggressive phenotype and showed high propensity to migration, invasion, and apoptosis inhibition due to *BIRC5* gene expression. For these reasons, PTC1 could have a pivotal role in PTC progression (153). To overcome the lack of nutrients and oxygen within the tumor mass, tumor cells foster the formation of newly synthesized vessels endowed with irregular structure and properties. Recently, it has been demonstrated that patient-derived xenografts of thyroid spheroids obtained from PTCs show “stem-like” features and promote neoangiogenesis in zebrafish *in vivo* model (154). Interestingly, Cirello et al. proposed an additional experimental model resembling the original thyroid tissue, composed of thyroid stem-like cells and endothelial and hematopoietic cells (155). These 3D models allowed to evaluate the therapeutic response to antiangiogenic compounds and other anticancer drugs and to assess the impact of several proangiogenic factors, as VEGF, FGF, and TSH, in TC progression (155, 156). Moreover, also pericytes can regulate the interaction between tumor and endothelial cells. Specifically, pericytes protect tumor cells by releasing proangiogenic factors. In TCs, it has been demonstrated that pericytes confer resistance to *BRAF*^{V600E} inhibitors and tyrosine-kinase inhibitors (TKI) in *BRAF*^{WT/V600E}-PTCs by secreting trombospondin (TSP-1) and TGF- β (157).

Promising Target Therapy Approach for TME Cells in Thyroid Tumor

New treatment approaches have focused on the development of specific inhibitor compounds and neutralizing antibodies able to block chemokines, CAFs, TCSCs proliferation, and EMT. The aberrant activation of Sonic Hedgehog signaling is a common feature of ATCs, and it represents an important

regulator of cancer cells and CAFs. Cancer cells secrete Shh ligand that encourages the peritumoral stroma, CAFs included, to produce a multitude of factors such as IGF, Wnt, and VEGF, which enhance cancer progression (158). In addition, this pathway is also activated in ATC and PTC cells in the absence of Shh in a Smo-dependent way through the downstream activation of Gli transcription factors caused by the oncogenic RAS/BRAF/MEK. Parascandolo et al. highlighted a specific positive correlation between stromal inhibition and reduction in TC progression. Coculture experiments and stimulation with conditioned medium showed that CAFs support TCP1 TC cells invasion, migration, and non-adherent growth abilities. These effects are both Smo and Shh dependent because they were abolished by the administration of cyclopamine and the 5E1 antibody. Furthermore, an increased Shh secretion has been observed in fibroblasts treated with conditioned medium derived from TC cells highlighting a bidirectional paracrine cross-talk, suggesting that targeting Shh pathway in ATC cells as well as in TME, especially in CAFs, could be exploited as potential target therapy (159). Visciano et al. elegantly studied that CXCL8 is a pivotal mediator of stemness and EMT in TC cells (77). Liotti et al. showed the mechanism through which CXCL8 exerts its autocrine function. The binding of CXCL8 to its receptor, CXCR1, is responsible for the formation of thyrospheres, self-renewal, and tumor-initiating ability. The identification of this autocrine protumorigenic loop could represent a therapeutic approach. Consistently, the treatment with the anti-CXCL8 blocking antibody decreases number and diameter of thyrospheroids, while anti-CXCL1 antibodies did not exert any effect on sphere formation (160). Furthermore, Liotti et al. studied the effect of reparixin, a CXCR1 receptor inhibitor. This treatment dramatically decreases cell survival, proliferation, EMT, and stemness of different TC cell lines (161).

In the last 10 years, different studies have been focused on the development of low molecular weight inhibitor drugs targeting EMT-initiating factors. The combination of BRAF inhibitors, dabrafenib, and MEK1/2 inhibitor, trametinib, have been suggested as a therapy for recurrent TCs (162). Wnt/ β -catenin signaling pathway are involved in the EMT program of TC cells, and its inhibition could represent a potential therapy. Indeed, Hardin et al. found that the silencing of β -catenin reduces EMT markers expression in TC (21). Moreover, Gao and Han reported that the silencing of C-Met/PI3K/AKT pathway reverses EMT and metastasis of TC cells (163). The most promising treatments targeting TME in TCSCs are shown in **Figure 4**.

CONCLUDING REMARKS

The gold standard therapy for all kinds of TCs is surgery associated with radioactive iodine (RAI) therapy. Unfortunately,

a group of “advanced thyroid cancers” including <10% of differentiated TCs, many MTCs, as well as ATCs are not responsive to the standard therapeutic approach and evolve in distant metastatic sites. The 5-years survival rate is <50% in these patients compared with iodine-sensitive well-differentiated TC patients (110). Specific therapeutic targets have been identified for treatment of RAI refractory thyroid tumors. Several genetic alterations in the main molecular pathways, related with TC progression, such as *BRAF* and *RAS* mutations and *RET/PTC* gene rearrangements have been identified and allowed to develop therapeutic strategies for TC patients. To date, FDA has approved the use of different kinase inhibitor drugs, targeting the MAPK pathway (MKIs), such as Levatinib and Sorafenib for advanced RAI-R well-differentiated TCs and Cabozantinib and Vandetanib for MTCs. Due to their systemic toxicity and the ability by tumors to activate alternative proliferation pathways, these drugs partially induce beneficial effects. Moreover, the conventional therapy targets only the proliferating CSCs but no CSCs in a quiescent or slow proliferative state. TCSCs are responsible for TC initiation, progression, relapse, and metastatic dissemination. Given their plasticity, TCSCs are able to remain in a quiescent state within the TME niche. This can explain their persistence after the conventional therapies such as chemo- and radiotherapy. Therefore, a comprehensive knowledge of TCSCs biology may lead to the development of more effective therapeutic strategies. Efficient therapeutic approaches need to be explored to target both TCSCs and their progeny. Immunotherapy and epigenetic drugs in combination with standard therapy could represent promising strategies for TC treatment.

AUTHOR CONTRIBUTIONS

VV, FV, ML, and MT conceptualized and wrote the manuscript. CD'A, GP, AT, MG, SF, DG, and LM contributed to draft the manuscript. All authors contributed to the article and approved the submitted version.

FUNDING

This work was supported by funding from AIRC under IG 2018 (ID: 14415 project - P.I.) to MT.

ACKNOWLEDGMENTS

VV and AT are research fellows funded by PON AIM line1. We thank Francesco Calo' for his graphical contribution. We apologize to our colleagues whose work we have not been able to include due to space constraints.

REFERENCES

- Filetti S, Durante C, Hartl D, Leboulleux S, Locati LD, Newbold K, et al. Thyroid cancer: ESMO Clinical Practice Guidelines for diagnosis, treatment and follow-up. *Ann Oncol.* (2019) 30:1856–83. doi: 10.1093/annonc/mdz400
- Cabanillas ME, McFadden DG, Durante C. Thyroid cancer. *Lancet.* (2016) 388:2783–95. doi: 10.1016/S0140-6736(16)30172-6

3. Pellegriti G, Frasca F, Regalbuto C, Squatrito S, Vigneri R. Worldwide increasing incidence of thyroid cancer: update on epidemiology and risk factors. *J Cancer Epidemiol.* (2013) 2013:965212. doi: 10.1155/2013/965212
4. Rahbari R, Zhang L, Kebebew E. Thyroid cancer gender disparity. *Future Oncol.* (2010) 6:1771–9. doi: 10.2217/fon.10.127
5. Rajoria S, Suriano R, Shanmugam A, Wilson YL, Schantz SP, Geliebter J, et al. Metastatic phenotype is regulated by estrogen in thyroid cells. *Thyroid.* (2010) 20:33–41. doi: 10.1089/thy.2009.0296
6. Faria CC, Peixoto MS, Carvalho DP, Fortunato RS. The emerging role of estrogens in thyroid redox homeostasis and carcinogenesis. *Oxid Med Cell Longev.* (2019) 2019:2514312. doi: 10.1155/2019/2514312
7. Fortunato RS, Braga WM, Ortenzi VH, Rodrigues DC, Andrade BM, Miranda-Alves L, et al. Sexual dimorphism of thyroid reactive oxygen species production due to higher NADPH oxidase 4 expression in female thyroid glands. *Thyroid.* (2013) 23:111–9. doi: 10.1089/thy.2012.0142
8. Clarke MF. Clinical and therapeutic implications of cancer stem cells. *N Engl J Med.* (2019) 380:2237–45. doi: 10.1056/NEJMr1804280
9. Turdo A, Veschi V, Gaggiani M, Chinnici A, Bianca P, Todaro M, et al. Meeting the challenge of targeting cancer stem cells. *Front Cell Dev Biol.* (2019) 7:16. doi: 10.3389/fcell.2019.00016
10. Valent P, Bonnet D, De Maria R, Lapidot T, Copland M, Melo JV, et al. Cancer stem cell definitions and terminology: the devil is in the details. *Nat Rev Cancer.* (2012) 12:767–75. doi: 10.1038/nrc3368
11. Takano T, Amino N. Fetal cell carcinogenesis: a new hypothesis for better understanding of thyroid carcinoma. *Thyroid.* (2005) 15:432–8. doi: 10.1089/thy.2005.15.432
12. Gibelli B, El-Fattah A, Giugliano G, Proh M, Grosso E. Thyroid stem cells—danger or resource? *Acta Otorhinolaryngol Ital.* (2009) 29:290–5.
13. Quiros RM, Ding HG, Gattuso P, Prinz RA, Xu X. Evidence that one subset of anaplastic thyroid carcinomas are derived from papillary carcinomas due to BRAF and p53 mutations. *Cancer.* (2005) 103:2261–8. doi: 10.1002/cncr.21073
14. Nikiforova MN, Ciampi R, Salvatore G, Santoro M, Gandhi M, Knauf JA, et al. Low prevalence of BRAF mutations in radiation-induced thyroid tumors in contrast to sporadic papillary carcinomas. *Cancer Lett.* (2004) 209:1–6. doi: 10.1016/j.canlet.2003.12.004
15. Hoshi N, Kusakabe T, Taylor BJ, Kimura S. Side population cells in the mouse thyroid exhibit stem/progenitor cell-like characteristics. *Endocrinology.* (2007) 148:4251–8. doi: 10.1210/en.2006-0490
16. Hardin H, Montemayor-Garcia C, Lloyd RV. Thyroid cancer stem-like cells and epithelial-mesenchymal transition in thyroid cancers. *Hum Pathol.* (2013) 44:1707–13. doi: 10.1016/j.humpath.2013.01.009
17. Yasui K, Shimamura M, Mitsutake N, Nagayama Y. SNAIL induces epithelial-to-mesenchymal transition and cancer stem cell-like properties in aldehyde dehydrogenase-negative thyroid cancer cells. *Thyroid.* (2013) 23:989–96. doi: 10.1089/thy.2012.0319
18. Takano T. Fetal cell carcinogenesis of the thyroid: a modified theory based on recent evidence. *Endocr J.* (2014) 61:311–20. doi: 10.1507/endocrj.EJ13-0517
19. Takano T. Fetal cell carcinogenesis of the thyroid: theory and practice. *Semin Cancer Biol.* (2007) 17:233–40. doi: 10.1016/j.semcancer.2006.02.001
20. Todaro M, Iovino F, Eterno V, Cammareri P, Gambaro G, Espina V, et al. Tumorigenic and metastatic activity of human thyroid cancer stem cells. *Cancer Res.* (2010) 70:8874–85. doi: 10.1158/0008-5472.CAN-10-1994
21. Hardin H, Zhang R, Helein H, Buehler D, Guo Z, Lloyd RV. The evolving concept of cancer stem-like cells in thyroid cancer and other solid tumors. *Lab Invest.* (2017) 97:1142–51. doi: 10.1038/labinvest.2017.41
22. Iliopoulos D, Hirsch HA, Wang G, Struhl K. Inducible formation of breast cancer stem cells and their dynamic equilibrium with non-stem cancer cells via IL6 secretion. *Proc Natl Acad Sci USA.* (2011) 108:1397–402. doi: 10.1073/pnas.1018898108
23. Vermeulen L, de Sousa e Melo F, Richel DJ, Medema JP. The developing cancer stem-cell model: clinical challenges and opportunities. *Lancet Oncol.* (2012) 13:e83–9. doi: 10.1016/S1470-2045(11)70257-1
24. Hoek KS, Goding CR. Cancer stem cells versus phenotype-switching in melanoma. *Pigment Cell Melanoma Res.* (2010) 23:746–59. doi: 10.1111/j.1755-148X.2010.00757.x
25. Zane M, Scavo E, Catalano V, Bonanno M, Todaro M, De Maria R, et al. Normal vs cancer thyroid stem cells: the road to transformation. *Oncogene.* (2016) 35:805–15. doi: 10.1038/onc.2015.138
26. Zito G, Richiusa P, Bommarito A, Carissimi E, Russo L, Coppola A, et al. *In vitro* identification and characterization of CD133(pos) cancer stem-like cells in anaplastic thyroid carcinoma cell lines. *PLoS ONE.* (2008) 3:e3544. doi: 10.1371/journal.pone.0003544
27. Giani F, Vella V, Nicolosi ML, Fierabracci A, Lotta S, Malaguarnera R, et al. Thyrospheres from normal or malignant thyroid tissue have different biological, functional, and genetic features. *J Clin Endocrinol Metab.* (2015) 100:E1168–78. doi: 10.1210/jc.2014-4163
28. Malaguarnera R, Frasca F, Garozzo A, Giani F, Pandini G, Vella V, et al. Insulin receptor isoforms and insulin-like growth factor receptor in human follicular cell precursors from papillary thyroid cancer and normal thyroid. *J Clin Endocrinol Metab.* (2011) 96:766–74. doi: 10.1210/jc.2010-1255
29. Friedman S, Lu M, Schultz A, Thomas D, Lin RY. CD133+ anaplastic thyroid cancer cells initiate tumors in immunodeficient mice and are regulated by thyrotropin. *PLoS ONE.* (2009) 4:e5395. doi: 10.1371/journal.pone.0005395
30. Li W, Reeb AN, Sewell WA, Elhomsy G, Lin RY. Phenotypic characterization of metastatic anaplastic thyroid cancer stem cells. *PLoS ONE.* (2013) 8:e65095. doi: 10.1371/journal.pone.0065095
31. Ahn SH, Henderson YC, Williams MD, Lai SY, Clayman GL. Detection of thyroid cancer stem cells in papillary thyroid carcinoma. *J Clin Endocrinol Metab.* (2014) 99:536–44. doi: 10.1210/jc.2013-2558
32. Shimamura M, Nagayama Y, Matsuse M, Yamashita S, Mitsutake N. Analysis of multiple markers for cancer stem-like cells in human thyroid carcinoma cell lines. *Endocr J.* (2014) 61:481–90. doi: 10.1507/endocrj.EJ13-0526
33. Murugan AK, Xing M. Anaplastic thyroid cancers harbor novel oncogenic mutations of the ALK gene. *Cancer Res.* (2011) 71:4403–11. doi: 10.1158/0008-5472.CAN-10-4041
34. Bommarito A, Richiusa P, Carissimi E, Pizzolanti G, Rodolico V, Zito G, et al. BRAFV600E mutation, TIMP-1 upregulation, and NF-kappaB activation: closing the loop on the papillary thyroid cancer trilogy. *Endocr Relat Cancer.* (2011) 18:669–85. doi: 10.1530/ERC-11-0076
35. Ilie MI, Lassalle S, Long-Mira E, Hofman V, Zangari J, Benaïm G, et al. In papillary thyroid carcinoma, TIMP-1 expression correlates with BRAF (V600E) mutation status and together with hypoxia-related proteins predicts aggressive behavior. *Virchows Arch.* (2013) 463:437–44. doi: 10.1007/s00428-013-1453-x
36. Vasko V, Saji M, Hardy E, Kruhlik M, Larin A, Savchenko V, et al. Akt activation and localisation correlate with tumour invasion and oncogene expression in thyroid cancer. *J Med Genet.* (2004) 41:161–70. doi: 10.1136/jmg.2003.015339
37. Ricarte-Filho JC, Ryder M, Chitale DA, Rivera M, Heguy A, Ladanyi M, et al. Mutational profile of advanced primary and metastatic radioactive iodine-refractory thyroid cancers reveals distinct pathogenetic roles for BRAF, PIK3CA, and AKT1. *Cancer Res.* (2009) 69:4885–93. doi: 10.1158/0008-5472.CAN-09-0727
38. Li X, Abdel-Mageed AB, Mondal D, Kandil E. The nuclear factor kappa-B signaling pathway as a therapeutic target against thyroid cancers. *Thyroid.* (2013) 23:209–18. doi: 10.1089/thy.2012.0237
39. Castellone MD, De Falco V, Rao DM, Bellelli R, Muthu M, Basolo F, et al. The beta-catenin axis integrates multiple signals downstream from RET/papillary thyroid carcinoma leading to cell proliferation. *Cancer Res.* (2009) 69:1867–76. doi: 10.1158/0008-5472.CAN-08-1982
40. Dawson MA. The cancer epigenome: concepts, challenges, and therapeutic opportunities. *Science.* (2017) 355:1147–52. doi: 10.1126/science.aam7304
41. Rodriguez-Rodero S, Fernandez AF, Fernandez-Morera JL, Castro-Santos P, Bayon GF, Ferrero C, et al. DNA methylation signatures identify biologically distinct thyroid cancer subtypes. *J Clin Endocrinol Metab.* (2013) 98:2811–21. doi: 10.1210/jc.2012-3566
42. Mancikova V, Buj R, Castelblanco E, Inglada-Perez L, Diez A, de Cubas AA, et al. DNA methylation profiling of well-differentiated thyroid cancer uncovers markers of recurrence free survival. *Int J Cancer.* (2014) 135:598–610. doi: 10.1002/ijc.28703
43. Ellis RJ, Wang Y, Stevenson HS, Boufraqech M, Patel D, Nilubol N, et al. Genome-wide methylation patterns in papillary thyroid cancer are distinct based on histological subtype and tumor genotype. *J Clin Endocrinol Metab.* (2014) 99:E329–37. doi: 10.1210/jc.2013-2749

44. Hu S, Liu D, Tufano RP, Carson KA, Rosenbaum E, Cohen Y, et al. Association of aberrant methylation of tumor suppressor genes with tumor aggressiveness and BRAF mutation in papillary thyroid cancer. *Int J Cancer*. (2006) 119:2322–9. doi: 10.1002/ijc.22110
45. Alvarez-Nunez F, Bussaglia E, Mauricio D, Ybarra J, Vilar M, Lerma E, et al. PTEN promoter methylation in sporadic thyroid carcinomas. *Thyroid*. (2006) 16:17–23. doi: 10.1089/thy.2006.16.17
46. Brown TC, Juhlin CC, Healy JM, Prasad ML, Korah R, Carling T. Frequent silencing of RASSF1A via promoter methylation in follicular thyroid hyperplasia: a potential early epigenetic susceptibility event in thyroid carcinogenesis. *JAMA Surg*. (2014) 149:1146–52. doi: 10.1001/jamasurg.2014.1694
47. Liu D, Yang C, Bojdani E, Murugan AK, Xing M. Identification of RASAL1 as a major tumor suppressor gene in thyroid cancer. *J Natl Cancer Inst*. (2013) 105:1617–27. doi: 10.1093/jnci/djt249
48. Soares P, Bex G, van Roy F, Sobrinho-Simoes M. E-cadherin gene alterations are rare events in thyroid tumors. *Int J Cancer*. (1997) 70:32–8. doi: 10.1002/(SICI)1097-0215(19970106)70:1<32::AID-IJC5>3.0.CO;2-7
49. Rocha AS, Soares P, Seruca R, Maximo V, Matias-Guiu X, Cameselle-Teijeiro J, et al. Abnormalities of the E-cadherin/catenin adhesion complex in classical papillary thyroid carcinoma and in its diffuse sclerosing variant. *J Pathol*. (2001) 194:358–66. doi: 10.1002/path.905
50. Vu-Phan D, Koenig RJ. Genetics and epigenetics of sporadic thyroid cancer. *Mol Cell Endocrinol*. (2014) 386:55–66. doi: 10.1016/j.mce.2013.07.030
51. de Moraes RM, Sobrinho AB, de Souza Silva CM, de Oliveira JR, da Silva ICR, de Toledo Nobrega O. The role of the NIS (SLC5A5) gene in papillary thyroid cancer: a systematic review. *Int J Endocrinol*. (2018) 2018:9128754. doi: 10.1155/2018/9128754
52. Blake A, Dragan M, Tirona RG, Hardy DB, Brackstone M, Tuck AB, et al. G protein-coupled KISS1 receptor is overexpressed in triple negative breast cancer and promotes drug resistance. *Sci Rep*. (2017) 7:46525. doi: 10.1038/srep46525
53. Matthaiou S, Kostakis ID, Kykalos S, Machairas N, Spartalis E, Ntikoudi E, et al. KISS1 and KISS1R expression in primary and metastatic colorectal cancer. *J Buon*. (2018) 23:598–603.
54. Guzman S, Brackstone M, Wondisford F, Babwah AV, Bhattacharya M. KISS1/KISS1R and breast cancer: metastasis promoter. *Semin Reprod Med*. (2019) 37:197–206. doi: 10.1055/s-0039-3400968
55. Savvidis C, Papaiconomou E, Petraki C, Msaouel P, Koutsilieris M. The role of KISS1/KISS1R system in tumor growth and invasion of differentiated thyroid cancer. *Anticancer Res*. (2015) 35:819–26.
56. Puppin C, Passon N, Lavarone E, Di Loreto C, Frasca F, Vella V, et al. Levels of histone acetylation in thyroid tumors. *Biochem Biophys Res Commun*. (2011) 411:679–83. doi: 10.1016/j.bbrc.2011.06.182
57. Gao X, Wu X, Zhang X, Hua W, Zhang Y, Maimaiti Y, et al. Inhibition of BRD4 suppresses tumor growth and enhances iodine uptake in thyroid cancer. *Biochem Biophys Res Commun*. (2016) 469:679–85. doi: 10.1016/j.bbrc.2015.12.008
58. Xu K, Chen D, Qian D, Zhang S, Zhang Y, Guo S, et al. AZD5153, a novel BRD4 inhibitor, suppresses human thyroid carcinoma cell growth *in vitro* and *in vivo*. *Biochem Biophys Res Commun*. (2018) 499:531–7. doi: 10.1016/j.bbrc.2018.03.184
59. Zhang W, Sun W, Qin Y, Wu C, He L, Zhang T, et al. Knockdown of KDM1A suppresses tumour migration and invasion by epigenetically regulating the TIMP1/MMP9 pathway in papillary thyroid cancer. *J Cell Mol Med*. (2019) 23:4933–44. doi: 10.1111/jcmm.14311
60. Borbone E, Troncione G, Ferraro A, Jasencakova Z, Stojic L, Esposito F, et al. Enhancer of zeste homolog 2 overexpression has a role in the development of anaplastic thyroid carcinomas. *J Clin Endocrinol Metab*. (2011) 96:1029–38. doi: 10.1210/jc.2010-1784
61. Asa SL, Ezzat S. The epigenetic landscape of differentiated thyroid cancer. *Mol Cell Endocrinol*. (2018) 469:3–10. doi: 10.1016/j.mce.2017.07.012
62. Sasanakietkul T, Murtha TD, Javid M, Korah R, Carling T. Epigenetic modifications in poorly differentiated and anaplastic thyroid cancer. *Mol Cell Endocrinol*. (2018) 469:23–37. doi: 10.1016/j.mce.2017.05.022
63. Zarkesh M, Zadeh-Vakili A, Azizi F, Foroughi F, Akhavan MM, Hedayati M. Altered epigenetic mechanisms in thyroid cancer subtypes. *Mol Diagn Ther*. (2018) 22:41–56. doi: 10.1007/s40291-017-0303-y
64. Rodriguez-Rodero S, Delgado-Alvarez E, Diaz-Naya L, Martin Nieto A, Menendez Torre E. Epigenetic modulators of thyroid cancer. *Endocrinol Diabetes Nutr*. (2017) 64:44–56. doi: 10.1016/j.endinu.2016.09.006
65. Zafon C, Gil J, Perez-Gonzalez B, Jorda M. DNA methylation in thyroid cancer. *Endocr Relat Cancer*. (2019) 26:R415–R39. doi: 10.1530/ERC-19-0093
66. Vitale G, Dicitore A, Pepe D, Gentilini D, Grassi ES, Borghi MO, et al. Synergistic activity of everolimus and 5-aza-2'-deoxycytidine in medullary thyroid carcinoma cell lines. *Mol Oncol*. (2017) 11:1007–22. doi: 10.1002/1878-0261.12070
67. Russo D, Damante G, Puxeddu E, Durante C, Filetti S. Epigenetics of thyroid cancer and novel therapeutic targets. *J Mol Endocrinol*. (2011) 46:R73–81. doi: 10.1530/JME-10-0150
68. Russo D, Durante C, Bulotta S, Puppin C, Puxeddu E, Filetti S, et al. Targeting histone deacetylase in thyroid cancer. *Expert Opin Ther Targets*. (2013) 17:179–93. doi: 10.1517/14728222.2013.740013
69. Roberti A, Valdes AF, Torrecillas R, Fraga MF, Fernandez AF. Epigenetics in cancer therapy and nanomedicine. *Clin Epigenetics*. (2019) 11:81. doi: 10.1186/s13148-019-0675-4
70. Mitmaker EJ, Griff NJ, Grogan RH, Sarkar R, Kebebew E, Duh QY, et al. Modulation of matrix metalloproteinase activity in human thyroid cancer cell lines using demethylating agents and histone deacetylase inhibitors. *Surgery*. (2011) 149:504–11. doi: 10.1016/j.surg.2010.10.007
71. Vesely MD, Kershaw MH, Schreiber RD, Smyth MJ. Natural innate and adaptive immunity to cancer. *Annu Rev Immunol*. (2011) 29:235–71. doi: 10.1146/annurev-immunol-031210-101324
72. Vahidian F, Duijf PHG, Safarzadeh E, Derakhshani A, Baghbanzadeh A, Baradaran B. Interactions between cancer stem cells, immune system and some environmental components: friends or foes? *Immunol Lett*. (2019) 208:19–29. doi: 10.1016/j.imlet.2019.03.004
73. Varricchi G, Loffredo S, Marone G, Modestino L, Fallahi P, Ferrari SM, et al. The immune landscape of thyroid cancer in the context of immune checkpoint inhibition. *Int J Mol Sci*. (2019) 20:3934. doi: 10.3390/ijms20163934
74. Gogali F, Paterakis G, Rassidakis GZ, Kaltsas G, Liakou CI, Gousis P, et al. Phenotypical analysis of lymphocytes with suppressive and regulatory properties (Tregs) and NK cells in the papillary carcinoma of thyroid. *J Clin Endocrinol Metab*. (2012) 97:1474–82. doi: 10.1210/jc.2011-1838
75. Cho JW, Kim WW, Lee YM, Jeon MJ, Kim WG, Song DE, et al. Impact of tumor-associated macrophages and BRAF(V600E) mutation on clinical outcomes in patients with various thyroid cancers. *Head Neck*. (2019) 41:686–91. doi: 10.1002/hed.25469
76. Liu CL, Lee JJ, Liu TP, Chang YC, Hsu YC, Cheng SP. Blood neutrophil-to-lymphocyte ratio correlates with tumor size in patients with differentiated thyroid cancer. *J Surg Oncol*. (2013) 107:493–7. doi: 10.1002/jso.23270
77. Visciano C, Liotti F, Prevete N, Cali G, Franco R, Collina F, et al. Mast cells induce epithelial-to-mesenchymal transition and stem cell features in human thyroid cancer cells through an IL-8-Akt-Slug pathway. *Oncogene*. (2015) 34:5175–86. doi: 10.1038/nc.2014.441
78. Piccolo V, Curina A, Genua M, Ghisletti S, Simonatto M, Sabo A, et al. Opposing macrophage polarization programs show extensive epigenomic and transcriptional cross-talk. *Nat Immunol*. (2017) 18:530–40. doi: 10.1038/ni.3710
79. Yuan A, Hsiao YJ, Chen HY, Chen HW, Ho CC, Chen YY, et al. Opposite effects of M1 and M2 macrophage subtypes on lung cancer progression. *Sci Rep*. (2015) 5:14273. doi: 10.1038/srep14273
80. Ryder M, Ghossein RA, Ricarte-Filho JC, Knauf JA, Fagin JA. Increased density of tumor-associated macrophages is associated with decreased survival in advanced thyroid cancer. *Endocr Relat Cancer*. (2008) 15:1069–74. doi: 10.1677/ERC-08-0036
81. Jung KY, Cho SW, Kim YA, Kim D, Oh BC, Park DJ, et al. Cancers with higher density of tumor-associated macrophages were associated with poor survival rates. *J Pathol Transl Med*. (2015) 49:318–24. doi: 10.4132/jptm.2015.06.01
82. Kim S, Cho SW, Min HS, Kim KM, Yeom GJ, Kim EY, et al. The expression of tumor-associated macrophages in papillary thyroid carcinoma.

- Endocrinol Metab (Seoul)*. (2013) 28:192–8. doi: 10.3803/EnM.2013.28.3.192
83. Fang W, Ye L, Shen L, Cai J, Huang F, Wei Q, et al. Tumor-associated macrophages promote the metastatic potential of thyroid papillary cancer by releasing CXCL8. *Carcinogenesis*. (2014) 35:1780–7. doi: 10.1093/carcin/bgu060
 84. Cho SW, Kim YA, Sun HJ, Kim YA, Oh BC, Yi KH, et al. CXCL16 signaling mediated macrophage effects on tumor invasion of papillary thyroid carcinoma. *Endocr Relat Cancer*. (2016) 23:113–24. doi: 10.1530/ERC-15-0196
 85. Knauf JA, Sartor MA, Medvedovic M, Lundsmith E, Ryder M, Salzano M, et al. Progression of BRAF-induced thyroid cancer is associated with epithelial-mesenchymal transition requiring concomitant MAP kinase and TGFbeta signaling. *Oncogene*. (2011) 30:3153–62. doi: 10.1038/onc.2011.44
 86. Ryder M, Gild M, Hohl TM, Pamer E, Knauf J, Ghossein R, et al. Genetic and pharmacological targeting of CSF-1/CSF-1R inhibits tumor-associated macrophages and impairs BRAF-induced thyroid cancer progression. *PLoS ONE*. (2013) 8:e54302. doi: 10.1371/journal.pone.0054302
 87. Angell TE, Lechner MG, Smith AM, Martin SE, Groshen SG, Maceri DR, et al. Circulating myeloid-derived suppressor cells predict differentiated thyroid cancer diagnosis and extent. *Thyroid*. (2016) 26:381–9. doi: 10.1089/thy.2015.0289
 88. Suzuki S, Shibata M, Gonda K, Kanke Y, Ashizawa M, Ujiie D, et al. Immunosuppression involving increased myeloid-derived suppressor cell levels, systemic inflammation and hypoalbuminemia are present in patients with anaplastic thyroid cancer. *Mol Clin Oncol*. (2013) 1:959–64. doi: 10.3892/mco.2013.170
 89. Najjar YG, Finke JH. Clinical perspectives on targeting of myeloid derived suppressor cells in the treatment of cancer. *Front Oncol*. (2013) 3:49. doi: 10.3389/fonc.2013.00049
 90. Scouten WT, Francis GL. Thyroid cancer and the immune system: a model for effective immune surveillance. *Expert Rev Endocrinol Metab*. (2006) 1:353–66. doi: 10.1586/17446651.1.3.353
 91. Proietti A, Ugolini C, Melillo RM, Crisman G, Elisei R, Santoro M, et al. Higher intratumoral expression of CD1a, tryptase, and CD68 in a follicular variant of papillary thyroid carcinoma compared to adenomas: correlation with clinical and pathological parameters. *Thyroid*. (2011) 21:1209–15. doi: 10.1089/thy.2011.0059
 92. Melillo RM, Guarino V, Avilla E, Galdiero MR, Liotti F, Prevete N, et al. Mast cells have a protumorigenic role in human thyroid cancer. *Oncogene*. (2010) 29:6203–15. doi: 10.1038/onc.2010.348
 93. Galdiero MR, Bianchi P, Grizzi F, Di Caro G, Basso G, Ponzetta A, et al. Occurrence and significance of tumor-associated neutrophils in patients with colorectal cancer. *Int J Cancer*. (2016) 139:446–56. doi: 10.1002/ijc.30076
 94. Donskov F. Immunomonitoring and prognostic relevance of neutrophils in clinical trials. *Semin Cancer Biol*. (2013) 23:200–7. doi: 10.1016/j.semcancer.2013.02.001
 95. Wikberg ML, Ling A, Li X, Oberg A, Edin S, Palmqvist R. Neutrophil infiltration is a favorable prognostic factor in early stages of colon cancer. *Hum Pathol*. (2017) 68:193–202. doi: 10.1016/j.humpath.2017.08.028
 96. Jablonska J, Leschner S, Westphal K, Lienenklaus S, Weiss S. Neutrophils responsive to endogenous IFN-beta regulate tumor angiogenesis and growth in a mouse tumor model. *J Clin Invest*. (2010) 120:1151–64. doi: 10.1172/JCI37223
 97. Houghton AM, Rzymkiewicz DM, Ji H, Gregory AD, Egea EE, Metz HE, et al. Neutrophil elastase-mediated degradation of IRS-1 accelerates lung tumor growth. *Nat Med*. (2010) 16:219–23. doi: 10.1038/nm.2084
 98. Galdiero MR, Varricchi G, Loffredo S, Bellevicine C, Lansione T, Ferrara AL, et al. Potential involvement of neutrophils in human thyroid cancer. *PLoS ONE*. (2018) 13:e0199740. doi: 10.1371/journal.pone.0199740
 99. Voutsadakis IA. Expression and function of immune ligand-receptor pairs in NK cells and cancer stem cells: therapeutic implications. *Cell Oncol (Dordr)*. (2018) 41:107–21. doi: 10.1007/s13402-018-0373-9
 100. Gogali E, Paterakis G, Rassidakis GZ, Liakou CI, Liapi C. CD3(-)CD16(-)CD56(bright) immunoregulatory NK cells are increased in the tumor microenvironment and inversely correlate with advanced stages in patients with papillary thyroid cancer. *Thyroid*. (2013) 23:1561–8. doi: 10.1089/thy.2012.0560
 101. Wennerberg E, Pfefferle A, Ekblad L, Yoshimoto Y, Kremer V, Kaminsky VO, et al. Human anaplastic thyroid carcinoma cells are sensitive to NK cell-mediated lysis via ULBP2/5/6 and chemoattract NK cells. *Clin Cancer Res*. (2014) 20:5733–44. doi: 10.1158/1078-0432.CCR-14-0291
 102. Antonelli A, Ferrari SM, Fallahi P, Piaggi S, Di Domenico Antonio A, Galleri D, et al. Variable modulation by cytokines and thiazolidinediones of the prototype Th1 chemokine CXCL10 in anaplastic thyroid cancer. *Cytokine*. (2012) 59:218–22. doi: 10.1016/j.cyto.2012.04.042
 103. Franco AT, Malaguarnera R, Refetoff S, Liao XH, Lundsmith E, Kimura S, et al. Thyrotrophin receptor signaling dependence of Braf-induced thyroid tumor initiation in mice. *Proc Natl Acad Sci USA*. (2011) 108:1615–20. doi: 10.1073/pnas.1015557108
 104. Parhar RS, Zou M, Al-Mohanna FA, Baitei EY, Assiri AM, Meyer BF, et al. IL-12 immunotherapy of Braf(V600E)-induced papillary thyroid cancer in a mouse model. *Lab Invest*. (2016) 96:89–97. doi: 10.1038/labinvest.2015.126
 105. Sultan M, Coyle KM, Vidovic D, Thomas ML, Gujar S, Marcato P. Hide-and-seek: the interplay between cancer stem cells and the immune system. *Carcinogenesis*. (2017) 38:107–18. doi: 10.1093/carcin/bgw115
 106. Chen L, Han X. Anti-PD-1/PD-L1 therapy of human cancer: past, present, and future. *J Clin Invest*. (2015) 125:3384–91. doi: 10.1172/JCI80011
 107. Bastman JJ, Serracino HS, Zhu Y, Koenig MR, Mateescu V, Sams SB, et al. Tumor-infiltrating T cells and the PD-1 checkpoint pathway in advanced differentiated and anaplastic thyroid cancer. *J Clin Endocrinol Metab*. (2016) 101:2863–73. doi: 10.1210/jc.2015-4227
 108. Pan Q, Li Q, Liu S, Ning N, Zhang X, Xu Y, et al. Concise review: targeting cancer stem cells using immunologic approaches. *Stem Cells*. (2015) 33:2085–92. doi: 10.1002/stem.2039
 109. Riley RS, June CH, Langer R, Mitchell MJ. Delivery technologies for cancer immunotherapy. *Nat Rev Drug Discov*. (2019) 18:175–96. doi: 10.1038/s41573-018-0006-z
 110. Naoum GE, Morkos M, Kim B, Arafat W. Novel targeted therapies and immunotherapy for advanced thyroid cancers. *Mol Cancer*. (2018) 17:51. doi: 10.1186/s12943-018-0786-0
 111. Gulubova MV, Ivanova KV. The expression of tumor-associated macrophages and multinucleated giant cells in papillary thyroid carcinoma. *Open Access Maced J Med Sci*. (2019) 7:3944–9. doi: 10.3889/oamjms.2019.715
 112. Willingham SB, Volkmer JP, Gentles AJ, Sahoo D, Dalerba P, Mitra SS, et al. The CD47-signal regulatory protein alpha (SIRPα) interaction is a therapeutic target for human solid tumors. *Proc Natl Acad Sci USA*. (2012) 109:6662–7. doi: 10.1073/pnas.1121623109
 113. Rath GM, Schneider C, Dedieu S, Rothhut B, Soula-Rothhut M, Ghoneim C, et al. The C-terminal CD47/IAP-binding domain of thrombospondin-1 prevents camptothecin- and doxorubicin-induced apoptosis in human thyroid carcinoma cells. *Biochim Biophys Acta*. (2006) 1763:1125–34. doi: 10.1016/j.bbamcr.2006.08.001
 114. Martins MB, Marcello MA, Batista Fde A, Cunha LL, Morari EC, Soares FA, et al. CD8+ TIL recruitment may revert the association of MAGE A3 with aggressive features in thyroid tumors. *J Immunol Res*. (2014) 2014:921864. doi: 10.1155/2014/921864
 115. Bieche I, Ruffet E, Zweibaum A, Vilde F, Lidereau R, Franc B. MUC1 mucin gene, transcripts, and protein in adenomas and papillary carcinomas of the thyroid. *Thyroid*. (1997) 7:725–31. doi: 10.1089/thy.1997.7.725
 116. Schott M, Seissler J, Lettmann M, Fouxon V, Scherbaum WA, Feldkamp J. Immunotherapy for medullary thyroid carcinoma by dendritic cell vaccination. *J Clin Endocrinol Metab*. (2001) 86:4965–9. doi: 10.1210/jcem.86.10.7949
 117. Ahn S, Kim TH, Kim SW, Ki CS, Jang HW, Kim JS, et al. Comprehensive screening for PD-L1 expression in thyroid cancer. *Endocr Relat Cancer*. (2017) 24:97–106. doi: 10.1530/ERC-16-0421
 118. Bai Y, Niu D, Huang X, Jia L, Kang Q, Dou F, et al. PD-L1 and PD-1 expression are correlated with distinctive clinicopathological features in papillary thyroid carcinoma. *Diagn Pathol*. (2017) 12:72. doi: 10.1186/s13000-017-0662-z
 119. Hanahan D, Coussens LM. Accessories to the crime: functions of cells recruited to the tumor microenvironment. *Cancer Cell*. (2012) 21:309–22. doi: 10.1016/j.ccr.2012.02.022

120. Quail DF, Joyce JA. Microenvironmental regulation of tumor progression and metastasis. *Nat Med.* (2013) 19:1423–37. doi: 10.1038/nm.3394
121. Ferrari SM, Fallahi P, Galdiero MR, Ruffilli I, Elia G, Ragusa F, et al. Immune and inflammatory cells in thyroid cancer microenvironment. *Int J Mol Sci.* (2019) 20:4413. doi: 10.3390/ijms20184413
122. Cunha LL, Marcello MA, Ward LS. The role of the inflammatory microenvironment in thyroid carcinogenesis. *Endocr Relat Cancer.* (2014) 21:R85–R103. doi: 10.1530/ERC-13-0431
123. Rotondi M, Coperchini F, Latrofa F, Chiovato L. Role of chemokines in thyroid cancer microenvironment: is CXCL8 the main player? *Front Endocrinol (Lausanne).* (2018) 9:314. doi: 10.3389/fendo.2018.00314
124. Huang FJ, Zhou XY, Ye L, Fei XC, Wang S, Wang W, et al. Follicular thyroid carcinoma but not adenoma recruits tumor-associated macrophages by releasing CCL15. *BMC Cancer.* (2016) 16:98. doi: 10.1186/s12885-016-2114-7
125. Kong L, Zhou Y, Bu H, Lv T, Shi Y, Yang J. Deletion of interleukin-6 in monocytes/macrophages suppresses the initiation of hepatocellular carcinoma in mice. *J Exp Clin Cancer Res.* (2016) 35:131. doi: 10.1186/s12885-016-0412-1
126. Schneider MR, Hoeflich A, Fischer JR, Wolf E, Sordat B, Lahm H. Interleukin-6 stimulates clonogenic growth of primary and metastatic human colon carcinoma cells. *Cancer Lett.* (2000) 151:31–8. doi: 10.1016/S0304-3835(99)00401-2
127. Wan S, Zhao E, Kryczek I, Vatan L, Sadovskaya A, Ludema G, et al. Tumor-associated macrophages produce interleukin 6 and signal via STAT3 to promote expansion of human hepatocellular carcinoma stem cells. *Gastroenterology.* (2014) 147:1393–404. doi: 10.1053/j.gastro.2014.08.039
128. Yin Y, Yao S, Hu Y, Feng Y, Li M, Bian Z, et al. The immune-microenvironment confers chemoresistance of colorectal cancer through macrophage-derived IL6. *Clin Cancer Res.* (2017) 23:7375–87. doi: 10.1158/1078-0432.CCR-17-1283
129. Murai H, Murakami S, Ishida K, Sugawara M. Elevated serum interleukin-6 and decreased thyroid hormone levels in postoperative patients and effects of IL-6 on thyroid cell function *in vitro*. *Thyroid.* (1996) 6:601–6. doi: 10.1089/thy.1996.6.601
130. Provatopoulou X, Georgiadou D, Sergentanis TN, Kalogera E, Spyridakis J, Gounaris A, et al. Interleukins as markers of inflammation in malignant and benign thyroid disease. *Inflamm Res.* (2014) 63:667–74. doi: 10.1007/s00011-014-0739-z
131. Zheng R, Chen G, Li X, Wei X, Liu C, Derwahl M. Effect of IL-6 on proliferation of human thyroid anaplastic cancer stem cells. *Int J Clin Exp Pathol.* (2019) 12:3992–4001.
132. Kalluri R. The biology and function of fibroblasts in cancer. *Nat Rev Cancer.* (2016) 16:582–98. doi: 10.1038/nrc.2016.73
133. Xing M. BRAF mutation in papillary thyroid cancer: pathogenic role, molecular bases, and clinical implications. *Endocr Rev.* (2007) 28:742–62. doi: 10.1210/er.2007-0007
134. Jolly LA, Novitskiy S, Owens P, Massoll N, Cheng N, Fang W, et al. Fibroblast-mediated collagen remodeling within the tumor microenvironment facilitates progression of thyroid cancers driven by BrafV600E and pten loss. *Cancer Res.* (2016) 76:1804–13. doi: 10.1158/0008-5472.CAN-15-2351
135. Fozzatti L, Alamino VA, Park S, Giusiano L, Volpini X, Zhao L, et al. Interplay of fibroblasts with anaplastic tumor cells promotes follicular thyroid cancer progression. *Sci Rep.* (2019) 9:8028. doi: 10.1038/s41598-019-44361-6
136. Kang YE, Kim JT, Lim MA, Oh C, Liu L, Jung SN, et al. Association between circulating fibroblast growth factor 21 and aggressiveness in thyroid cancer. *Cancers (Basel).* (2019) 11:1154. doi: 10.3390/cancers11081154
137. Parascandolo A, Rappa F, Cappello F, Kim J, Cantu DA, Chen H, et al. Extracellular superoxide dismutase expression in papillary thyroid cancer mesenchymal stem/stromal cells modulates cancer cell growth and migration. *Sci Rep.* (2017) 7:41416. doi: 10.1038/srep41416
138. Islekel H, Oktay G, Terzi C, Canda AE, Fuzun M, Kupelioglu A. Matrix metalloproteinase-9,-3 and tissue inhibitor of matrix metalloproteinase-1 in colorectal cancer: relationship to clinicopathological variables. *Cell Biochem Funct.* (2007) 25:433–41. doi: 10.1002/cbf.1325
139. Maeta H, Ohgi S, Terada T. Protein expression of matrix metalloproteinases 2 and 9 and tissue inhibitors of metalloproteinase 1 and 2 in papillary thyroid carcinomas. *Virchows Arch.* (2001) 438:121–8. doi: 10.1007/s004280000286
140. Bjerre C, Vinther L, Belling KC, Wurtz SO, Yadav R, Lademann U, et al. TIMP1 overexpression mediates resistance of MCF-7 human breast cancer cells to fulvestrant and down-regulates progesterone receptor expression. *Tumour Biol.* (2013) 34:3839–51. doi: 10.1007/s13277-013-0969-7
141. Zhang WJ, Song B, Yang T. MMP-2, MMP-9, TIMP-1, and TIMP-2 in the peripheral blood of patients with differentiated thyroid carcinoma. *Cancer Manag Res.* (2019) 11:10675–81. doi: 10.2147/CMAR.S233776
142. Doyle LM, Wang MZ. Overview of extracellular vesicles, their origin, composition, purpose, and methods for exosome isolation and analysis. *Cells.* (2019) 8:727. doi: 10.3390/cells8070727
143. Wortzel I, Dror S, Kenific CM, Lyden D. Exosome-mediated metastasis: communication from a distance. *Dev Cell.* (2019) 49:347–60. doi: 10.1016/j.devcel.2019.04.011
144. Hessvik NP, Llorente A. Current knowledge on exosome biogenesis and release. *Cell Mol Life Sci.* (2018) 75:193–208. doi: 10.1007/s00018-017-2595-9
145. Hardin H, Helein H, Meyer K, Robertson S, Zhang R, Zhong W, et al. Thyroid cancer stem-like cell exosomes: regulation of EMT via transfer of lncRNAs. *Lab Invest.* (2018) 98:1133–42. doi: 10.1038/s41374-018-0065-0
146. Fabregat I, Malfetton A, Soukupova J. New insights into the crossroads between EMT and stemness in the context of cancer. *J Clin Med.* (2016) 5:37. doi: 10.3390/jcm5030037
147. Lan L, Luo Y, Cui D, Shi BY, Deng W, Huo LL, et al. Epithelial-mesenchymal transition triggers cancer stem cell generation in human thyroid cancer cells. *Int J Oncol.* (2013) 43:113–20. doi: 10.3892/ijo.2013.1913
148. Lan L, Luo Y, Cui D, Shi BY, Deng W, Huo LL, et al. Epithelial-mesenchymal transition induces cancer stem cell generation in human thyroid cancer cells *in vitro*. *Zhonghua Yi Xue Za Zhi.* (2013) 93:1261–5.
149. Liu J, Brown RE. Immunohistochemical detection of epithelialmesenchymal transition associated with stemness phenotype in anaplastic thyroid carcinoma. *Int J Clin Exp Pathol.* (2010) 3:755–62.
150. Heiden KB, Williamson AJ, Doscas ME, Ye J, Wang Y, Liu D, et al. The sonic hedgehog signaling pathway maintains the cancer stem cell self-renewal of anaplastic thyroid cancer by inducing snail expression. *J Clin Endocrinol Metab.* (2014) 99:E2178–87. doi: 10.1210/jc.2014-1844
151. Hardin H, Guo Z, Shan W, Montemayor-Garcia C, Asioli S, Yu XM, et al. The roles of the epithelial-mesenchymal transition marker PRRX1 and miR-146b-5p in papillary thyroid carcinoma progression. *Am J Pathol.* (2014) 184:2342–54. doi: 10.1016/j.ajpath.2014.04.011
152. Ma R, Minsky N, Morshed SA, Davies TF. Stemness in human thyroid cancers and derived cell lines: the role of asymmetrically dividing cancer stem cells resistant to chemotherapy. *J Clin Endocrinol Metab.* (2014) 99:E400–9. doi: 10.1210/jc.2013-3545
153. Mato E, Gonzalez C, Moral A, Perez JI, Bell O, Lerma E, et al. ABCG2/BCRP gene expression is related to epithelial-mesenchymal transition inducer genes in a papillary thyroid carcinoma cell line (TPC-1). *J Mol Endocrinol.* (2014) 52:289–300. doi: 10.1530/JME-14-0051
154. Cirello V, Gaudenzi G, Grassi ES, Colombo C, Vicentini L, Ferrero S, et al. Tumor and normal thyroid spheroids: from tissues to zebrafish. *Minerva Endocrinol.* (2018) 43:1–10. doi: 10.23736/S0391-1977.17.02610-4
155. Cirello V, Vaira V, Grassi ES, Vezzoli V, Ricca D, Colombo C, et al. Multicellular spheroids from normal and neoplastic thyroid tissues as a suitable model to test the effects of multitargeted kinase inhibitors. *Oncotarget.* (2017) 8:9752–66. doi: 10.18632/oncotarget.14187
156. Rajabi S, Dehghan MH, Dastmalchi R, Jalali Mashayekhi F, Salami S, Hedayati M. The roles and role-players in thyroid cancer angiogenesis. *Endocr J.* (2019) 66:277–93. doi: 10.1507/endocrj.EJ18-0537
157. Prete A, Lo AS, Sadow PM, Bhasin SS, Antonello ZA, Vodopivec DM, et al. Pericytes elicit resistance to vemurafenib and sorafenib therapy in thyroid carcinoma via the TSP-1/TGFbeta1 axis. *Clin Cancer Res.* (2018) 24:6078–97. doi: 10.1158/1078-0432.CCR-18-0693
158. Castellone MD, Laukkanen MO. TGF-beta1, WNT, and SHH signaling in tumor progression and in fibrotic diseases. *Front Biosci (Schol Ed).* (2017) 9:31–45. doi: 10.2741/s470
159. Parascandolo A, Laukkanen MO, De Rosa N, Ugolini C, Cantisani MC, Cirafici AM, et al. A dual mechanism of activation of the Sonic Hedgehog

- pathway in anaplastic thyroid cancer: crosstalk with RAS-BRAF-MEK pathway and ligand secretion by tumor stroma. *Oncotarget*. (2018) 9:4496–510. doi: 10.18632/oncotarget.23388
160. Liotti F, Collina F, Pone E, La Sala L, Franco R, Prevete N, et al. Interleukin-8, but not the related chemokine CXCL1, sustains an autocrine circuit necessary for the properties and functions of thyroid cancer stem cells. *Stem Cells*. (2017) 35:135–46. doi: 10.1002/stem.2492
161. Liotti F, De Pizzol M, Allegretti M, Prevete N, Melillo RM. Multiple anti-tumor effects of Reparixin on thyroid cancer. *Oncotarget*. (2017) 8:35946–61. doi: 10.18632/oncotarget.16412
162. Antonelli A, La Motta C. Novel therapeutic clues in thyroid carcinomas: The role of targeting cancer stem cells. *Med Res Rev*. (2017) 37:1299–317. doi: 10.1002/med.21448
163. Gao W, Han J. Overexpression of ING5 inhibits HGF-induced proliferation, invasion and EMT in thyroid cancer cells via regulation of the c-Met/PI3K/Akt signaling pathway. *Biomed Pharmacother*. (2018) 98:265–70. doi: 10.1016/j.biopha.2017.12.045

Conflict of Interest: The authors declare that the research was conducted in the absence of any commercial or financial relationships that could be construed as a potential conflict of interest.

Copyright © 2020 Veschi, Verona, Lo Iacono, D'Accardo, Porcelli, Turdo, Gaggianesi, Forte, Giuffrida, Memeo and Todaro. This is an open-access article distributed under the terms of the Creative Commons Attribution License (CC BY). The use, distribution or reproduction in other forums is permitted, provided the original author(s) and the copyright owner(s) are credited and that the original publication in this journal is cited, in accordance with accepted academic practice. No use, distribution or reproduction is permitted which does not comply with these terms.

Chapter 2

Recapitulating thyroid cancer histotypes through engineering embryonic stem cells

*Veschi V, *Turdo A, *Modica C, **Verona F**, Di Franco S, Gaggianesi M, Tirrò E, Di Bella S, Iacono ML, Pantina VD, Porcelli G, Mangiapane LR, Bianca P, Rizzo A, Sciacca E, Pillitteri I, Vella V, Belfiore A, Bongiorno MR, Pistone G, Memeo L, Colarossi L, Giuffrida D, Colarossi C, Vigneri P, Todaro M, Stassi G.

*Co-first authors

Published in Nature Communications, 2023
















Recapitulating thyroid cancer histotypes through engineering embryonic stem cells

Received: 25 February 2022

Accepted: 21 February 2023

Published online: 11 March 2023

 Check for updates

Veronica Veschi ^{1,9}, Alice Turdo ^{2,9}, Chiara Modica ^{1,9}, Francesco Verona², Simone Di Franco ¹, Miriam Gaggianesi ¹, Elena Tirrò ^{1,3}, Sebastiano Di Bella ², Melania Lo Iacono², Vincenzo Davide Pantina ¹, Gaetana Porcelli ², Laura Rosa Mangiapane², Paola Bianca², Aroldo Rizzo⁴, Elisabetta Sciacca⁵, Irene Pillitteri ², Veronica Vella⁶, Antonino Belfiore ⁶, Maria Rita Bongiorno², Giuseppe Pistone², Lorenzo Memeo ⁷, Lorenzo Colarossi ⁷, Dario Giuffrida⁷, Cristina Colarossi⁷, Paolo Vigneri ³, Matilde Todaro^{2,8} & Giorgio Stassi ¹ ✉

Thyroid carcinoma (TC) is the most common malignancy of endocrine organs. The cell subpopulation in the lineage hierarchy that serves as cell of origin for the different TC histotypes is unknown. Human embryonic stem cells (hESCs) with appropriate in vitro stimulation undergo sequential differentiation into thyroid progenitor cells (TPCs-day 22), which mature into thyrocytes (day 30). Here, we create follicular cell-derived TCs of all the different histotypes based on specific genomic alterations delivered by CRISPR-Cas9 in hESC-derived TPCs. Specifically, TPCs harboring *BRAF*^{V600E} or *NRAS*^{Q61R} mutations generate papillary or follicular TC, respectively, whereas addition of *TP53*^{R248Q} generate undifferentiated TCs. Of note, TCs arise by engineering TPCs, whereas mature thyrocytes have a very limited tumorigenic capacity. The same mutations result in teratocarcinomas when delivered in early differentiating hESCs. Tissue Inhibitor of Metalloproteinase 1 (TIMP1)/Matrix metalloproteinase 9 (MMP9)/Cluster of differentiation 44 (CD44) ternary complex, in cooperation with Kisspeptin receptor (KISS1R), is involved in TC initiation and progression. Increasing radioiodine uptake, KISS1R and TIMP1 targeting may represent a therapeutic adjuvant option for undifferentiated TCs.

Follicular cell-derived TCs mostly develop through the aberrant growing of endodermal layer-derived follicular epithelial cells and comprise the main histological differentiated and undifferentiated subtypes^{1,2}. Differentiated TCs include the most common papillary (PTC, 80-85%) and follicular (FTC, 10-15%) TCs. Although most

differentiated TCs are indolent tumors with a favorable outcome, 5–20% of them have a high risk of relapse and death³. Anaplastic TC (ATC) represents 1-2% of all TC cases and behaves very aggressively by invading adjacent tissues and metastasizing distant organs⁴. ATC can be derived either from the follicular thyroid epithelium gland by losing

¹Department of Surgical Oncological and Stomatological Sciences, University of Palermo, Palermo, Italy. ²Department of Health Promotion Sciences, Internal Medicine and Medical Specialties, University of Palermo, Palermo, Italy. ³Department of Clinical and Experimental Medicine, A.O.U. Policlinico-Vittorio Emanuele, Center of Experimental Oncology and Hematology, University of Catania, Catania, Italy. ⁴Villa Sofia-Cervello Hospital, Palermo, Italy. ⁵Queen Mary University, Experimental Medicine & Rheumatology, London, United Kingdom. ⁶Endocrinology Unit, Department of Clinical and Experimental Medicine, University of Catania, Garibaldi-Nesima Hospital, Catania, Italy. ⁷Department of Experimental Oncology, Mediterranean Institute of Oncology, Viagrande, Catania, Italy. ⁸A.O.U.P. "Paolo Giaccone", University of Palermo, Palermo, Italy. ⁹These authors contributed equally: Veronica Veschi, Alice Turdo, Chiara Modica. ✉ e-mail: giorgio.stassi@unipa.it

the biological features, including the iodine uptake (de novo), or more frequently from a dedifferentiation process of a pre-existing differentiated TC, following the accumulation of multiple mutations⁵. Despite the intense efforts to improve therapeutic regimens, there are no effective therapies available for metastatic TC patients. The majority of TC metastases do not express the sodium/iodine symporter (NIS) and are not responsive to radioactive iodine, the most effective non-surgical therapy in TC^{6–8}. Thus, there is an urgent need to develop experimental models to study the fundamental mechanisms underlying tumorigenesis and metastasis formation, particularly in radioiodine-resistant patients.

Despite major advances in the know-how of TC's hallmarks and biological behavior, the cell subpopulation in the lineage hierarchy that serves as cell of origin for the different TC histotypes, following the acquisition of somatic mutations, remains unknown. A critical issue argues whether the different TC histotypes mirror a distinct transformed cell subpopulation or the same target cell harboring different genetic mutations. The existence of different follicular histotypes of cells-derived TCs endowed with distinctive biological behavior led to formulate several carcinogenesis models that describe the cell of origin^{1,2}. However, these models do not reflect the phenotypic and genetic intertumoral heterogeneity of follicular cell-derived TCs. In adults mammals, tissue homeostasis and repair of injured organs depends on small reservoirs of tissue-specific stem cells able to self-renew and differentiate. Indeed, the hierarchical organization of adult tissue has been accomplished to slow aging, help the organism recover from injury, and finally protect cells from accumulating damage that would ultimately lead to cancer. Although the progenitor cells with limited lifespan escape the risk of accumulating mutations, adult stem cells and their immediate offsprings could potentially be transformed either by acquiring mutations inducing self-renewal, or by inheriting existing mutations from stem cells⁹. This model introduced the concept of tumorigenesis assuming stem cells as source of tumor formation in light of their longevity and innate self-renewal capacity, essential for the accumulation of genetic or epigenetic alterations^{10,11}. To explain the different tumor histopathology and behavior, a genetic mutation model, in which a variety of genetic mutations occurs within the same “target cell”, was conceptualized². For most cancers, the “target cell” of transforming mutations is unknown. Nevertheless, there are considerable evidence that certain types of leukemia arise from mutations which accumulate in hematopoietic progenitor cells^{12–14}. This observation mostly reflects the need to better understand the oncogenic events which occur in tissue-resident stem cells in order to explain the transition from non-malignant hyper-proliferative lesions to well-established cancers endowed with different biological behaviors. Although we and other research groups have identified a subpopulation of cancer stem cells (CSCs)/progenitor cells that is crucially involved in the TC initiation, the transformation stage in the hierarchy lineage remains elusive¹⁵. Here, we show the ability of human embryonic stem cells (hESCs) to recapitulate the cellular hierarchy of thyroid gland and reproduce the oncogenic process upon CRISPR-based genetic editing.

Results

hESCs engineered with the most common TC genetic alterations recapitulate TC histotypes

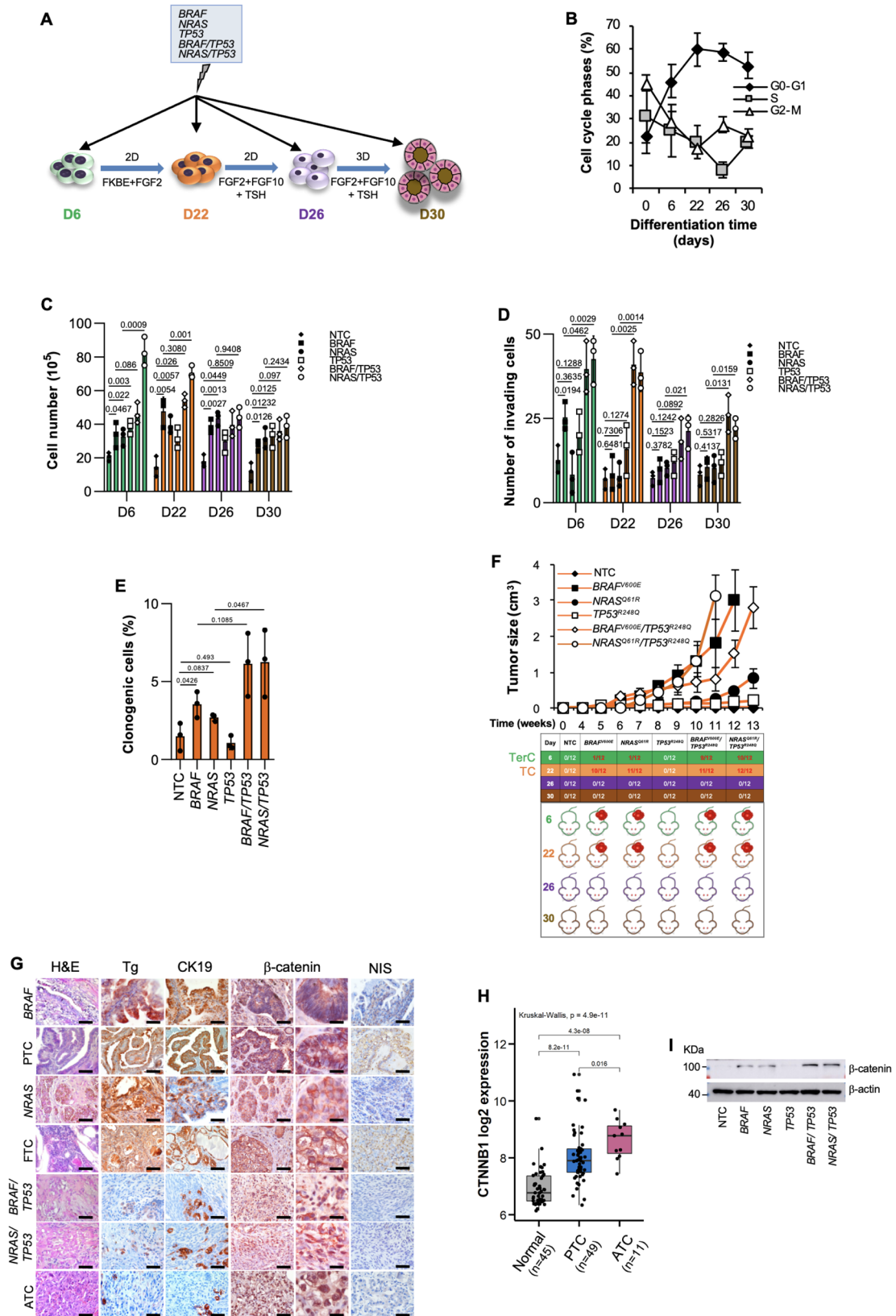
To establish a model that mirrors the follicular cell-derived TC histotypes, hESCs-derived thyroid progenitor cells (TPCs) and their differentiation lineages were obtained following Longmire's established protocol¹⁶ and genetically modified using a CRISPR/Cas9 technology by introducing the most common TC genetic alterations including *BRAF*, *NRAS* and *TP53* (Fig. 1A and Supplementary Fig. 1a). According to literature, cells at day 6, upon activation of BMP-FGF2 signaling, promoted thyroid lineage specification gradually increasing, up to day 30, the expression levels of thyroid markers PAX8, TTF1, TSH-R, TPO, Tg

and NIS (Supplementary Figs. 1b–e)^{16–18}. D22 cells triggered the expression of specific thyroid lineage markers, PAX8 and TTF1, which are retained and concomitantly complemented, at D26 and D30, by the activation of thyroid differentiation markers, TSH-R, TPO, Tg, and NIS (Supplementary Figs. 1c–e). Besides, D22 cells expressed high levels of other putative thyroid progenitor cell hallmarks such as CD133, ABCG2, Nestin and HNF-4 α ¹⁹, along with the thyroid transcription factors *HHEX* and *FOXE1*²⁰ (Supplementary Figs. 1f–j). All together these data indicate that D22 thyroid lineage is enriched in thyroid progenitor cells (TPCs). Mature lung markers *SCGB1A1*, *AQP5*, *SFTPB* and *SFTPC* were barely detectable in the thyroid lineage from days 22 to 30 (Supplementary Fig. 1k). While throughout hESC differentiation, cells at days 0, 6 and 22 were progressively enriched in G0-G1 and depleted in G2-M/S phase fractions, most of the differentiated thyroid precursors at days 26 and 30 displayed a slight decrease of G0-G1 and increase of G2-M phases (Fig. 1B).

D22 TPCs showed a similar cell cycle profile upon *BRAF*, *NRAS* and *TP53* mutational background introduction. Sanger and Next-generation sequencing analyses exhibited a high-efficiency percentage of the introduced exogenous genetic mutations that was consistent with a correlation coefficient of 0.85% (Supplementary Figs. 2a–c and Supplementary Table 1). hESC-derived anterior foregut endoderm at day 6 and D22 TPCs, harboring *TP53*^{R248Q} in combination with *BRAF*^{V600E} or *NRAS*^{Q61R}, showed more pronounced proliferative, invasive capabilities and clonogenic activity, compared to NTC control (Fig. 1C–E). Upon the acquisition of specific genetic alterations, except the inactivating point *TP53*^{R248Q} mutation alone, exclusively cells at days 6 and 22 retained tumorigenic capacity (Fig. 1F). Subcutaneous injection of the genetically engineered D22 TPCs generated avatars that recapitulate the recognizable phenotypic and morphological features of follicular cell-derived TC histotypes, whereas D6 cells-derived xenograft masses resembled a teratocarcinoma phenotype expressing S-100, CDX2, Oct3/4 and p40 (Fig. 1G and Supplementary Fig. 2d).

Specifically, *BRAF*^{V600E} and *NRAS*^{Q61R}-engineered D22 cells led to the formation of tumors that reflect the cellular heterogeneity of patient-derived PTC and FTC phenotype, respectively, mainly characterized by different degrees of nuclear atypia and variable mitotic activity (Fig. 1G).

Although the inactivation of p53 alone was not required for the tumor initiation, D22 TPCs harboring *TP53*^{R248Q} in combination with *BRAF*^{V600E} or *NRAS*^{Q61R} generated undifferentiated tumors with a pleomorphic and undifferentiated morphology recapitulating the heterogeneity and the phenotypic characteristics of ATC, expressing low levels of Tg, CK19 and NIS as compared with the well-differentiated TC histotypes (Fig. 1F, G and Supplementary Fig. 2e). In line with current knowledge, these data suggest that *TP53* mutations are required for tumor evolution and a higher disease stage exclusively in cooperation with other oncogenic hits²¹. Accordingly, *TP53* mutation was more frequently positively associated with undifferentiated tumors showing aggressive features and distant metastases^{22–24} (Supplementary Fig. 2f). This phenomenon is in line with the analysis of *TP53* germline mutation distribution in a large cohort of patients affected by Li-Fraumeni syndrome, which highlighted a rare positive association with inherited risk of developing TCs (Supplementary Fig. 2g). Moreover, in accordance with the positive association between *CTNNB1* mRNA levels and aggressive histotypes of TC²⁵, D22 TPCs engineered with *TP53*^{R248Q} in combination with *BRAF*^{V600E} or *NRAS*^{Q61R} mutations displayed β -catenin accumulation and nuclear localization (Fig. 1G–I and Supplementary Fig. 2h). In D22 cells, *BRAF*^{V600E} and *NRAS*^{Q61R} alone or in combination with *TP53*^{R248Q} mutation promoted the expression of CSC-, EMT-, and metastasis-related genes (Fig. 2A). These findings suggest that thyroid carcinogenesis follows a genetic mutation model in which the TPCs are the elective target of genetic alterations.



TIMP1-MMP9-CD44 complex sustains tumor initiation capability of engineered D22 TPCs

To explore the signaling pathway implicated in the tumorigenesis of engineered TPCs, we sought to analyze the reprogramming of the transcriptomic profile sustained by specific oncogenic alterations.

From transcriptomic analysis of engineered D22 TPCs with *BRAF*^{V600E} or *NRAS*^{Q61R} alone and in combination with *TP53*^{R248Q} mutation emerged a common higher expression of *HGF*, *TIMP1*, *MMP9* and *CD44* compared with D30 mature thyroid cells (Fig. 2A, B and Supplementary Fig. 3a). As the previously reported activation of HGF/MET

Fig. 1 | hESCs engineered with the most common TC genetic alterations recapitulate thyroid cancer histotypes. **A** Model of directed differentiation of human embryonic stem cell (hESC) into thyroid lineage. To promote thyroid lineage specification, hESCs were exposed to the indicated stimuli. Treatment with FGF10, KGF, BMP4 and EGF is reported as FKBE. **B** Cell cycle analysis in non-targeting control (NTC) hESC-derived cells at the indicated stage of thyroid differentiation lineage. The data show percentage of cell number in G0/G1, S, and G2/M cell cycle phases. Data are expressed as mean \pm SD of three independent experiments. **C** Cell proliferation in hESC-derived cells, engineered with the indicated mutations, at the indicated stage of thyroid differentiation lineage, at 7 days. **D** Invasion analysis in cells engineered as in (C) at 72 h. **E** Clonogenic assay in D22 thyroid progenitor cells (TPCs) engineered as in (C) at 21 days. For (C–E) statistical significance was calculated using the two-tailed unpaired t test and data are mean \pm standard error of three independent experiments. **F** (*upper panel*) Growth kinetics of xenograft tumors generated by subcutaneous injection of D22 TPCs. (*lower panel*) Frequency

of teratocarcinoma (TerC) or TCs obtained by the injection of hESC-derived cells harboring different mutational background, at different stages of thyroid differentiation lineage. Data are shown as mean \pm SD. $n = 12$ mice per group. **G** H&E staining and immunohistochemistry analysis of thyroglobulin (Tg), cytokeratin 19 (CK19), β -catenin and NIS on xenograft tumors obtained following injection of D22 TPCs engineered with different mutational background and compared with patient-derived PTC, FTC and ATC. Number of tissues analyzed $n = 5$. Mutational status of human tissues: PTC *BRAF* mutated ID#6, FTC *NRAS* mutated, and ATC *BRAF/TP53* mutated ID#96. Scale bars, 100 μ m. **H** Correlation analysis in Gene Expression Omnibus (GEO) (GSE33630) of *CTNNB1* mRNA expression levels in normal thyroid tissue, PTC and ATC. Boxes represent the interquartile range (IQR) and midline represents the median. Statistical significance was calculated using Kruskal-Wallis test. **I** Immunoblot analysis of β -catenin in D22 TPCs engineered as in (c). β -actin was used as loading control. Source data are provided as a Source Data file.

signaling pathway in ATCs²⁶, HGF was found among the top differentially upregulated genes in D22 compared with D30 (Fig. 2A, B).

These findings are in line with TIMP1 and CD44 protein expression patterns and MMP9 activity in genetically edited cells at days 22 and 30 stage of thyroid differentiation lineage (Fig. 2C, D, and Supplementary Fig. 3b). mRNA and protein analysis of hESCs at different stages of differentiation revealed that expression levels of TIMP1, MMP9 and CD44, in a time-dependent manner, increase from D0 to D22, and then decrease to D30 (Supplementary Figs. 3C–E). In accordance with the lack of tumorigenic activity, *TP53*^{R248Q} mutation alone did not endorse the expression of these molecules (Fig. 2A–D and Supplementary Figs. 3a, b). Although TIMP1 is a natural inhibitor of MMPs involved in the matrix remodeling during carcinogenesis, it converges toward cancer cell survival by binding MMP9/CD44 complex and mediating PI3K/AKT pathway activation^{27,28}. TIMP1, together with its binding protein CD63, has emerged as a predictive biomarker with regard to tumor therapeutic response and spreading²⁹. Differentiated cells at days 26 and 30, characterized by negligible expression levels of TIMP1, MMP9 and CD44, were unable to induce tumor growth (Supplementary Figs. 3f, g). Interestingly, the overexpression of TIMP1 together with CD44 and MMP9, is able to significantly increase the proliferation rate and in lesser extent the invasive capacity of D30 cells harboring *NRAS*^{Q61R}/*TP53*^{R248Q} mutations, whose cells have acquired a weak tumorigenic activity, tardily generating small tumors. This phenomenon could be attributed to the concurrent epigenetic alterations, induced by the ternary complex, along the differentiation process (Fig. 2E and Supplementary Figs. 4a–d).

In the light of these data, we investigated whether the expression of each member of the ternary complex TIMP1-MMP9-CD44 correlated with thyroid tumor. Analysis of a large cohort of primary TCs showed a significant positive association with the expression of *TIMP1*, *MMP9* and *CD44* (Fig. 2F and Supplementary Fig. 4e)³⁰. Following the ternary complex formation, TIMP1 leads to the activation of MMP9, which in turn cleaves the CD44 extra-cellular domain hence releasing the intracellular fragment into the cytoplasm³¹. The CD44 fragment translocates into the nucleus, where it acts as a transcription factor, by regulating the expression of several target genes including the variant isoforms of CD44 (CD44v)³².

Some of CD44v have been considered as functional markers of cancer progression³³. We have recently reported that constitutive and reprogrammed metastatic cancer cells are identifiable by the expression of CD44v6, which is positively associated with PI3K/AKT pathway activation³⁴.

We next evaluated whether TIMP1, interacting with CD63, is required for cell survival and migration, cooperating with CD44v6. D22 cell-derived xenograft tumors, harboring *BRAF*^{V600E} and *NRAS*^{Q61R} alone or in combination with *TP53*^{R248Q} mutation expressed comparable levels of TIMP1, CD63, MMP9 and CD44v6 with those found in the matching PTC, FTC and ATC histotypes (Fig. 2G, H, and Supplementary

Figs. 4f, g). In accordance with the inability to promote tumor initiation, *TP53*^{R248Q} mutation alone lacked the capability to induce CD44v6 expression in D22 TPCs (Supplementary Fig. 4h). TIMP1 targeting significantly impaired the proliferative and invasive capacity of the engineered D22 TPCs, regardless the introduced genetic alteration, by impeding the activation of PI3K/AKT pathway, even in presence of TIMP1 exogenous cytokine, driven by a reduced expression level of CD44v6³⁴ (Fig. 3A–D, and Supplementary Figs. 5a–d).

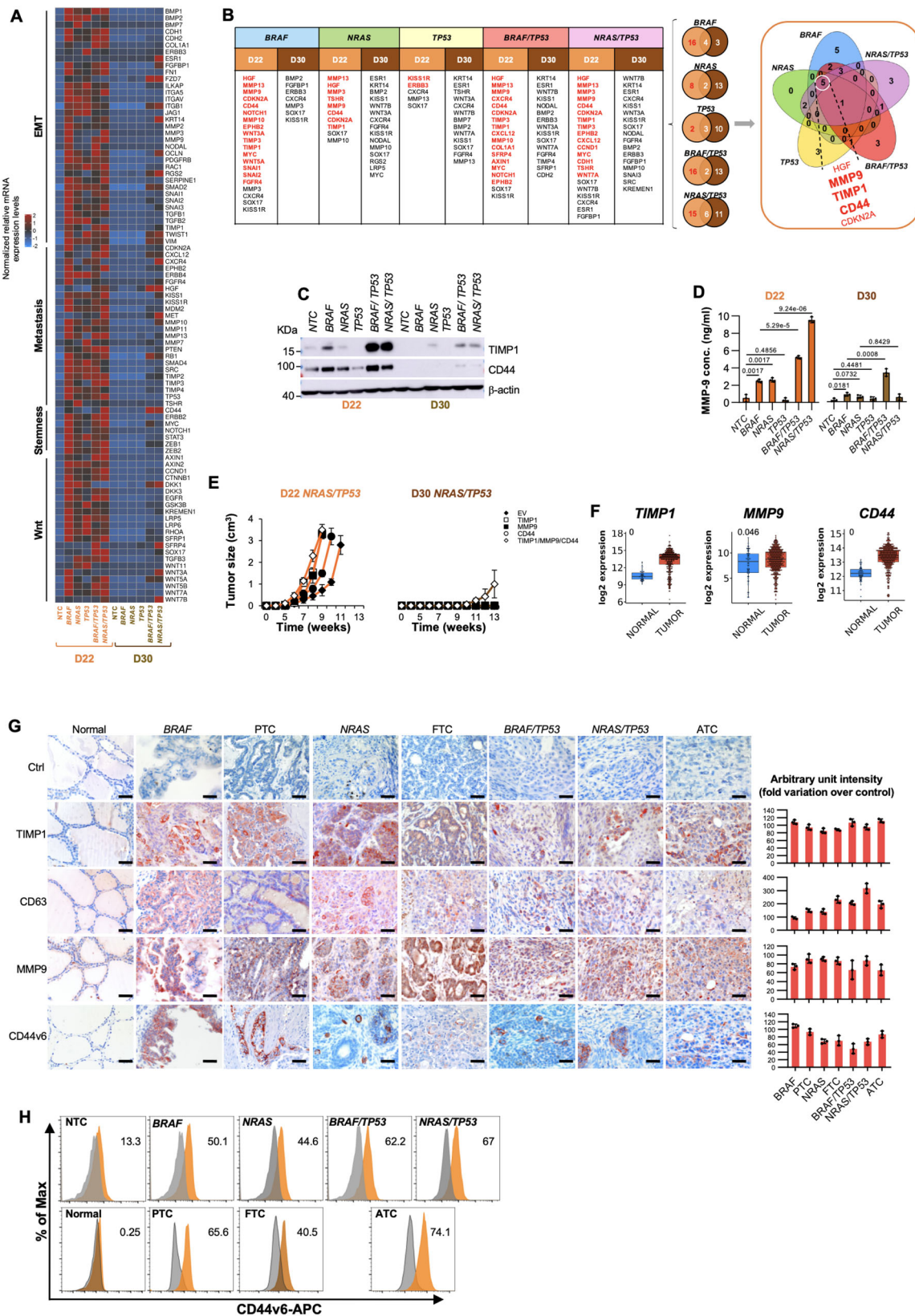
Transduction of engineered D22 TPCs with a lentiviral vector encoding for *CD44v6* short hairpin RNA (shRNA) sequences, significantly decreased AKT phosphorylation, proliferative and invasive potential (Fig. 3E–G and Supplementary Fig. 5e–g). Conversely, CD44v6 overexpression led to an upregulation of pAKT, whose protein expression levels were restored by the targeting of TIMP1, to lower levels expressed by untreated TPCs (Fig. 3H and Supplementary Figs. 5h–j). These findings suggest that TIMP1 through CD44v6 is required for the activation of PI3K/AKT pathway.

Likewise, in the TPCs harboring the different mutation profiles, TIMP1 blockade downregulated the expression of Wnt, EMT- and stemness-related genes, as also confirmed by enrichment analysis computed with Reactome Database (Fig. 3I and Supplementary Figs. 6a–d). Specifically, targeting of TIMP1 hampered the mRNA levels of β -catenin targets, such as *AXIN2*, *MYC* and *CCND1* and the cell growth rate, which were both restored in presence of Wnt pathway agonists, Wnt3A and R-spondin1 (Supplementary Figs. 6e–h). In line with these findings, engineered D22 TPCs and their derived mouse avatars, showed similar transcriptomic profiles and an enrichment of pathways related to EMT- and stemness-associated signature, as well as PI3K/AKT and MAPK signaling, comparable to that observed in primary PTC- and ATC tissues (Fig. 4A–D and Supplementary Figs. 7a, b). Altogether, these data indicate that specific mutations regulate the expression of TIMP1/CD44v6 complex, which sustain the tumor growth of the different TC histotypes through the activation of PI3K/AKT pathway.

KISSIR is a prognostic factor and a potential therapeutic target in advanced TCs

Given that, *BRAF*^{V600E} or *NRAS*^{Q61R} in combination with *TP53*^{R248Q} mutations gave rise to tumors that resemble the ATC phenotype, we evaluated whether these genetic alterations are required for the metastatic potential of TPCs. Cells were orthotopically injected and their xenograft-derived lesions analyzed for the gene expression related to the metastatic signaling profile.

TPCs engineered for *BRAF*^{V600E}/*TP53*^{R248Q} and *NRAS*^{Q61R}/*TP53*^{R248Q}, robustly generated orthotopic and metastatic tumors (Fig. 5A). Immunohistochemical analysis showed that TIMP1/MMP9/CD44 ternary complex expression in primary tumor avatars paralleled an increase of the expression levels of TWIST, SNAIL in the xenograft metastasis, resembling the phenotypic landscape of PTC and ATC patient-derived primary and metastatic lesions (Fig. 5A, B).



From the transcriptomic analysis emerged a high expression of *KISS1* and *KISS1R* in TC metastatic lesions and in xenografts derived from TPCs harboring the mutation of *BRAF* or *NRAS* in combination with *TP53*, likely induced by the functional inactivation of p53, along with the activation of Wnt signaling and EMT-related pathways (Fig. 5C, D and Supplementary Figs. 8a–d). Although *KISS1* is known as

a metastasis suppressor gene, recent evidence highlighted its role in triggering the molecular events of the metastatic cascade^{35–38}. Consistently, by binding its cognate receptor, *KISS1* promotes invasion, intravasation and secondary lesion engraftments^{37,39}.

Immunohistochemistry and transcriptomic analysis of a cohort of TC patients (Supplementary Table 2 and Supplementary Fig. 8e)

Fig. 2 | The ternary complex TIMP1-MMP9-CD44 sustains the tumor initiation capability of engineered D22 TPCs. **A** Heatmap of Wnt-, stemness-, metastasis- and EMT-related genes in D22 TPCs and in D30 mature thyrocytes engineered with the indicated mutations. Data are presented as $2^{-\Delta Ct}$ normalized values of three independent experiments. **B** Table and Venn diagrams of common (black color) and exclusive upregulated genes (red color) with $\log_{2}FC > 1.5$ in D22 TPCs vs thyrocytes (D30). **C** Immunoblot analysis of TIMP1 and CD44 in hESC-derived cells harboring different mutational background, at D22 and D30. β -actin was used as loading control. One representative of three independent experiments is shown. Source data are provided as a Source Data file. **D** MMP9 production in cells as in (C) at 48 h. Statistical significance was calculated using the unpaired two-tailed t test. Data are expressed as mean \pm SD of three independent experiments. **E** Growth kinetics of xenograft tumors generated by subcutaneous injection of the indicated engineered D22 TPCs and D30 cells overexpressing *TIMP1*, *MMP9* and *CD44* alone and in combination. Data are shown as mean \pm SD. $n = 10$ mice per group. **F** Relative

mRNA expression levels of *TIMP1*, *MMP9* and *CD44* in normal ($n = 59$) and tumor ($n = 509$) thyroid tissue from TCGA database, thyroid carcinoma (THCA) branch. Boxes represent the IQR and midline represents the median. Statistical significance was calculated using the Wilcoxon test. **G** (left panel) Immunohistochemical analysis of TIMP1, CD63, MMP9 and CD44v6 on xenografts obtained by injecting engineered D22 TPCs and compared with normal thyroid tissue, patient-derived PTC, FTC and ATC. Ctrl= negative control. The number of tissues analyzed $n = 5$. Mutational status of human tissues: PTC *BRAF* mutated ID#6, FTC *NRAS* mutated, and ATC *BRAF/TP53* mutated ID#96. Scale bars, 100 μ m. (right panel) Histograms represent the percentage of TIMP1, CD63, MMP9 and CD44v6 positive cells. Data are expressed as mean \pm SD of three independent experiments. **H** CD44v6 flow cytometry analysis (orange histograms) and corresponding isotype-matched control (grey histograms), in engineered D22 TPCs and compared with isolated normal thyroid cells and patient-derived PTC, FTC and ATC cells.

revealed that *KISS1* and *KISS1R* expression levels are positively associated with the aggressive phenotype including PTC-derived metastatic lesions and ATCs, in line with a RNAseq and DFS probability analysis of a large cohort of thyroid carcinoma, showing a significant correlation between high levels of *KISS1R* and the risk of developing TC metastatic disease (Fig. 5E–G and Supplementary Figs. 8f–i).

KISS1R targeting reduced both proliferative and invasive activity and also inhibited the activation of the PI3K/AKT and ERK pathways (Supplementary Figs. 9a–f). Indeed, several clinical trials have been designed to target concomitantly PI3K/AKT and MAPK pathway (NCT01830504). Although surgical resection in combination with radioactive iodine and l-thyroxine treatment is known to be effective in differentiated TCs³, patients who developed distant metastases or affected by ATCs are refractory to radioactive iodine^{7,8}. Indeed, ATC and metastatic disease are still incurable due to their systemic nature and resistance to the currently accessible therapeutic approaches. In accordance with targeting of molecules regulating NIS trafficking, tyrosine kinases or HDAC and overexpression of *PAX8* gene^{40–43}, we intriguingly observed that inhibition of *KISS1R* together with *TIMP1* induced the expression of thyroid differentiation markers such as *PAX8*, *TG*, *TSHR*, *TPO*, *TFE1* and *NIS*, which sustained the increase of functional radioiodine uptake in *BRAF/TP53* and *NRAS/TP53* mutant D22 TPCs, whose ¹²⁵Iodine retention levels were similar to those of untreated PTC established cell lines (Fig. 6A–G and Supplementary Fig. 9g). In xenograft thyroid tumors derived from the subcutaneous injection of mutated D22 TPCs, the intra-tumoral administration of *TIMP1* and *KISS1R* inhibitors^{44–46} lead to a significant delay in tumor growth, characterized by a marked expression of *NIS*, and a prolonged percentage of mice survival (Fig. 6H, I).

Thus, these data indicate *KISS1R* and *TIMP1* blockade as adjuvant therapy to sensitize undifferentiated TCs to radioiodine-based therapeutic regimen, reprogramming thyroid cancer cells behaving aggressively toward a more differentiated phenotype.

Our findings suggest that TC histopathology and behavior are determined by distinct genetic alterations and that while the ternary complex is crucial for the promotion of TC, *KISS1R* sustains the metastatic growth (Fig. 7A). Triggering of *KISS1R* leads to the acquisition of an invasive phenotype through the activation of both PI3K and ERK-mediated *MMP9* signaling pathway⁴⁷, which positively regulated the expression of EMT-associated genes (Fig. 7B and Supplementary Fig. 9h).

Discussion

In this study, we reproduced the oncogenic events that occur in tissue-resident stem cells/progenitor cells during TC transformation. We demonstrated that genetic mutations occurring in tissue-resident progenitor cells, characterized by a long-lasting cell lifespan, govern the evolutionary dynamics of thyroid tumorigenesis. Thus, this phenomenon could explain the TC incidence rates dictated by the rare

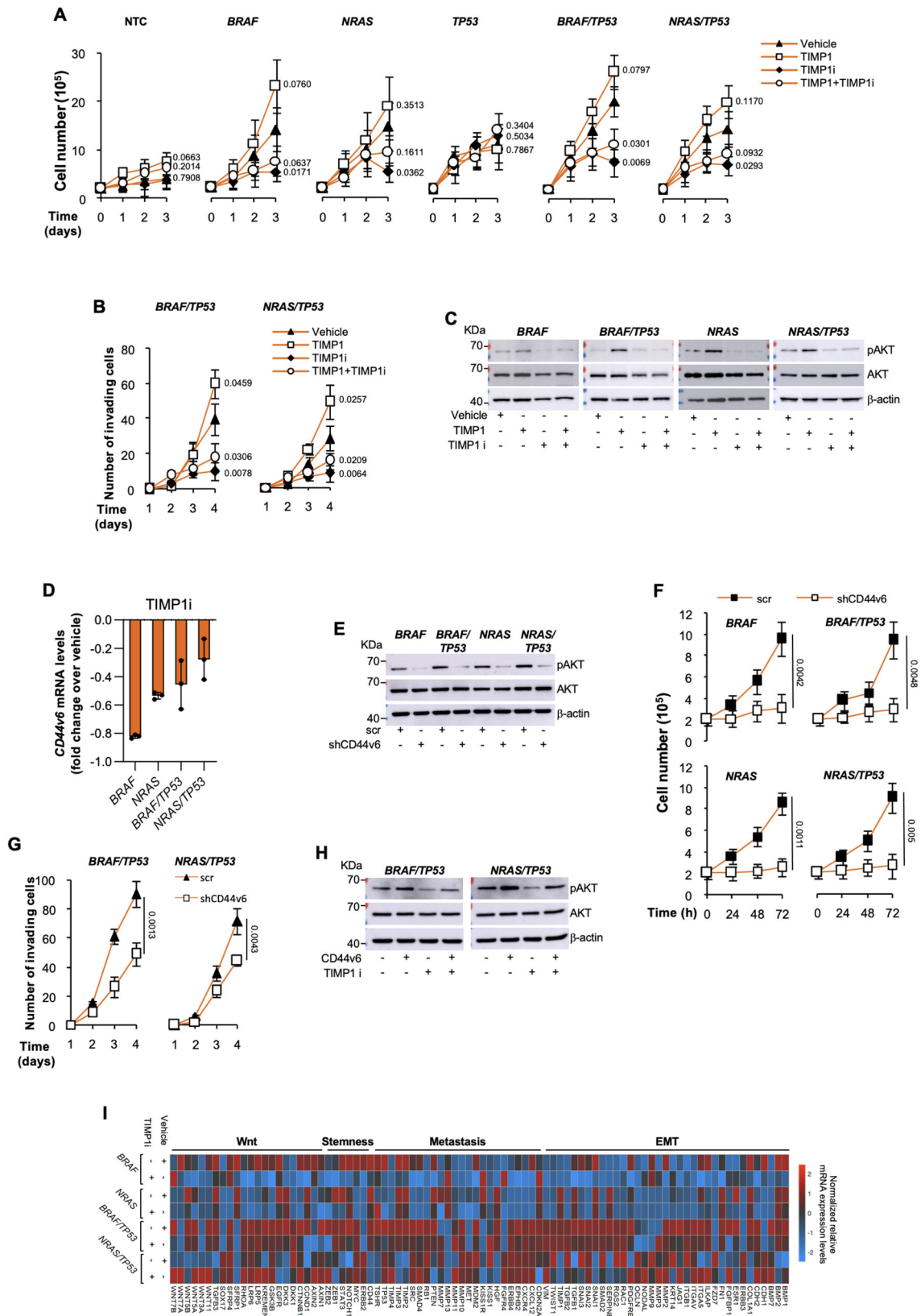
(1/1000) presence of stem/progenitor cells in the thyroid gland⁴⁸, which is renewed few times during the whole life⁴⁹. We recapitulated all the different TC histotypes based on the induction of specific genomic alteration delivered by CRISPR-Cas9 in human ESC-derived TPCs at day 22. Thus, this is a genetic edited model of tumor transformation derived from human ESCs-derived cells. Scientists have either generated in vitro a normal functional thyroid gland starting from murine ESCs¹⁶ or they have introduced oncogenic driver mutations in breast, colon, or pancreas organoids by using CRISPR/Cas9 technology to induce tumor transformation^{50–52}. Nowadays, the most common genetic and epigenetic alterations reported in TC, lead to the constitutive activation of two main signaling pathways: *i*) the MAPK and *ii*) PI3K/AKT/mTOR signaling pathways, which promote uncontrolled cell division, cell migration and longevity⁵³. The spectrum of altered genes, including point somatic mutations, which differ on TC histotypes, endorse tumor initiation and progression. *BRAF* is mutated in 35–40% of PTCs and in 25–35% of ATCs, while it is not mutated in FTCs. *RAS* point mutations are reported in 18–52% of FTCs and in 6–55% of ATCs⁵⁴.

Accordingly, we show that *BRAF*^{V600E} or *NRAS*^{Q61R} recapitulates PTC and FTC histotypes, respectively, at transcriptomic, morphological and phenotypic levels. The mutation of tumor suppressor gene *TP53* rarely occurs in differentiated PTC and FTC while it is frequently reported in ATC (70%)^{54,55}, positing that ATC can also arise from a *BRAF*-mutated PTC following a further acquisition in *TP53* mutations.

In line with these notions, our data reveal that *TP53* mutation alone is not sufficient to drive TC tumorigenesis, whereas only in association with *BRAF*^{V600E} or *NRAS*^{Q61R} generate undifferentiated TCs endowed with an enrichment of metastatic-associated gene signatures, contributing to the aggressive behavior that characterizes the ATC. This evidence ascertains that TC carcinogenesis follows a genetic mutation model, in which *NRAS*, *BRAF* and *TP53* mutations occur in TPCs.

By integrating transcriptomic analyses in primary and metastatic TC lesions of human patients and xenografts derived from TPCs harboring *BRAF*^{V600E} or *NRAS*^{Q61R} in combination with *TP53*^{R248Q} mutations, emerged *TIMP1/MMP9/CD44* complex as fundamental for TC promotion, while the activation of *KISS1/KISS1R* signaling crucial for the metastatic growth. In accordance, *TP53*^{R248Q} alone was not able to induce the expression of the ternary complex *TIMP1/MMP9/CD44*. We previously demonstrated that cells expressing a *CD44* isoform, *CD44v6*, display activation of PI3K/AKT and Wnt pathways, which cooperate to sustain their self-renewal, survival and metastatic potential^{34,56,57}. *TIMP1* promotes the activation of AKT in TPCs engineered with the selected point mutations, whereas its inhibition is associated with significantly decreased levels of *CD44v6* and genes related to signaling of β -catenin, whose expression levels are positively correlated with TC poor prognosis²⁵.

Moreover, we show that poor TC prognosis is associated with high expression levels of *KISS1/KISS1R*, which could be a promising



functional marker for defining specific therapeutic targets and responsive advanced TC patients. The majority of non-metastatic differentiated TCs can be cured by surgical resection, radioactive iodine, and TSH suppression³, whereas metastatic TC patients are still incurable. Of note, KISS1R and TIMP1 inhibition in TPCs harboring *BRAF*^{V600E} or *NRAS*^{Q61R} in combination with *TP53*^{R248Q} mutations results in

increased expression of NIS, thus restoring the functional radioiodine uptake. We propose that KISS1R and TIMP1 targeting may be further explored as adjunct therapy to sensitize ATCs to the standard radiometabolic therapy.

Future research studies can take advantage of our experimental model based on the engineering of hESC-derived cells, even though

Fig. 3 | TIMP1 blockade and CD44v6 silencing significantly impair survival and invasive capacity of D22 TPCs. **A** Cell proliferation in D22 TPCs engineered with the indicated mutations treated with vehicle, TIMP1, TIMP1 inhibitor (TIMP1i) alone or in combination up to 3 days. **B** Invasion analysis in D22 TPCs harboring the indicated mutations treated as in **(A)** up to 4 days. For **(A and B)** statistical significance was calculated using the two-tailed unpaired t test and data are mean \pm standard error of three independent experiments. **C** Immunoblot of pAKT and AKT in engineered D22 TPCs treated as in **(A)** for 48 h. β -actin was used as loading control. One representative of three independent experiments is shown. Source data are provided as a Source Data file. **D** Relative mRNA expression levels of *CD44v6* in D22 TPCs engineered with the indicated mutations and treated with TIMP1 inhibitor (TIMP1i) for 24 h. Data are presented as fold change over vehicle \pm SD of three independent experiments. **E** Immunoblot analysis of pAKT and AKT levels in D22 TPCs engineered with the indicated mutations and transduced with control shRNA (scramble, scr) or CD44v6 shRNA (shCD44v6). β -actin was used as

loading control. One representative of three independent experiments is shown. Source data are provided as a Source Data file. **F** Cell proliferation in D22 TPCs engineered with the indicated mutations transduced with control shRNA (scramble, scr) or CD44v6 shRNA (shCD44v6), up to 72 h. **G** Invasion analysis in D22 TPCs harboring the indicated mutations transduced with control scramble (scr) or shCD44v6, up to 4 days. For **(F and G)** statistical significance was calculated using the two-tailed unpaired t test and data are mean \pm standard error of three independent experiments. **H** Immunoblot analysis of pAKT and AKT in the indicated engineered D22 TPCs overexpressing CD44v6, untreated and treated with TIMP1i for 48 h. β -actin was used as loading control. One representative of three independent experiments is shown. Source data are provided as a Source Data file. **I** Heatmap of Wnt-, EMT- stemness and metastasis-related genes in D22 TPCs engineered with the indicated mutations and treated with vehicle or TIMP1i for 24 h. Data are presented as normalized $2^{-\Delta Ct}$ values of three independent experiments.

artificial, to generate tumors with specific mutations in progenitor cells and to further investigate genes and pathways responsible of therapy resistance. It is likely that this model could be applied to study the tumorigenesis mechanisms in different organs derived from the definitive endoderm during their lineage differentiation. The engineering of hESC-derived TPCs can be exploited for both the generation of tumors with specific mutations, and the study of molecular signatures responsible for tumor transformation and therapy resistance.

Methods

Ethics statement

Institutional Review Board (IRB) approval for the collection of human tissues derived from TC patients was obtained from the Ethical Committee of the Mediterranean Institute of Oncology, Catania, Italy (authorization n° 16/21 on February 9th, 2021). The study complied with all the ethical regulations for work with human participants. Written informed consents were obtained from all the patients, including consent to publish information about age and sex.

Human embryonic stem cell (hESC) culture and directed differentiation

The human embryonic stem cell (hESC) line, WA09 (#WA09-RB-001), was purchased by Wi Cell and cultured in mTESR1 media (Stemcell Technologies). Definitive endoderm was induced by culturing cells for five days with the StemDiff definitive endoderm kit (Stemcell Technologies). In order to induce anterior foregut endoderm differentiation, definitive endoderm cells were cultured for one additional day in serum-free medium, composed by 75% IMDM (ThermoFisher Scientific) and 25% Ham's Modified F12 medium (EuroClone), N2 (ThermoFisher Scientific), B27 (ThermoFisher Scientific), BSA (0.05%, US Biological), L-glutamine (200 mM, Euroclone) and ascorbic acid (0.05 mg/ml, Sigma-Aldrich) (Serra, M. et al. 2017), supplemented with Noggin (100 ng/ml, Novus Biologicals) and the TGF- β RI, ALK4 and ALK7 inhibitor SB431542 (10 μ M, Sigma-Aldrich). Lineage differentiation into thyroid progenitor cells was assessed by exposing cells, up to day 22, to the serum-free media containing FGF10 (10 ng/ml, Novus Biologicals), KGF (10 ng/ml, Peprotech), BMP4 (10 ng/ml, R&D), EGF (20 ng/ml, Peprotech), FGF2 (500 ng/ml, Peprotech) and heparin sodium salt (100 ng/ml, Sigma-Aldrich). For differentiation in mature thyrocytes, cells were cultured in serum-free medium, supplemented with FGF2 (100 ng/ml, Peprotech), FGF10 (100 ng/ml, Novus Biologicals), heparin sodium salt (100 ng/ml, Sigma-Aldrich) and TSH (1 mU/ml, Novus Biologicals). The ROCK inhibitor Y-27632 (10 μ M, Sigma-Aldrich) was added after every cell passage. Cells at any stage of differentiation were seeded on matrigel-coated dishes, specifically by using the Corning hESC-qualified matrix up to day 6 and BD matrigel from day 6 to day 30. For all the experiments, cells at each stage of differentiation were maintained in the specific cell culture differentiation media.

BCPAP (catalog number ACC 273), TT2609co2 (catalog number ACC 510) and Cal62 (catalog number ACC 448), human PTC, FTC and ATC cells, respectively, were obtained from DSMZ and cultured according to the manufacturer's instructions.

Cells were routinely authenticated performing short tandem repeat (STR) analysis, using a 24 loci-based multiplex PCR assay (GlobalFiler™ STR kit, Applied Biosystem).

The conditioned medium (CM) of hESCs-derived TPCs (D22) and their differentiation lineage (D30) was collected after exposure of specific medium to subconfluent cells for 48 h. Quantification of pro- and active MMP9 was performed using the quantikine ELISA kit (R&D systems). D22 TPCs were treated with TIMP1 (50 ng/ml; BioLegend), TIMP1 inhibitor (1 μ g/ml; R&D), KISSIR inhibitor (10 nM; Tocris). Cytokines or inhibitors were added every 48 h to cell culture. D22 TPCs were pre-treated with Wnt-3a (200 ng/ml, R&D systems) and R-spondin1 (500 ng/ml) for 16 h. Then, TIMP1 inhibitor (1 μ g/ml) was added for 48 h.

Animals and tumor models

All the in vivo procedures complied with the institutional (University of Palermo) animal care committee guidelines (authorization #1281/2015-PR, Italian Ministry of Health). 4-6 weeks old female NOD.Cg-Prkdcscid/J (NOD SCID) mice were purchased by Charles River Laboratories and maintained in a barrier facility for animals in a temperature-controlled system characterized by 22 Celsius degrees and 50% humidity with a 12 h dark/light cycle within cages (Tecniplast) with radiation-sterilized bedding (SAWI Research Bedding, JELUWERK). Mice were given *ad libitum* access to 0.45 μ m-filtered tap water in sterile drinking bottles and to pelleted chow (Special Diets Services-811900 VRF1 (P)).

To evaluate the tumorigenic capacity of hESC-derived thyroid progenitor cells and mature thyrocytes, 3×10^6 *BRAF*, *NRAS* and *TP53* engineered hESCs at different day of differentiation (D6/22/26/30) were resuspended in a 150 μ l solution of 1:1 SCM/Matrigel (BD Biosciences) and subcutaneously injected in 4-6 weeks old female NOD.Cg-Prkdcscid/J (NOD SCID) mice (12 mice/group).

To assess the individual contribution of each member of the ternary complex in TC tumorigenesis process, 3×10^6 hESC-derived cells at D22 and at D30 engineered for *NRAS/TP53* mutations and overexpressing *TIMP1*, *MMP9* and *CD44* alone and in combination were resuspended in a 150 μ l solution of 1:1 SCM/Matrigel (BD Biosciences) and subcutaneously injected in 4-6 weeks old female NOD.Cg-Prkdcscid/J (NOD SCID) mice (10 mice/group).

To evaluate the effect of treatment with TIMP1 and KISSIR inhibitors, alone or in combination, 3.5×10^6 *NRAS/TP53* engineered hESCs at D22 were resuspended in 150 μ l of a solution composed of 1:1 SCM/Matrigel (BD Biosciences) subcutaneously injected in 4-6 weeks old female NOD.Cg-Prkdcscid/J (NOD SCID) mice (6 mice/group). Mice were immediately randomized in four groups and treated via

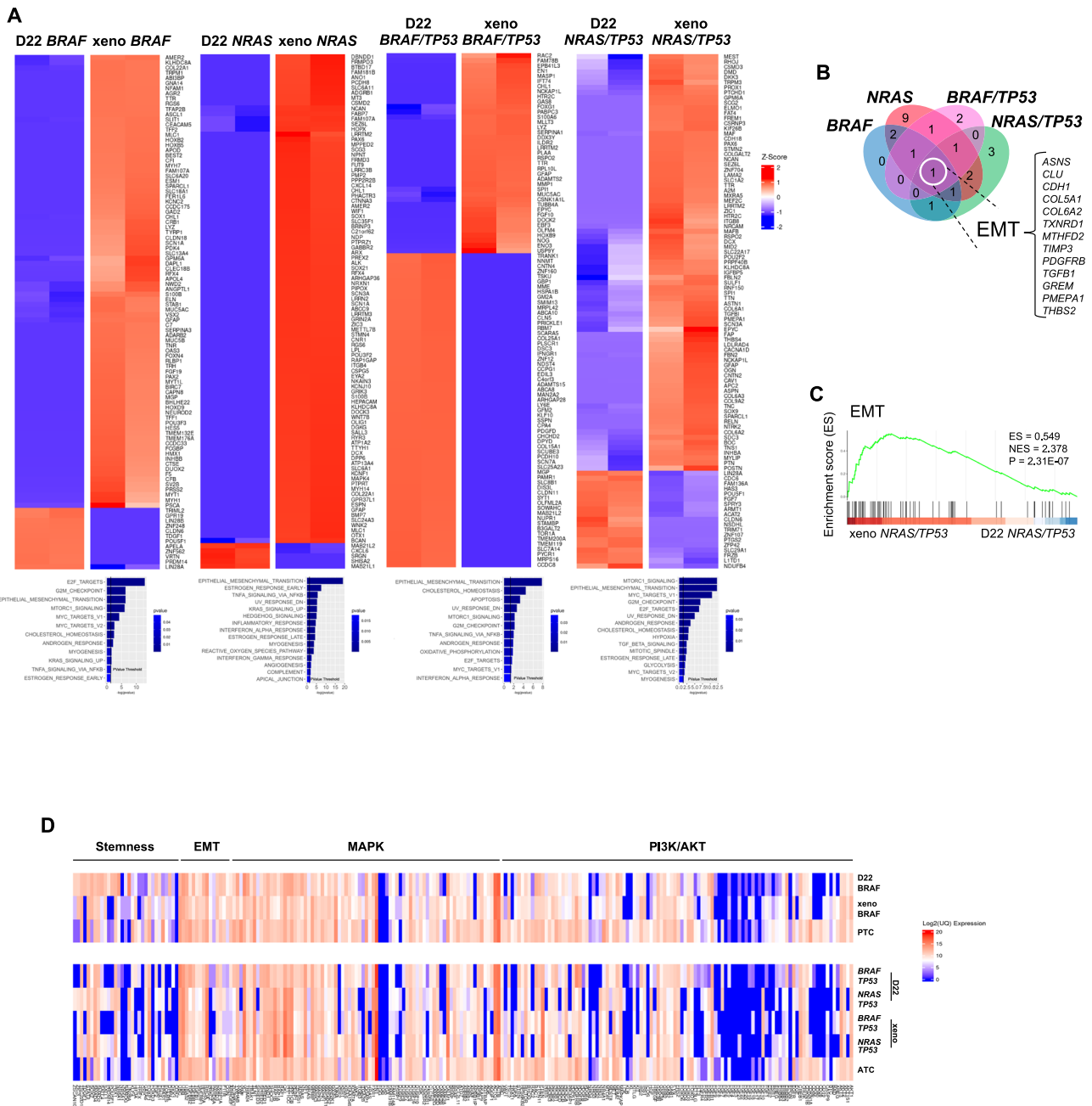


Fig. 4 | MAPK and PI3K/AKT pathways, along with EMT-associated signature, are enriched in D22 TPCs, mouse avatars and human PTC and ATC. A (upper panels) Heatmaps showing the top 100 differentially expressed genes (DEGs) with logFC > 2 obtained by total transcriptome analysis (mRNAseq), in engineered D22 TPCs harboring the pathogenetic TC mutations versus their derived-xenograft tumors. (lower panels) Barplots indicate the significantly enriched pathways (p value < 0.05) performed using a Gene set enrichment analysis (GSEA) on Hallmark category from MSigDB database of differentially expressed genes (DEGs) obtained by RNAseq. **B** Venn diagram of the common enriched pathways in

xenograft tumors versus D22 TPCs. List of the common 13 differentially regulated genes, associated with EMT-pathway. **C** Gene set enrichment analysis (GSEA) of EMT pathway in xeno *NRAS/TP53* versus *D22 NRAS/TP53* (ES = 0.549, NES = 2.378, $p = 2.31E-07$). Statistical significance was calculated using Benjamini & Hochberg test. **D** Heatmap showing normalized mRNA expression values of genes involved in PI3K/AKT-, MAPK-, EMT- and stemness-related pathways in the indicated engineered D22 TPCs, D22-derived xenograft tumors and human PTC and ATC. Mutational status of human tissues: PTC *BRAF* mutated ID#6, and ATC *BRAF/TP53* mutated ID#96. Values are expressed as Log₂ upper quartile (UQ).

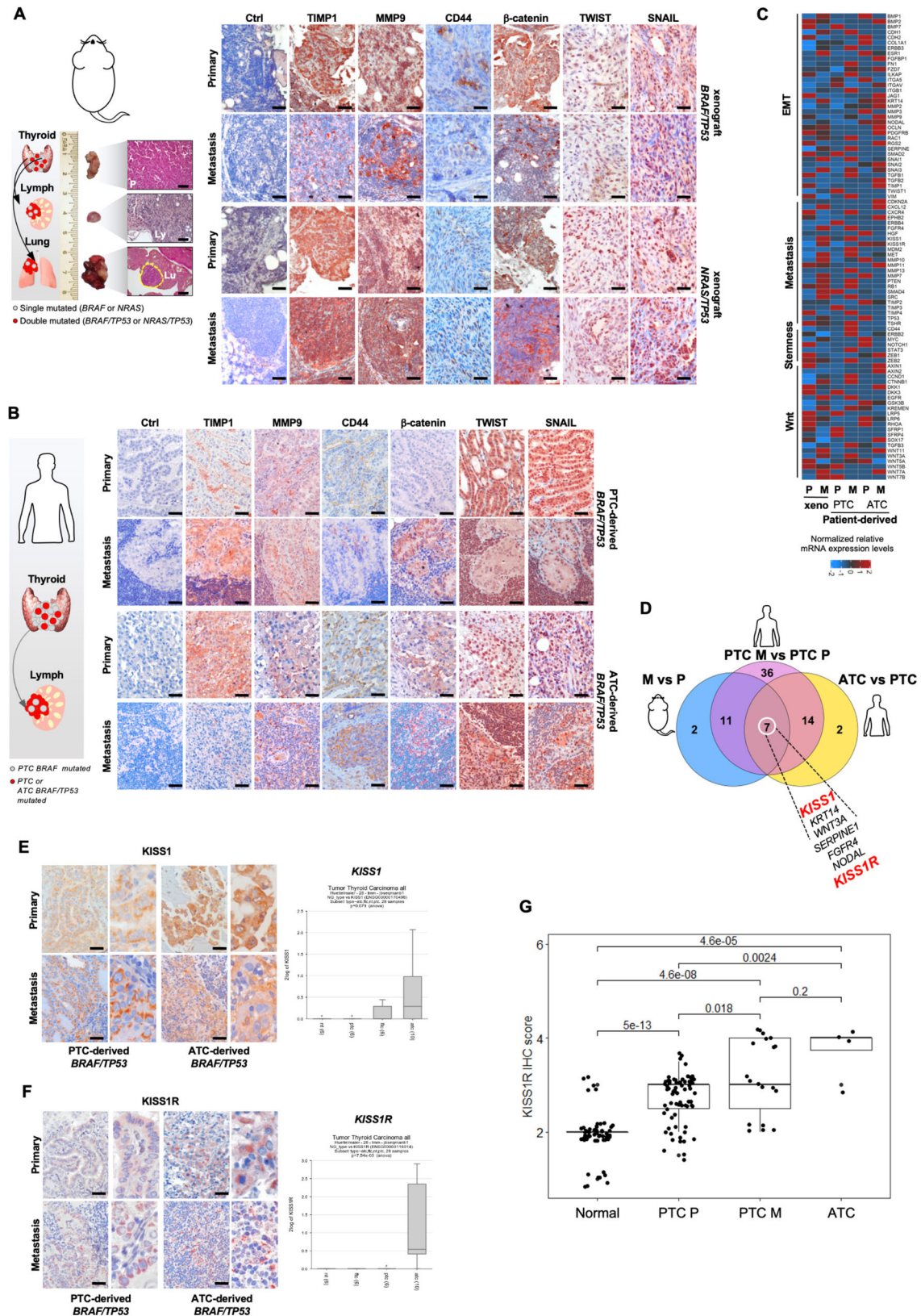
intratumoral administration with KISS1R inhibitor (10 μ M; Tocris) every day for 14 days and with a neutralizing antibody against TIMP-1 (1 μ g/ml; R&D) once a week for 4 weeks alone or in combination.

Tumor size was monitored using a digital caliper twice per week and the volume determined by the formula: largest diameter x (smallest diameter)² x $\pi/6$.

To evaluate the migration ability of D22 TPCs, bearing *BRAF* and *NRAS* mutations alone and in combination with *TP53*, 3×10^5 cells were

orthotopically injected into the thyroid gland of 4-6 weeks old female NOD.Cg-Prkdcscid/J (NOD SCID) (12 mice/group).

Mice sacrifice was performed in accordance with the Directive 2010/63/EU guidelines (D.lgs 26/2016) with the maximum diameter of the tumor = 2 cm, or when any sign of suffering was observed. The maximal tumor size was not exceeded. Animals involved in the study were sacrificed at the pre-established end point or in presence of any morbidity sign. Mice at the experimental endpoint were subjected to



rapid loss of consciousness through isoflurane inhalation and then sacrificed by cervical dislocation.

CRISPR/Cas9 gene editing

In order to perform gene editing, cells of each stage of thyroid differentiation were transfected with CRISPR/cas9 all-in-one GFP vector

(1 μ g) and pMA-T customized donor DNA plasmid specific for BRAF^{V600E}, NRAS^{Q61R} and TP53^{R248Q} mutations (1 μ g) (ThermoFisher Scientific) by using the DNA transfection reagent (X-tremeGENE HP, Roche) according to the manufacturer's instructions. The CRISPR Nuclease Vector with GFP Reporter (ThermoFisher Scientific) was used as nontargeting control (NTC). Following DNA incubation, transfection

Fig. 5 | KISS1R is a prognostic factor and a potential therapeutic target in advanced TCs. **A** (left panel) H&E analysis of primary tumor (P), lymphnodes (Ly) and lung (Lu) metastatic lesions, generated by orthotopic injection of D22 TPCs engineered with the indicated mutations. Scale bars, 100 μ m. (right panel) Immunohistochemical analysis of TIMP1, MMP9, CD44, β -catenin, TWIST and SNAIL on primary and metastasis mouse avatars. Ctrl= negative control. Scale bars, 100 μ m. **B** Immunohistochemical analysis of TIMP1, MMP9, CD44, β -catenin, TWIST and SNAIL on primary and metastatic PTC (ID#61) and ATC (ID#96) patient-derived tumors harboring *BRAF/TP53* mutations. Ctrl= negative control. Scale bars, 100 μ m. For **(A and B)** $n = 5$ tissues analyzed. **C** Heatmap of Wnt-, EMT- stemness and metastasis-related genes ($2^{-\Delta Ct}$ expression values) in primary (P), metastatic (M) tumor xenografts and primary (P) and metastatic (M) PTC- and ATC-patient derived tumors, harboring *BRAF/TP53* mutations. Data are presented as normalized mRNA expression values of three independent experiments. **D** Venn diagram showing common upregulated genes with $\log_{2}FC > 3.5$ in metastasis (M) versus primary (P)

tumor xenografts, in PTC-derived metastasis (PTC M) versus primary tumors (PTC P) and in ATC primary versus PTC primary tumors. **E** and **F**, (left panels) Immunohistochemical analysis of KISS1 (**E**) and KISS1R (**F**) on primary and metastatic PTC (ID#61) and ATC (ID#96) patient-derived tumors harboring *BRAF/TP53* mutations. $n = 5$ tissues analyzed. Scale bars, 100 μ m. (right panels) R2 database analysis of *KISS1* (**E**) and *KISS1R* (**F**) mRNA expression levels in normal thyroid (nt, $n = 6$), PTC ($n = 6$), FTC ($n = 6$) and ATC ($n = 10$) patient-derived tissues (R2 database Tumor Thyroid Carcinoma all - Huettelmaier - 28 - tmm - jbsqrnanb1). Boxes represent the IQR and midline represents the median. Statistical significance was calculated using ANOVA test. **G** Immunohistochemistry score analysis of KISS1R expression in normal thyroid tissue ($n = 56$), primary PTC tumors (PTC P, $n = 73$), PTC-derived loco-regional lymphnode metastasis (PTC M, $n = 19$) and primary ATC tumors ($n = 5$). Mutational status of 97 primary and metastatic human tissues is reported in Supplementary Data 2. Boxes represent the IQR and midline represents the median. Statistical significance was calculated using Kruskal-Wallis test.

medium was replaced with the specific cell culture differentiation media. After 48 h, enrichment of GFP-positive cells was performed by FACSMelody cell sorter. All the in vitro and in vivo experiments, in cells of any stage of differentiation, have been performed at the same time upon transfection.

To detect *BRAF*^{V600E}, *NRAS*^{Q61R} and *TP53*^{R248Q} mutations, DNA from engineered cells was extracted using the DNeasy Blood & Tissue Kit (Qiagen) and amplified by using the HotStarTaq Plus Master Mix Kit (Qiagen). Purification of amplified products was achieved with the MinElute PCR Purification Kit (Qiagen). BigDye Terminator v3.1 Cycle Sequencing Kit and BigDye X-Terminator Purification Kit (Applied Biosystems) were used for the purification and base pair sequence, respectively. Capillary electrophoresis was performed by ABI PRISM 3130 Genetic Analyzer or by BMR Genomics service (Padua, Italy). The obtained electropherograms were visually analyzed using 4Peaks Software (Griekspoor and Tom Groothuis, nucleobytes.com). The Synthego online tool (<https://design.synthego.com/#/validate>) was used to predict potential off-target sites for gRNAs and the top three predicted off-targets were analyzed by DNA sequencing.

All the primers used for sequencing analysis were listed in Supplementary Table 3.

DNA extraction and next generation sequencing (NGS)

DNA was extracted from engineered cells using DNeasy Blood & Tissue Kit (Qiagen) according to manufacturer's instructions. Yields of extracted DNA were assessed by dsDNA HS Assay kit on Qubit 3.0 Fluorometer (both from ThermoFisher Scientific). Libraries were prepared using a custom primer panel designed with the Ion AmpliSeq Designer tool (<https://www.ampliseq.com/login/login.action>). The panel encompasses 1525 amplicons covering 25 genes, including *BRAF*, *TP53* and *NRAS* genes. NGS libraries were generated with Ion AmpliSeq library kit plus (ThermoFisher Scientific) and the customized panel starting from 10 nanograms of genomic DNA for each primer pool. The libraries were barcoded employing the Ion Xpress barcode adapter kit (ThermoFisher Scientific), quantified by qPCR with the Ion Library TaqMan Quantitation kit (ThermoFisher Scientific), and diluted to equimolar amounts before pooling. The Ion Chef System was used for automated template preparation and chip loading. Sequencing was carried out on Ion GeneStudio S5 Plus System using the Ion 510 & Ion 520 & Ion 530 Kit (all from ThermoFisher Scientific). Raw data were then aligned to the hg19 reference genome and Torrent Suite v.5.10.1 (ThermoFisher Scientific) was used to perform initial quality control, including chip loading density, median read length and number of mapped reads. Ion Reporter v5.18.2.0 (ThermoFisher Scientific) was employed to single nucleotide variant (SNV) annotations. Cut offs of 3% for variant allele frequency (VAF), read depth > 100, Phred quality score > 40 and p value < 0.0001 were used for filtering in order to exclude false positive variants.

BRAF^{V600E}, *NRAS*^{Q61R} and *TP53*^{R248Q} mutation percentage in h-ESCs-derived cells at different stage of thyroid differentiation lineage detected by Sanger and NGS technologies are reported in Supplementary Table 1.

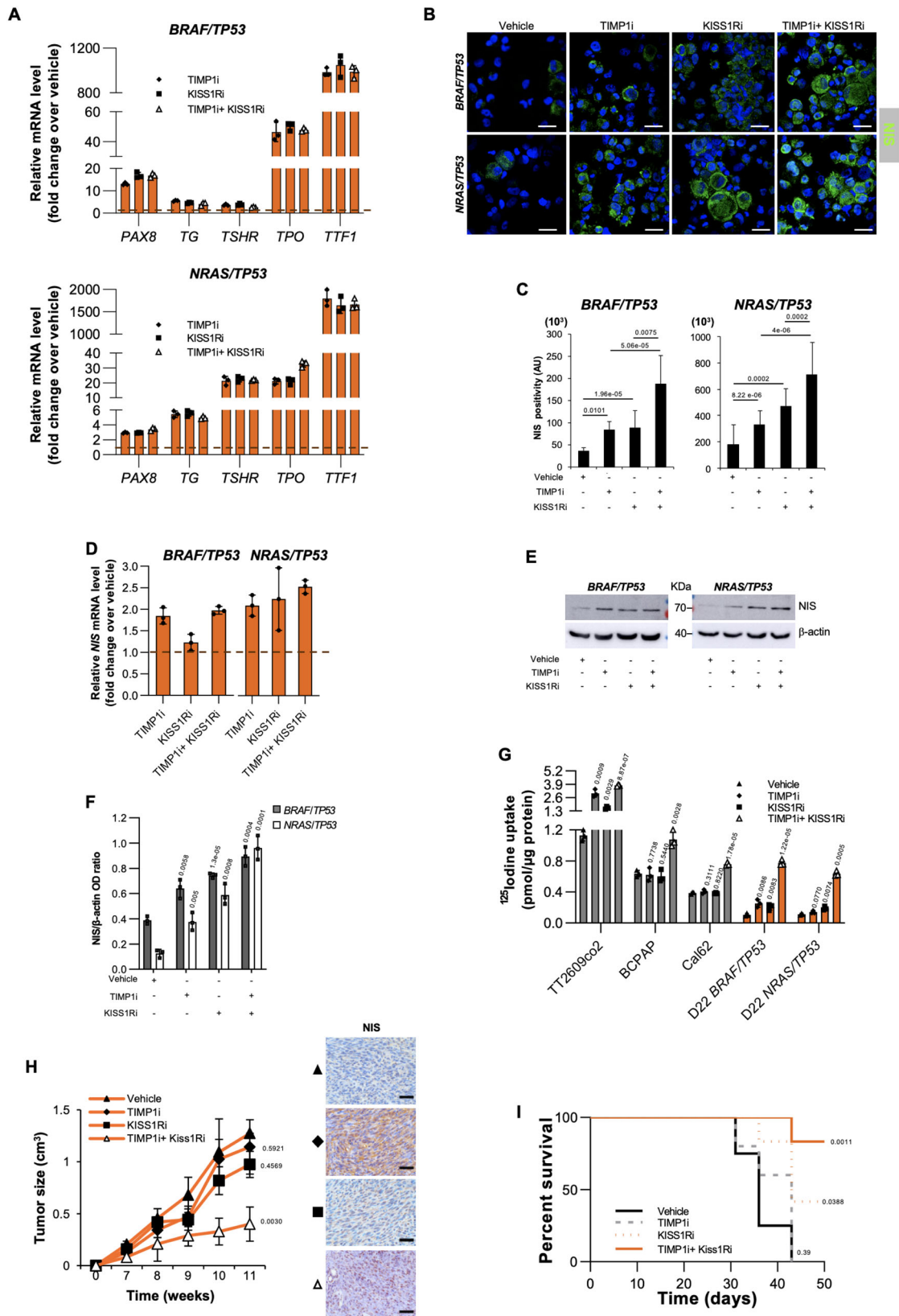
Patients

Fresh frozen or formalin-fixed paraffin-embedded (FFPE) tissues from 97 TC patients, including 73 PTC primary tumors (PTC P; ID#1-73), 19 loco-regional lymphnode metastases (PTC M; ID#74-92), and 5 ATCs who underwent thyroidectomy were collected and analyzed in accordance with the ethical policy of the Mediterranean Institute of Oncology on Human Experimentation. The clinicopathological characteristics of TC patients are shown in Supplementary Table 2 and their mutational background evaluated by Next Generation Sequencing (NGS) analysis is provided in Supplementary Data 2.

Flow cytometry analysis

Cycle analysis of hESCs-derived cells at different stage of thyroid differentiation was analyzed by incubating cells with 1 ml of Nicoletti Buffer (0.1% of Sodium citrate, 0.1% of Triton x-100, 50 μ g/ml of Propidium Iodide, 10 μ g/ml of Rnase solution) in the dark at 4 $^{\circ}$ C overnight. DNA content was evaluated by BD FACS Lyric flow cytometer (BD Clinical system, BD Biosciences).

For FACS analysis, hESCs-derived TPCs were washed in PBS and exposed for 1 h at 4 $^{\circ}$ C to CD44v6 (2F10 APC, mouse IgG1, R&D systems, 5 μ l/sample), Oct3/4 (40/Oct-3 Alexa-fluor647, mouse IgG1k, BD Biosciences, 20 μ l/sample), Sox2 (245610 PE, mouse IgG2a BD Biosciences, 20 μ l/sample), Nanog (N31-355 PE, mouse IgG1, BD Biosciences, 20 μ l/sample), CXCR4 (FAB170P PE, mouse IgG2a, R&D system, 1 μ l/sample), c-kit (YB5.B8 PE, mouse IgG1 BD Biosciences, 20 μ l/sample), Sox17 (P7-969 PE, mouse IgG1k, BD Biosciences, 5 μ l/sample), Fox A2 (N17-280 PE, mouse IgG1, BD Biosciences 5 μ l/sample), PAX8 (PAX8/1492 APC, mouse IgG2a, Novus 5 μ l/sample), TTF1 (REA1090 FITC, mouse IgG1, MACS Miltenyi Biotec, 16 μ l/sample), TSH-R (4C1 FITC, IgG2a Santa Cruz, 2 μ l/sample), TPO (203340, Anti-rabbit IgG H+L Alexa-488, Abcam, 2 μ l/sample), Thyroglobulin (SPM221 PE, mouse IgG1, Novus, 2 μ l/sample), NIS (SPM186, goat antimouse IgG (H+L) Alexa-488, Abcam, 5 μ l/sample), CD133 (W6B3C1 FITC, mouse IgG1, BD Bioscience, 20 μ l/sample), ABCG2 (5D3/CD338 APC, mouse IgG2b, BD Bioscience, 10 μ l/sample), Nestin (25/Nestin PerCP 5.5, mouse IgG1, BD Bioscience, 5 μ l/sample), HNF-4 α (H-1, goat anti-mouse IgG (H+L) Alexa-488, Santa Cruz, 4 μ l/sample), or corresponding isotype matched controls (IMC) and analyzed using the FACS Lyric cytometer (BD Biosciences). All the listed antibodies have been validated following manufacturer's information, using appropriate positive and negative controls. To perform antibody titration 4 different dilutions were tested starting from the manufacturer's recommended concentration, including the 0.5 and 2x concentrations.



Titration of the antibodies has been routinely performed at antibody arrival, and every 3 months after storage.

Tissues from normal, PTC, FTC and ATC thyroids were digested mechanically and enzymatically with collagenase (Life Technologies) and hyaluronidase (Sigma Chemical Co.) and thyrocytes were isolated, purified and cultured in DMEM 10% fetal bovine serum (FBS)

(Life Technologies)⁵⁸. Following enzymatic dissociation with Accutase (A1110501, ThermoFisher), 1×10^5 cells were stained in 200 μl of staining buffer (PBS with 0.5% BSA) with specific fluorescence-conjugated antibody, or the corresponding, according to the manufacturer's recommendations. For the detection of intracellular markers, cells were fixed in 2% paraformaldehyde and

Fig. 6 | KISSIR and TIMP1 targeting restore the functional iodine uptake by increasing NIS expression. **A** Relative mRNA expression levels of *PAX8*, *TG*, *TSHR*, *TPO* and *TFPI* in the indicated engineered D22 treated with KISSIRi (KISSIRi) alone or in combination with TIMP1 inhibitor (TIMP1i) for 24 h. Data are presented as fold change over vehicle \pm SD of three independent experiments. **B** and **c** Immunofluorescence analysis of NIS and cell positivity in D22 TPCs engineered with the indicated mutations and treated as in (A) for 72 h. Nuclei were counterstained by TOTO-3. Statistical significance was calculated using the unpaired two-tailed t test. Scale bars, 20 μ m. Data are mean \pm SD of 3 independent experiments. **D** Relative mRNA expression levels of *NIS* in cells engineered and treated as in (A) for 24 h. Data are presented as fold change over vehicle \pm SD of three independent experiments. **E** and **F** Immunoblot of NIS (**E**) and relative optical density ratio (**F**) in cells as in (A) for 48 h. β -actin was used as loading control. One representative of three independent experiments is shown. Source

data are provided as a Source Data file. **G** Radioiodine uptake in the indicated established thyroid cancer cell lines and engineered D22 TPCs treated as in (A) for 48 h. For (F and G) statistical significance was calculated using the two-tailed unpaired t test and data are mean \pm standard error of three independent experiments. **H** (left panel) Growth kinetics of xenograft tumors generated by subcutaneous injection of D22 TPCs engineered for *NRAS*^{Q61R}/*TP53*^{R248Q} treated with TIMP1 inhibitor (TIMP1i) and KISSIRi (KISSIRi) alone and in combination. Statistical significance was calculated using the unpaired two-tailed t test. Data are shown as mean \pm SD. *n* = 6 mice per group. (right panels) Immunohistochemical analysis of NIS on xenograft tumors obtained following injection of D22 TPCs engineered for *NRAS*^{Q61R}/*TP53*^{R248Q} treated as indicated, left panel. Scale bars, 100 μ m. **I** Kaplan-Meier graph showing the murine survival of D22 TPCs engineered with *NRAS*^{Q61R}/*TP53*^{R248Q} treated as in (H). The statistical significance between groups was evaluated using a log rank Mantel-Cox test.

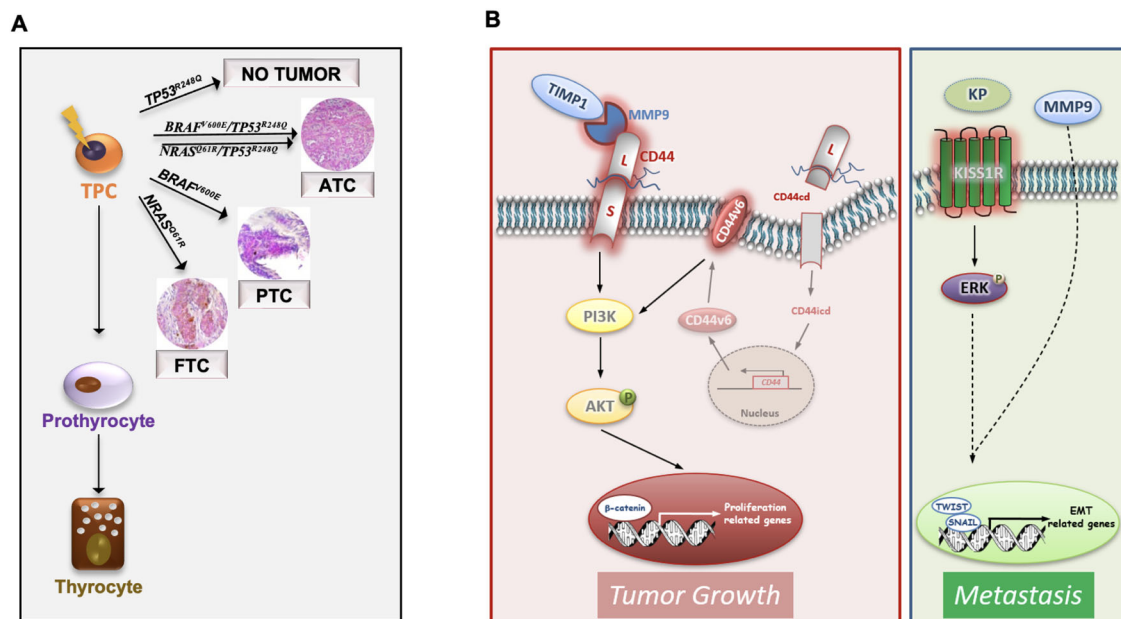


Fig. 7 | Model of TC tumorigenesis and progression. **A** Schematic model illustrating that the most common TC genetic alterations (*BRAF*^{V600E}, *NRAS*^{Q61R}, *BRAF*^{V600E}/*TP53*^{R248Q} and *NRAS*^{Q61R}/*TP53*^{R248Q}) in thyroid progenitor cell (TPC) recapitulate the different TC histotypes (FTC, PTC and ATC). Of note *TP53*^{R248Q} alone is not required for TC initiation. **B** Model of ternary complex (TIMP1/MMP9/CD44) and KISSIR driven pathways in engineered D22 TPCs. TIMP1 and pro-MMP9 complex

formation activates MMP9 and consequently leads to the cleavage of CD44. The CD44 intracytoplasmic domain (CD44icd) translocates into the nucleus where it induces *CD44v6* transcription. *CD44v6* promotes TPC proliferation through PI3K/AKT pathway. The binding of kisspeptins (KP) to KISSIR activates ERK and cooperates with MMP9 to promote the transcription of EMT-related genes, including *TWIST* and *SNAIL*, driving metastatic engraftment.

permeabilized using PBS 0.1% Triton X-100. The dead cells were excluded using the 7-AAD (BD Biosciences). Data were analyzed by FlowJo software.

Cell proliferation, clonogenic and invasion assay

The proliferative potential of hESC at different day of thyroid differentiation was assessed by using Tripan blue exclusion test.

Clonogenicity of TPCs bearing different mutations was determined by plating 1, 2, 4, 8, 16, 32, 64, 128 cells per well and evaluated with the Extreme Limiting Dilution Analysis (ELDA) 'limdil' function (<http://bioinf.wehi.edu.au/software/elda/index.html>). The invasive potential of hESCs (D6, D22, D26, D30) and of *BRAF*/*TP53* and *NRAS*/*TP53* mutated TPCs, pretreated with vehicle, TIMP1, TIMP1 inhibitor (TIMP1i) alone or in combination, was estimated by seeding 2×10^3 into 8 μ m pore size transwell coated with growth factor reduced matrigel (BD Biosciences). Advanced DMEM/F12 medium (Thermo fisher) supplemented with 10% FBS (Lonza) was used as chemoattractant in the lower chamber of transwell. Invading cells were calculated microscopically up to 72 h.

Cell transfection and lentiviral transduction

Production of lentiviral particles was achieved through the transfection of HEK-293T packaging cells (catalog number CRL-3216, obtained from ATCC), with lentiviral vector expressing *TIMP1*, *MMP9*, *CD44* (Horizon Discovery) and *CD44v6*³⁴ or with a lentiviral plasmid carrying a specific sh*CD44v6*³⁴, together with psPAX2 (Addgene) and pMD2.G (Addgene) in OPTIMEM (Gibco) medium supplemented with DNA transfection reagent (XtremeGENE HP, Roche). pLOC (Horizon Discovery) and pTWEEN-GFP plasmids or scrambled (PLKO.1, Addgene) vector was used as control, respectively. Lentiviral transduction was performed by exposing hESCs (D22, D30) to lentiviral particles in presence of polybrene (8 μ g/ml) (Sigma-Aldrich). Selection of resistant clones, where suitable, was performed by treating cells with puromycin (0.5 μ g/ml) (Sigma-Aldrich).

Immunohistochemistry and immunofluorescence

Immunohistochemical analysis was performed on 4- μ m-thick paraffin-embedded tumor sections using specific antibody against Tg (EPR9730, rabbit monoclonal, Abcam, 1:100 dilution), CK19 (B170,

mouse IgG1, Leica, 1:50 dilution), β -catenin (E-5, mouse IgG1,k, Santa Cruz, 1:25 dilution), NIS (SPM186, mouse IgG1,k, Abcam, 1:50 dilution), TIMP1 (M7293, mouse IgG1,k, Dako, 1:50 dilution), CD63 (MX-49.129.5, mouse IgG1,k, Santa Cruz, 1:50 dilution), MMP9 (4A3, mouse IgG1, ThermoFisher, 1:100 dilution), CD44v6 (2F10, mouse IgG1, R&D systems, 1:100 dilution), CD44 (156-3c11, mouse monoclonal, Cell Signaling, 1:50), Twist (Twist2C1a, mouse IgG1, Abcam, 1:25 dilution), Snail (63371, rabbit polyclonal, Abcam, 1:50 dilution), KISS1 (34010, rabbit polyclonal, Novus Bio, 1:200 dilution), KISS1R (TA351332, rabbit polyclonal, Origene, 1:50 dilution), TSHR (4C1, mouse IgG2a κ , Santa Cruz, 1:50 dilution), S100 (GA504, rabbit polyclonal, Dako, 1:1000 dilution), CDX2 (AMT28, mouse monoclonal IgG1, Novocastra, 1:50 dilution), Oct3/4 (C-10, mouse IgG1, Santa Cruz, 1:200), p40 (PA0163, Leica), P53 (DO-7, mouse monoclonal IgG2b, Novocastra, 1:100 dilution). Single stainings were revealed by the byotyne-streptavidine system (Dako). Antibody detection was performed using the 3-amino-9-ethylcarbazole (Dako). Romlin (bio-optica) has been used only for KISS1 staining. Aqueous hematoxylin (Sigma) was used to counterstain nuclei.

Immunostaining intensity has been calculated by Image J software (Analyze Histogram), by analyzing 5 serial sections from 3 tumor xenografts or patient-derived tumors. Arbitrary unit intensity has been normalized on cell count and expressed as fold variation over control. Immunohistochemistry score of KISS1R expression has been measured as the percentage of positive cells (1 = 1–12%; 1.5 = 13–25%; 2 = 26–38%; 2.5 = 39–50%; 3 = 51–62%; 3.5 = 63–75%; 4 = >75%). H&E staining was performed using standard protocols.

For immunofluorescence, ESC-derived thyroid follicles grown on matrigel droplets or D22 TPCs grown on coverslips, were fixed, and exposed overnight at 4 °C to the following antibodies: NIS (SPM186, mouse IgG1,k, Abcam), CK19 (BI70, mouse IgG1, Leica), TSHR (4C1, mouse IgG2a κ , Santa Cruz) and KISS1R (NBP2-57942, rabbit polyclonal, Novus). Primary antibody staining was revealed by using anti-rabbit or antimouse secondary antibody conjugated with Alexa Fluor-488 (Life Technologies). Nuclei were counterstained using TOTO-3 iodide (Life Technologies). NIS positivity was determined by using Image J software (Analyze Histogram), normalized on cell count (Analyze Particles) and expressed as arbitrary units (AU). At least 3 fields for each sample were counted. All the reported antibodies for both immunohistochemistry and immunofluorescence analyses have been validated following manufacturer's information, using appropriate positive and negative controls.

Western blot

hESCs-derived TPCs and their differentiation lineage (D30) were collected and washed twice with ice-cold PBS, before being lysed using a buffer containing 10 mM Tris-HCL (Sigma-Aldrich), 50 mM NaCl (Sigma-Aldrich), 30 mM sodium pyruvate (Sigma-Aldrich), 50 nM NaF (Sigma-Aldrich), 5 μ M ZnCl₂ (Sigma-Aldrich), 1% triton (Bio-Rad) supplemented with protease and phosphatase inhibitor cocktails (Sigma-Aldrich), 0.1 nM sodium orthovanadate (Sigma-Aldrich), 10 mM sodium butyrate (Sigma-Aldrich) and 1 mM PMSF (Sigma-Aldrich). Total protein extracts were loaded onto SDS-PAGE gel and blotted on nitrocellulose membranes. Following the incubation with blocking solution (5% Blotto, not fat dry milk, Santa Cruz Biotechnology, PBS 0.1% Tween 20), membranes were exposed overnight at 4 °C to β -catenin (Ser33/37/Thr41, D13A1, rabbit IgG, CST, 1:500 dilution), TIMP1 (M7293, mouse IgG1,k, Dako, 1:400 dilution), CD44 (156-3C11, mouse IgG2a, CST, 1:500 dilution), phospho-AKT XP (Ser473; D9E, rabbit, IgG, CST, 1:1000 dilution), AKT (rabbit polyclonal, CST, 1:500 dilution), NIS (SPM186, mouse IgG1,k, Abcam, 1:1000 dilution), phospho-ERK 1/2 (Thr202/Tyr204; rabbit polyclonal, CST, 1:500 dilution), ERK 1/2 (137F5, rabbit IgG, CST, 1:1000 dilution). For protein expression normalization, β -actin (8H10D10, mouse, CST, 1:1000 dilution) was used as endogenous control.

All the listed antibodies have been validated following manufacturer's information, using appropriate positive controls. Anti-mouse or anti-rabbit HRP-conjugated antibodies (goat H+L, ThermoFisher Scientific) were used to reveal primary antibodies, which were finally detected using the Amersham imager 600 (GE Healthcare).

RNA extraction, real-time/digital PCR and RNA sequencing

Total RNA of hESCs-derived TPCs (D22) and their differentiation lineage (D26 and D30), engineered with *BRAF*^{V600E}, *NRAS*^{Q61R}, *TP53*^{R248Q}, *BRAF*^{V600E}/*TP53*^{R248Q} and *NRAS*^{Q61R}/*TP53*^{R248Q} CRISPR vectors, or frozen primary and metastasis tissue xenografts obtained from the injection of *BRAF*^{V600E}/*TP53*^{R248Q} D22 cells was obtained using TRIZOL reagent (Thermo Fisher Scientific). Total RNA from FFPE PTC and ATC primary and metastasis tissues was purified by using RNeasy FFPE Kit (Qiagen) following manufacturer's instructions. For gene expression array, 1 μ g of total RNA was retrotranscribed and analyzed with a PrimePCR EMT and stemness-related gene custom panel (Bio-Rad). For Real-time PCR, RNA was retrotranscribed using the High-Capacity cDNA Reverse Transcription Kit (Applied Biosystems) and qRT-PCR was performed using specific primers. Quantitative Real-time PCR analysis was performed in a Taqman master mix (Qiagen 1054588) containing the primer sets Hs01075870_m1 (*CD44v6*), Hs00765553_m1 (*CCND1*) and Hu-*GAPDH* (Applied Biosystems), or in a SYBR Green Master Mix (Qiagen, 1054586) using primers shown in Supplementary Table 4.

Relative mRNA expression levels were obtained using the comparative CT method ($\Delta\Delta$ Ct method). The cycle threshold (Ct) of the housekeeping genes *GAPDH* or *HPRT1* or their average was used to normalize the data. Heatmaps were generated using ComplexHeatmap (v2.6.2) and show 2^{- Δ Ct} values, row scaled per array. Venn diagrams were plotted through the VennDiagram (v1.6.20) R package. Gene expression data of *KISS1* and *KISS1R* in thyroid cancer patients ("Tumor Thyroid Carcinoma All" database) were obtained from R2: Genomics Analysis and Visualization Platform (<https://hgserver1.amc.nl/cgi-bin/r2/main.cgi>). Analysis of enriched pathways from the Reactome database was performed through EnrichR R library v3.0.

Total RNA from FFPE thyroid tumor tissue specimens was purified with RNeasy FFPE Kit (Qiagen). 200 ng of total RNA were retrotranscribed with the high-capacity c-DNA reverse Transcription kit (Applied Biosystem).

Droplet digital PCR (ddPCR) was performed using ddPCR supermix for probes no-dUTP (Bio-Rad), and *KISS1R* (FAM) and *GAPDH* (HEX) ddPCR GEX assays (Bio-Rad). Following droplets generation and RT-PCR amplification, samples were quantified using QX200 Digital Droplet Reader (Bio-Rad). The obtained data were analysed with QuantaSoft Software (Bio-Rad) and *KISS1R* expression levels were calculated using the *KISS1R* (copies/ μ l)/*GAPDH* (copies/ μ l) ratio. Total RNA-seq analysis was carried out on 28 samples, including engineered D22 TPCs, D22-derived xenograft tumor tissues and human tissues from primary tumors and metastatic lesions of PTC and ATC patients. Read alignment and gene expression quantification were performed using STAR and Stringtie, respectively. Differentially expressed genes (DEGs) analysis was conducted by R with edgeR library based on the following criteria: (1) adjusted $P < 0.05$ and (2) Log₂ FC ≥ 2 . The top 100 DEGs were selected. Gene set enrichment analysis (GSEA) was performed by using R library msigdb and querying the hallmark (H) category, which includes 50 pathways. Pathways statistically significant with p value < 0.05 were selected. Genes involved in PI3K/AKT-, MAPK-, EMT-related pathways were extracted from REACTOME signatures from MSigDB. Heatmaps were plotted using R library ggplot2 and ComplexHeatmap.

Nonradioactive assay

Iodine uptake of D22 TPCs, D30 and BCPAP cells has been measured by using Nonradioactive Iodine Assay kit (#D05076.96 wells; Bertin Pharma, Cayman Chemical), according to the manufacturer's

specifications. D22 TPCs, D30 and B-CPAP cells were plated (50000 cells in 24-well plates) and treated with KISS1R inhibitor (10 nM; Tocris) and TIMP1 inhibitor (1 µg/ml; R&D) alone or in combination for 48 h. Then, cell supernatant was analysed using Nonradioactive Iodine Assay kit (#D05076.96 wells; Bertin Pharma, Cayman Chemical).

Radioactive assay

D22 TPCs, B-CPAP, TT2609co2 and Cal62 cells were plated (50,000 cells in 24-well plates) and treated with KISS1R inhibitor (10 nM; Tocris) and TIMP1 inhibitor (1 µg/ml; R&D) alone or in combination for 72 h. Then, cells were incubated with iodine-125 (I25) (0.05 mCi; PerkinElmer). After 1 h, cells were washed twice in HBSS (Sigma-Aldrich) and lysed in 100 ml 2% SDS. Radioiodine uptake was determined using PerkinElmer Wallac 1470 Wizard instrument. Iodine 125 uptake was calculated normalized the counts per minute on the relative protein concentration revealed using Protein assay dye reagent concentrate (BIO-RAD).

Statistical analysis

Kruskal-Wallis test and pairwise Wilcoxon tests were used to compare the expression levels of *CTNNB1* in normal thyrocytes, papillary and anaplastic thyroid carcinomas from the GSE33630 series in Gene Expression Omnibus (GEO). The Wilcoxon test was used to compare the expression levels of *TIMP1*, *MMP9* and *CD44* in normal and tumorigenic samples from the The Cancer Genome Atlas (TCGA) thyroid carcinoma (THCA) branch. TNMplot database was used for the analysis of thyroid cancer RNAseq-based data, for *TIMP1/MMP9/CD44* and *KISS1R* gene expression analysis, respectively, using Kruskal-Wallis test.

Survival analyses were performed on data obtained from Gene Expression Profiling Interactive Analysis (GEPIA <http://gepia.cancer-pku.cn/>), showing the hazards ratio based on Cox PH Model, and expressed as disease-free survival (DFS) curves.

Following Kolmogorov-Smirnov test to assess the samples distribution, statistical significance was estimated by unpaired two-tailed t test, or by two-tailed Mann-Whitney test.

Reporting summary

Further information on research design is available in the Nature Portfolio Reporting Summary linked to this article.

Data availability

All data relevant to the study are included in the article, Supplementary Information, and Source Data. NGS sequencing data from hESC-derived cells at different stage of thyroid differentiation lineage and from 93 TC patients, as well as total RNA-seq transcriptomic data of engineered D22 TPCs, D22-derived xenograft tumor tissues and human tissues from primary tumors and metastatic lesions of PTC and ATC patients, generated in this study, have been deposited in a public open-access GEO repository under accession code BioProject ID PRJNA887246. *CTNNB1* expression values were obtained from the GSE33630 series in Gene Expression Omnibus (GEO). *TIMP1*, *MMP9* and *CD44* expression levels were obtained from The Cancer Genome Atlas (TCGA) thyroid carcinoma (THCA) branch. *KISS1* and *KISS1R* expression values were obtained from R2: Genomics Analysis and Visualization Platform (<https://hgserver1.lmc.nl/cgi-bin/r2/main.cgi>). TNMplot database was used for the analysis of thyroid cancer RNAseq-based data, for *TIMP1/MMP9/CD44* and *KISS1R* gene expression analysis, respectively. Survival analyses were performed on data obtained from Gene Expression Profiling Interactive Analysis (GEPIA <http://gepia.cancer-pku.cn/>). Data about the histotypes and the mutational background of TCs derived from patients along the whole manuscript, are provided in Supplementary Data 1 and 2. Source data are provided with this paper.

References

- Zane, M. et al. Normal vs cancer thyroid stem cells: the road to transformation. *Oncogene* **35**, 805–815 (2016).
- Veschi, V. et al. Cancer Stem Cells in Thyroid Tumors: From the Origin to Metastasis. *Front Endocrinol. (Lausanne)* **11**, 566 (2020).
- Haugen, B. R. et al. 2015 American Thyroid Association Management Guidelines for Adult Patients with Thyroid Nodules and Differentiated Thyroid Cancer: The American Thyroid Association Guidelines Task Force on Thyroid Nodules and Differentiated Thyroid Cancer. *Thyroid* **26**, 1–133 (2016).
- Maniakas, A. et al. Evaluation of Overall Survival in Patients With Anaplastic Thyroid Carcinoma, 2000–2019. *JAMA Oncol.* **6**, 1397–1404 (2020).
- Romitti, M. et al. Signaling pathways in follicular cell-derived thyroid carcinomas. (Rev.) *Int J. Oncol.* **42**, 19–28 (2013).
- Romei, C. et al. Clinical, pathological and genetic features of anaplastic and poorly differentiated thyroid cancer: A single institute experience. *Oncol. Lett.* **15**, 9174–9182 (2018).
- Durante, C. et al. Long-term outcome of 444 patients with distant metastases from papillary and follicular thyroid carcinoma: benefits and limits of radioiodine therapy. *J. Clin. Endocrinol. Metab.* **91**, 2892–2899 (2006).
- Schlumberger, M. et al. Definition and management of radioactive iodine-refractory differentiated thyroid cancer. *Lancet Diabetes Endocrinol.* **2**, 356–358 (2014).
- Lobo, N. A., Shimono, Y., Qian, D. & Clarke, M. F. The biology of cancer stem cells. *Annu Rev. Cell Dev. Biol.* **23**, 675–699 (2007).
- Lin, R. Y. Thyroid cancer stem cells. *Nat. Rev. Endocrinol.* **7**, 609–616 (2011).
- Derwahl, M. Linking stem cells to thyroid cancer. *J. Clin. Endocrinol. Metab.* **96**, 610–613 (2011).
- Jan, M. et al. Clonal evolution of preleukemic hematopoietic stem cells precedes human acute myeloid leukemia. *Sci. Transl. Med.* **4**, 149ra118 (2012).
- Shlush, L. I. et al. Identification of pre-leukaemic haematopoietic stem cells in acute leukaemia. *Nature* **506**, 328–333 (2014).
- Corces-Zimmerman, M. R., Hong, W. J., Weissman, I. L., Medeiros, B. C. & Majeti, R. Preleukemic mutations in human acute myeloid leukemia affect epigenetic regulators and persist in remission. *Proc. Natl Acad. Sci. USA* **111**, 2548–2553 (2014).
- Visvader, J. E. Cells of origin in cancer. *Nature* **469**, 314–322 (2011).
- Longmire, T. A. et al. Efficient derivation of purified lung and thyroid progenitors from embryonic stem cells. *Cell Stem Cell* **10**, 398–411 (2012).
- Kurmann, A. A. et al. Regeneration of Thyroid Function by Transplantation of Differentiated Pluripotent Stem Cells. *Cell Stem Cell* **17**, 527–542 (2015).
- Serra, M. et al. Pluripotent stem cell differentiation reveals distinct developmental pathways regulating lung- versus thyroid-lineage specification. *Development* **144**, 3879–3893 (2017).
- Fierabracci, A. Identifying thyroid stem/progenitor cells: advances and limitations. *J. Endocrinol.* **213**, 1–13 (2012).
- Fernandez, L. P., Lopez-Marquez, A. & Santisteban, P. Thyroid transcription factors in development, differentiation and disease. *Nat. Rev. Endocrinol.* **11**, 29–42 (2015).
- McFadden, D. G. et al. p53 constrains progression to anaplastic thyroid carcinoma in a Braf-mutant mouse model of papillary thyroid cancer. *Proc. Natl Acad. Sci. USA* **111**, E1600–E1609 (2014).
- Fagin, J. A. et al. High prevalence of mutations of the p53 gene in poorly differentiated human thyroid carcinomas. *J. Clin. Invest* **91**, 179–184 (1993).
- Ito, T. et al. Unique association of p53 mutations with undifferentiated but not with differentiated carcinomas of the thyroid gland. *Cancer Res* **52**, 1369–1371 (1992).

24. Donghi, R. et al. Gene p53 mutations are restricted to poorly differentiated and undifferentiated carcinomas of the thyroid gland. *J. Clin. Invest* **91**, 1753–1760 (1993).
25. Garcia-Rostan, G. et al. Beta-catenin dysregulation in thyroid neoplasms: down-regulation, aberrant nuclear expression, and CTNNB1 exon 3 mutations are markers for aggressive tumor phenotypes and poor prognosis. *Am. J. Pathol.* **158**, 987–996 (2001).
26. Todaro, M. et al. Tumorigenic and metastatic activity of human thyroid cancer stem cells. *Cancer Res* **70**, 8874–8885 (2010).
27. Xu, Y. P., Zhao, X. Q., Sommer, K. & Moubayed, P. Correlation of matrix metalloproteinase-2, -9, tissue inhibitor-1 of matrix metalloproteinase and CD44 variant 6 in head and neck cancer metastasis. *J. Zhejiang Univ. Sci.* **4**, 491–501 (2003).
28. Seiki, M. The cell surface: the stage for matrix metalloproteinase regulation of migration. *Curr. Opin. Cell Biol.* **14**, 624–632 (2002).
29. Aaberg-Jessen, C. et al. Co-expression of TIMP-1 and its cell surface binding partner CD63 in glioblastomas. *BMC Cancer* **18**, 270 (2018).
30. Bartha, A. & Gyorffy, B. TNMplot.com: A Web Tool for the Comparison of Gene Expression in Normal, Tumor and Metastatic Tissues. *Int. J. Mol. Sci.* **22**, 2622 (2021).
31. Lambert, E. et al. TIMP-1 binding to proMMP-9/CD44 complex localized at the cell surface promotes erythroid cell survival. *Int. J. Biochem Cell Biol.* **41**, 1102–1115 (2009).
32. Chetty, C. et al. MMP-9 induces CD44 cleavage and CD44 mediated cell migration in glioblastoma xenograft cells. *Cell Signal* **24**, 549–559 (2012).
33. Chen, C., Zhao, S., Karnad, A. & Freeman, J. W. The biology and role of CD44 in cancer progression: therapeutic implications. *J. Hematol. Oncol.* **11**, 64 (2018).
34. Todaro, M. et al. CD44v6 is a marker of constitutive and reprogrammed cancer stem cells driving colon cancer metastasis. *Cell Stem Cell* **14**, 342–356 (2014).
35. Savvidis, C., Papaiconomou, E., Petraki, C., Msaouel, P. & Koutsilieris, M. The role of KISS1/KISS1R system in tumor growth and invasion of differentiated thyroid cancer. *Anticancer Res* **35**, 819–826 (2015).
36. Beck, B. H. & Welch, D. R. The KISS1 metastasis suppressor: a good night kiss for disseminated cancer cells. *Eur. J. Cancer* **46**, 1283–1289 (2010).
37. Cvetkovic, D., Babwah, A. V. & Bhattacharya, M. Kisspeptin/KISS1R System in Breast Cancer. *J. Cancer* **4**, 653–661 (2013).
38. Li, Z., Liu, J., Inuzuka, H. & Wei, W. Functional analysis of the emerging roles for the KISS1/KISS1R signaling pathway in cancer metastasis. *J. Genet. Genom.* **49**, 181–184 (2022).
39. Blake, A. et al. G protein-coupled KISS1 receptor is overexpressed in triple negative breast cancer and promotes drug resistance. *Sci. Rep.* **7**, 46525 (2017).
40. Fletcher, A. et al. Targeting Novel Sodium Iodide Symporter Interactors ADP-Ribosylation Factor 4 and Valosin-Containing Protein Enhances Radioiodine Uptake. *Cancer Res* **80**, 102–115 (2020).
41. Oh, J. M. et al. A Novel Tyrosine Kinase Inhibitor Can Augment Radioactive Iodine Uptake Through Endogenous Sodium/Iodide Symporter Expression in Anaplastic Thyroid Cancer. *Thyroid* **30**, 501–518 (2020).
42. Wachter, S. et al. Epigenetic Modifications in Thyroid Cancer Cells Restore NIS and Radio-Iodine Uptake and Promote Cell Death. *J. Clin. Med.* **7**, 61 (2018).
43. Presta, I. et al. Recovery of NIS expression in thyroid cancer cells by overexpression of Pax8 gene. *BMC Cancer* **5**, 80 (2005).
44. Cheng, G. et al. Higher levels of TIMP-1 expression are associated with a poor prognosis in triple-negative breast cancer. *Mol. Cancer* **15**, 30 (2016).
45. Kim, T. H. & Cho, S. G. Kisspeptin inhibits cancer growth and metastasis via activation of EIF2AK2. *Mol. Med Rep.* **16**, 7585–7590 (2017).
46. Harihar, S. et al. Role of the tumor microenvironment in regulating the anti-metastatic effect of KISS1. *Clin. Exp. Metastasis* **37**, 209–223 (2020).
47. Li, Y. et al. Role of MMP-9 in epithelial-mesenchymal transition of thyroid cancer. *World J. Surg. Oncol.* **18**, 181 (2020).
48. Dumont, J. E., Lamy, F., Roger, P. & Maenhaut, C. Physiological and pathological regulation of thyroid cell proliferation and differentiation by thyrotropin and other factors. *Physiol. Rev.* **72**, 667–697 (1992).
49. Coclet, J., Foureau, F., Ketelbant, P., Galand, P. & Dumont, J. E. Cell population kinetics in dog and human adult thyroid. *Clin. Endocrinol. (Oxf.)* **31**, 655–665 (1989).
50. Dekkers, J. F. et al. Modeling Breast Cancer Using CRISPR-Cas9-Mediated Engineering of Human Breast Organoids. *J. Natl. Cancer Inst.* **112**, 540–544 (2020).
51. Lannagan, T. R. M. et al. Genetic editing of colonic organoids provides a molecularly distinct and orthotopic preclinical model of serrated carcinogenesis. *Gut* **68**, 684–692 (2019).
52. Huang, L. et al. Commitment and oncogene-induced plasticity of human stem cell-derived pancreatic acinar and ductal organoids. *Cell Stem Cell* **28**, 1090–1104 e1096 (2021).
53. Zaballos, M. A. & Santisteban, P. Key signaling pathways in thyroid cancer. *J. Endocrinol.* **235**, R43–R61 (2017).
54. Nikiforov, Y. E. & Nikiforova, M. N. Molecular genetics and diagnosis of thyroid cancer. *Nat. Rev. Endocrinol.* **7**, 569–580 (2011).
55. Xing, M. Molecular pathogenesis and mechanisms of thyroid cancer. *Nat. Rev. Cancer* **13**, 184–199 (2013).
56. Veschi, V. et al. Targeting chemoresistant colorectal cancer via systemic administration of a BMP7 variant. *Oncogene* **39**, 987–1003 (2020).
57. Mangiapane, L. R. et al. PI3K-driven HER2 expression is a potential therapeutic target in colorectal cancer stem cells. *Gut* **71**, 119–128 (2022).
58. Stassi, G. et al. Thyroid cancer resistance to chemotherapeutic drugs via autocrine production of interleukin-4 and interleukin-10. *Cancer Res* **63**, 6784–6790 (2003).

Acknowledgements

We are thankful to Francesco Calo' for graphics and Salvo Scarpulla for patient's data collection. V.Veschi is a research fellows funded by European Union- FESR FSE, PON Ricerca e Innovazione 2014–2020 (AIM line 1). AT is a research fellow funded by “Programma Operativo Complementare” 2014-2020. CM and MLI are researchers funded by European Union-FESR FSE PON Ricerca e Innovazione 2014-2020 DM 1062/2021. M.G. is a research fellow funded by PRIN (2017WNKSLR). The research leading to these results has received funding from AIRC IG (21445) to GS.

Author contributions

V.Veschi, A.T., C.M. and G.S. conceived and designed the experiments; V.Veschi, A.T., C.M., F.V., S.D.F., M.G., E.T., M.L.I., V.D.P., G.P., L.R.M., P.B., I.P., L.C. and M.T. carried out the experiments, analyzed and elaborated data; S.D.B. and E.S. executed the bioinformatics analysis; V.Vella and A.B. provided support for the radioactive assay; A.R., L.M. and D.G. supplied scientific suggestions and critical review; L.M., D.G. and C.C. provided clinical data of thyroid patients; M.R.B., G.P. and P.V. provided critical comments to the manuscript. V.Veschi, A.T., C.M. and G.S. wrote the manuscript. All authors revised the manuscript.

Competing interests

The authors declare no competing interests.

Additional information

Supplementary information The online version contains supplementary material available at <https://doi.org/10.1038/s41467-023-36922-1>.

Correspondence and requests for materials should be addressed to Giorgio Stassi.

Peer review information *Nature Communications* thanks Maria Abad and the other, anonymous, reviewer(s) for their contribution to the peer review of this work.

Reprints and permissions information is available at <http://www.nature.com/reprints>

Publisher's note Springer Nature remains neutral with regard to jurisdictional claims in published maps and institutional affiliations.

Open Access This article is licensed under a Creative Commons Attribution 4.0 International License, which permits use, sharing, adaptation, distribution and reproduction in any medium or format, as long as you give appropriate credit to the original author(s) and the source, provide a link to the Creative Commons license, and indicate if changes were made. The images or other third party material in this article are included in the article's Creative Commons license, unless indicated otherwise in a credit line to the material. If material is not included in the article's Creative Commons license and your intended use is not permitted by statutory regulation or exceeds the permitted use, you will need to obtain permission directly from the copyright holder. To view a copy of this license, visit <http://creativecommons.org/licenses/by/4.0/>.

© The Author(s) 2023

Conclusions

Targeted therapy against CSCs has emerged as a promising approach in the cure of cancer. CSCs, often referred to as tumor-initiating cells, are a small subpopulation of cells within a tumor that exhibit self-renewal, differentiation and tumorigenicity capabilities. They are implicated in tumor initiation, progression, and resistance to conventional treatments like chemotherapy and radiation therapy. Consequently, eradicating these CSCs has become a significant focus of cancer research, leading to the development of innovative targeted therapies. One notable strategy for targeting CSCs is the identification of specific molecular markers and pathways that are essential for their survival and proliferation. This approach aims to design drugs that selectively target these markers or disrupt the signaling pathways critical for CSCs function [103, 104].

Here, we identified the cell of origin from which different well differentiated and undifferentiated TCs histotypes derive. We showed that human embryonic stem cells (hESCs), after specific *in vitro* stimulation, undergo a stepwise differentiation process, culminating in the formation of thyroid progenitor cells (TPCs) at day 22, which subsequently mature into thyrocytes at day 30. In this study, we harnessed hESC-derived TPCs as the cell of origin recapitulating various histotypes of thyroid cancer follicular cells derived. Employing CRISPR-Cas9, we introduced the most common genetic mutations. Particularly, TPCs harboring BRAF^{V600E} or NRAS^{Q61R} mutations gave rise to PTC or FTC, respectively. The introduction of TP53^{R248Q} mutations led to the development of ATCs. Interestingly, our study revealed the involvement of the Tissue Inhibitor of Metalloproteinase 1 (TIMP1)/Matrix metalloproteinase 9 (MMP9)/Cluster of differentiation 44 (CD44) ternary complex, working in collaboration with the Kisspeptin receptor (KISS1R), in the initiation and progression of TC. Finally, we demonstrated that targeting KISS1R and

TIMP1 induced radioiodine uptake. It may represent promising adjuvant therapeutic strategies for managing ATC patients.

Bibliography

1. Hulbert, A.J., *Thyroid hormones and their effects: a new perspective*. Biol Rev Camb Philos Soc, 2000. **75**(4): p. 519-631.
2. Ravera, S., et al., *Structural insights into the mechanism of the sodium/iodide symporter*. Nature, 2022. **612**(7941): p. 795-801.
3. Felsenfeld, A.J. and B.S. Levine, *Calcitonin, the forgotten hormone: does it deserve to be forgotten?* Clin Kidney J, 2015. **8**(2): p. 180-7.
4. Filetti, S., et al., *Thyroid cancer: ESMO Clinical Practice Guidelines for diagnosis, treatment and follow-up*. Ann Oncol, 2019. **30**(12): p. 1856-1883.
5. Cabanillas, M.E., D.G. McFadden, and C. Durante, *Thyroid cancer*. Lancet, 2016. **388**(10061): p. 2783-2795.
6. Cancer Genome Atlas Research, N., *Integrated genomic characterization of papillary thyroid carcinoma*. Cell, 2014. **159**(3): p. 676-90.
7. Kimura, E.T., et al., *High prevalence of BRAF mutations in thyroid cancer: genetic evidence for constitutive activation of the RET/PTC-RAS-BRAF signaling pathway in papillary thyroid carcinoma*. Cancer Res, 2003. **63**(7): p. 1454-7.
8. Soares, P., et al., *BRAF mutations and RET/PTC rearrangements are alternative events in the etiopathogenesis of PTC*. Oncogene, 2003. **22**(29): p. 4578-80.
9. Frattini, M., et al., *Alternative mutations of BRAF, RET and NTRK1 are associated with similar but distinct gene expression patterns in papillary thyroid cancer*. Oncogene, 2004. **23**(44): p. 7436-40.
10. Schmid, K.W. and N.R. Farid, *How to define follicular thyroid carcinoma?* Virchows Arch, 2006. **448**(4): p. 385-93.
11. Luvhengo, T.E., et al., *Multi-Omics and Management of Follicular Carcinoma of the Thyroid*. Biomedicines, 2023. **11**(4).
12. Are, C. and A.R. Shaha, *Anaplastic thyroid carcinoma: biology, pathogenesis, prognostic factors, and treatment approaches*. Ann Surg Oncol, 2006. **13**(4): p. 453-64.
13. Untch, B.R. and J.A. Olson, Jr., *Anaplastic thyroid carcinoma, thyroid lymphoma, and metastasis to thyroid*. Surg Oncol Clin N Am, 2006. **15**(3): p. 661-79, x.
14. Sugitani, I., et al., *Super-radical surgery for anaplastic thyroid carcinoma: a large cohort study using the Anaplastic Thyroid Carcinoma Research Consortium of Japan database*. Head Neck, 2014. **36**(3): p. 328-33.
15. Yang, J. and J.A. Barletta, *Anaplastic thyroid carcinoma*. Semin Diagn Pathol, 2020. **37**(5): p. 248-256.
16. Xu, B. and R.A. Ghossein, *Advances in Thyroid Pathology: High Grade Follicular Cell-derived Thyroid Carcinoma and Anaplastic Thyroid Carcinoma*. Adv Anat Pathol, 2023. **30**(1): p. 3-10.
17. Brzezianska, E. and D. Pastuszek-Lewandoska, *A minireview: the role of MAPK/ERK and PI3K/Akt pathways in thyroid follicular cell-derived neoplasm*. Front Biosci (Landmark Ed), 2011. **16**(2): p. 422-39.
18. Liu, B. and A. Kuang, *[Genetic alterations in MAPK and PI3K/Akt signaling pathways and the generation, progression, diagnosis and therapy of thyroid cancer]*. Sheng Wu Yi Xue Gong Cheng Xue Za Zhi, 2012. **29**(6): p. 1221-5.
19. Seo, J.Y., et al., *A Multi-institutional Study of Prevalence and Clinicopathologic Features of Non-invasive Follicular Thyroid Neoplasm with Papillary-like Nuclear Features (NIFTP) in Korea*. J Pathol Transl Med, 2019. **53**(6): p. 378-385.
20. Guerra, A., et al., *The primary occurrence of BRAF(V600E) is a rare clonal event in papillary thyroid carcinoma*. J Clin Endocrinol Metab, 2012. **97**(2): p. 517-24.
21. Guerra, A., et al., *Concomitant BRAF(V600E) mutation and RET/PTC rearrangement is a frequent occurrence in papillary thyroid carcinoma*. Thyroid, 2014. **24**(2): p. 254-9.

22. Guerra, A., et al., *Genetic mutations in the treatment of anaplastic thyroid cancer: a systematic review*. BMC Surg, 2013. **13 Suppl 2**(Suppl 2): p. S44.
23. Hou, P., et al., *Genetic alterations and their relationship in the phosphatidylinositol 3-kinase/Akt pathway in thyroid cancer*. Clin Cancer Res, 2007. **13**(4): p. 1161-70.
24. Ricarte-Filho, J.C., et al., *Mutational profile of advanced primary and metastatic radioactive iodine-refractory thyroid cancers reveals distinct pathogenetic roles for BRAF, PIK3CA, and AKT1*. Cancer Res, 2009. **69**(11): p. 4885-93.
25. Osaki, M., M. Oshimura, and H. Ito, *PI3K-Akt pathway: its functions and alterations in human cancer*. Apoptosis, 2004. **9**(6): p. 667-76.
26. Shirokawa, J.M., et al., *Conditional apoptosis induced by oncogenic ras in thyroid cells*. Mol Endocrinol, 2000. **14**(11): p. 1725-38.
27. De Vita, G., et al., *Dose-dependent inhibition of thyroid differentiation by RAS oncogenes*. Mol Endocrinol, 2005. **19**(1): p. 76-89.
28. Vitagliano, D., et al., *Thyroid targeting of the N-ras(Gln61Lys) oncogene in transgenic mice results in follicular tumors that progress to poorly differentiated carcinomas*. Oncogene, 2006. **25**(39): p. 5467-74.
29. Nikiforova, M.N., et al., *RAS point mutations and PAX8-PPAR gamma rearrangement in thyroid tumors: evidence for distinct molecular pathways in thyroid follicular carcinoma*. J Clin Endocrinol Metab, 2003. **88**(5): p. 2318-26.
30. Fukahori, M., et al., *The associations between RAS mutations and clinical characteristics in follicular thyroid tumors: new insights from a single center and a large patient cohort*. Thyroid, 2012. **22**(7): p. 683-9.
31. Schulten, H.J., et al., *Comprehensive survey of HRAS, KRAS, and NRAS mutations in proliferative thyroid lesions from an ethnically diverse population*. Anticancer Res, 2013. **33**(11): p. 4779-84.
32. Nikiforov, Y.E. and M.N. Nikiforova, *Molecular genetics and diagnosis of thyroid cancer*. Nat Rev Endocrinol, 2011. **7**(10): p. 569-80.
33. Cohen, Y., et al., *BRAF mutation in papillary thyroid carcinoma*. J Natl Cancer Inst, 2003. **95**(8): p. 625-7.
34. Fukushima, T., et al., *BRAF mutations in papillary carcinomas of the thyroid*. Oncogene, 2003. **22**(41): p. 6455-7.
35. Xu, X., et al., *High prevalence of BRAF gene mutation in papillary thyroid carcinomas and thyroid tumor cell lines*. Cancer Res, 2003. **63**(15): p. 4561-7.
36. Xing, M., et al., *BRAF mutation predicts a poorer clinical prognosis for papillary thyroid cancer*. J Clin Endocrinol Metab, 2005. **90**(12): p. 6373-9.
37. Landa, I., et al., *Genomic and transcriptomic hallmarks of poorly differentiated and anaplastic thyroid cancers*. J Clin Invest, 2016. **126**(3): p. 1052-66.
38. Suzuki, K. and H. Matsubara, *Recent advances in p53 research and cancer treatment*. J Biomed Biotechnol, 2011. **2011**: p. 978312.
39. Yoo, S.K., et al., *Integrative analysis of genomic and transcriptomic characteristics associated with progression of aggressive thyroid cancer*. Nat Commun, 2019. **10**(1): p. 2764.
40. Grieco, M., et al., *PTC is a novel rearranged form of the ret proto-oncogene and is frequently detected in vivo in human thyroid papillary carcinomas*. Cell, 1990. **60**(4): p. 557-63.
41. Bongarzone, I., et al., *Molecular characterization of a thyroid tumor-specific transforming sequence formed by the fusion of ret tyrosine kinase and the regulatory subunit RI alpha of cyclic AMP-dependent protein kinase A*. Mol Cell Biol, 1993. **13**(1): p. 358-66.
42. Santoro, M., et al., *Molecular characterization of RET/PTC3; a novel rearranged version of the RET proto-oncogene in a human thyroid papillary carcinoma*. Oncogene, 1994. **9**(2): p. 509-16.
43. Wirth, L.J., et al., *Efficacy of Selpercatinib in RET-Altered Thyroid Cancers*. N Engl J Med, 2020. **383**(9): p. 825-835.
44. Kroll, T.G., et al., *PAX8-PPARgamma1 fusion oncogene in human thyroid carcinoma [corrected]*. Science, 2000. **289**(5483): p. 1357-60.
45. Nikiforova, M.N., et al., *PAX8-PPARgamma rearrangement in thyroid tumors: RT-PCR and immunohistochemical analyses*. Am J Surg Pathol, 2002. **26**(8): p. 1016-23.

46. Castro, P., et al., *PAX8-PPARgamma rearrangement is frequently detected in the follicular variant of papillary thyroid carcinoma*. J Clin Endocrinol Metab, 2006. **91**(1): p. 213-20.
47. Marques, A.R., et al., *Expression of PAX8-PPAR gamma 1 rearrangements in both follicular thyroid carcinomas and adenomas*. J Clin Endocrinol Metab, 2002. **87**(8): p. 3947-52.
48. Kelly, L.M., et al., *Identification of the transforming STRN-ALK fusion as a potential therapeutic target in the aggressive forms of thyroid cancer*. Proc Natl Acad Sci U S A, 2014. **111**(11): p. 4233-8.
49. Panebianco, F., et al., *Characterization of thyroid cancer driven by known and novel ALK fusions*. Endocr Relat Cancer, 2019. **26**(11): p. 803-814.
50. Pekova, B., et al., *NTRK Fusion Genes in Thyroid Carcinomas: Clinicopathological Characteristics and Their Impacts on Prognosis*. Cancers (Basel), 2021. **13**(8).
51. Pozdeyev, N., et al., *Genetic Analysis of 779 Advanced Differentiated and Anaplastic Thyroid Cancers*. Clin Cancer Res, 2018. **24**(13): p. 3059-3068.
52. Song, Y.S., et al., *Prognostic effects of TERT promoter mutations are enhanced by coexistence with BRAF or RAS mutations and strengthen the risk prediction by the ATA or TNM staging system in differentiated thyroid cancer patients*. Cancer, 2016. **122**(9): p. 1370-9.
53. Liu, J., et al., *The Genetic Duet of BRAF V600E and TERT Promoter Mutations Robustly Predicts Loss of Radioiodine Avidity in Recurrent Papillary Thyroid Cancer*. J Nucl Med, 2020. **61**(2): p. 177-182.
54. Melo, M., et al., *TERT, BRAF, and NRAS in Primary Thyroid Cancer and Metastatic Disease*. J Clin Endocrinol Metab, 2017. **102**(6): p. 1898-1907.
55. Melo, M., et al., *TERT promoter mutations are a major indicator of poor outcome in differentiated thyroid carcinomas*. J Clin Endocrinol Metab, 2014. **99**(5): p. E754-65.
56. Karunamurthy, A., et al., *Prevalence and phenotypic correlations of EIF1AX mutations in thyroid nodules*. Endocr Relat Cancer, 2016. **23**(4): p. 295-301.
57. Nicolson, N.G., et al., *Comprehensive Genetic Analysis of Follicular Thyroid Carcinoma Predicts Prognosis Independent of Histology*. J Clin Endocrinol Metab, 2018. **103**(7): p. 2640-2650.
58. Krishnamoorthy, G.P., et al., *EIF1AX and RAS Mutations Cooperate to Drive Thyroid Tumorigenesis through ATF4 and c-MYC*. Cancer Discov, 2019. **9**(2): p. 264-281.
59. Chung, J.K. and G.J. Cheon, *Radioiodine therapy in differentiated thyroid cancer: the first targeted therapy in oncology*. Endocrinol Metab (Seoul), 2014. **29**(3): p. 233-9.
60. Portulano, C., M. Paroder-Belenitsky, and N. Carrasco, *The Na⁺/I⁻ symporter (NIS): mechanism and medical impact*. Endocr Rev, 2014. **35**(1): p. 106-49.
61. Haugen, B.R., et al., *2015 American Thyroid Association Management Guidelines for Adult Patients with Thyroid Nodules and Differentiated Thyroid Cancer: The American Thyroid Association Guidelines Task Force on Thyroid Nodules and Differentiated Thyroid Cancer*. Thyroid, 2016. **26**(1): p. 1-133.
62. Jonklaas, J., et al., *Outcomes of patients with differentiated thyroid carcinoma following initial therapy*. Thyroid, 2006. **16**(12): p. 1229-42.
63. Ruel, E., et al., *Adjuvant radioactive iodine therapy is associated with improved survival for patients with intermediate-risk papillary thyroid cancer*. J Clin Endocrinol Metab, 2015. **100**(4): p. 1529-36.
64. Boucai, L., et al., *Genomic and Transcriptomic Characteristics of Metastatic Thyroid Cancers with Exceptional Responses to Radioactive Iodine Therapy*. Clin Cancer Res, 2023. **29**(8): p. 1620-1630.
65. Weber, M., et al., *Enhancing Radioiodine Incorporation into Radioiodine-Refractory Thyroid Cancer with MAPK Inhibition (ERRITI): A Single-Center Prospective Two-Arm Study*. Clin Cancer Res, 2022. **28**(19): p. 4194-4202.
66. Bible, K.C., et al., *2021 American Thyroid Association Guidelines for Management of Patients with Anaplastic Thyroid Cancer*. Thyroid, 2021. **31**(3): p. 337-386.
67. Hyman, D.M., et al., *Vemurafenib in Multiple Nonmelanoma Cancers with BRAF V600 Mutations*. N Engl J Med, 2015. **373**(8): p. 726-36.

68. Montero-Conde, C., et al., *Relief of feedback inhibition of HER3 transcription by RAF and MEK inhibitors attenuates their antitumor effects in BRAF-mutant thyroid carcinomas*. *Cancer Discov*, 2013. **3**(5): p. 520-33.
69. Subbiah, V., et al., *Dabrafenib and Trametinib Treatment in Patients With Locally Advanced or Metastatic BRAF V600-Mutant Anaplastic Thyroid Cancer*. *J Clin Oncol*, 2018. **36**(1): p. 7-13.
70. Subbiah, V., et al., *Dabrafenib plus trametinib in patients with BRAF V600E-mutant anaplastic thyroid cancer: updated analysis from the phase II ROAR basket study*. *Ann Oncol*, 2022. **33**(4): p. 406-415.
71. Ryder, M., et al., *Increased density of tumor-associated macrophages is associated with decreased survival in advanced thyroid cancer*. *Endocr Relat Cancer*, 2008. **15**(4): p. 1069-74.
72. Caillou, B., et al., *Tumor-associated macrophages (TAMs) form an interconnected cellular supportive network in anaplastic thyroid carcinoma*. *PLoS One*, 2011. **6**(7): p. e22567.
73. Luo, H., et al., *Characterizing dedifferentiation of thyroid cancer by integrated analysis*. *Sci Adv*, 2021. **7**(31).
74. Capdevila, J., et al., *PD-1 Blockade in Anaplastic Thyroid Carcinoma*. *J Clin Oncol*, 2020. **38**(23): p. 2620-2627.
75. Chakravarty, D., et al., *Small-molecule MAPK inhibitors restore radioiodine incorporation in mouse thyroid cancers with conditional BRAF activation*. *J Clin Invest*, 2011. **121**(12): p. 4700-11.
76. Untch, B.R., et al., *Tipifarnib Inhibits HRAS-Driven Dedifferentiated Thyroid Cancers*. *Cancer Res*, 2018. **78**(16): p. 4642-4657.
77. Subbiah, V., et al., *Pralsetinib for patients with advanced or metastatic RET-altered thyroid cancer (ARROW): a multi-cohort, open-label, registrational, phase 1/2 study*. *Lancet Diabetes Endocrinol*, 2021. **9**(8): p. 491-501.
78. Hong, D.S., et al., *KRAS(G12C) Inhibition with Sotorasib in Advanced Solid Tumors*. *N Engl J Med*, 2020. **383**(13): p. 1207-1217.
79. Ho, A.L., et al., *Tipifarnib in Head and Neck Squamous Cell Carcinoma With HRAS Mutations*. *J Clin Oncol*, 2021. **39**(17): p. 1856-1864.
80. Yu, Z., et al., *Cancer stem cells*. *Int J Biochem Cell Biol*, 2012. **44**(12): p. 2144-51.
81. Stine, R.R. and E.L. Matunis, *Stem cell competition: finding balance in the niche*. *Trends Cell Biol*, 2013. **23**(8): p. 357-64.
82. Lacina, L., et al., *Cancer Microenvironment: What Can We Learn from the Stem Cell Niche*. *Int J Mol Sci*, 2015. **16**(10): p. 24094-110.
83. Visvader, J.E., *Cells of origin in cancer*. *Nature*, 2011. **469**(7330): p. 314-22.
84. Takakura, N., *Formation and regulation of the cancer stem cell niche*. *Cancer Sci*, 2012. **103**(7): p. 1177-81.
85. Li, L. and W.B. Neaves, *Normal stem cells and cancer stem cells: the niche matters*. *Cancer Res*, 2006. **66**(9): p. 4553-7.
86. Yi, S.Y., et al., *Cancer stem cells niche: a target for novel cancer therapeutics*. *Cancer Treat Rev*, 2013. **39**(3): p. 290-6.
87. Todaro, M., et al., *Tumorigenic and metastatic activity of human thyroid cancer stem cells*. *Cancer Res*, 2010. **70**(21): p. 8874-85.
88. Zito, G., et al., *In vitro identification and characterization of CD133(pos) cancer stem-like cells in anaplastic thyroid carcinoma cell lines*. *PLoS One*, 2008. **3**(10): p. e3544.
89. Giani, F., et al., *Thyrospheres From Normal or Malignant Thyroid Tissue Have Different Biological, Functional, and Genetic Features*. *J Clin Endocrinol Metab*, 2015. **100**(9): p. E1168-78.
90. Gibelli, B., et al., *Thyroid stem cells--danger or resource?* *Acta Otorhinolaryngol Ital*, 2009. **29**(6): p. 290-5.
91. Kondo, T., S. Ezzat, and S.L. Asa, *Pathogenetic mechanisms in thyroid follicular-cell neoplasia*. *Nat Rev Cancer*, 2006. **6**(4): p. 292-306.
92. Takano, T. and N. Amino, *Fetal cell carcinogenesis: a new hypothesis for better understanding of thyroid carcinoma*. *Thyroid*, 2005. **15**(5): p. 432-8.

93. Takano, T., *Fetal cell carcinogenesis of the thyroid: theory and practice*. Semin Cancer Biol, 2007. **17**(3): p. 233-40.
94. Hardin, H., et al., *The evolving concept of cancer stem-like cells in thyroid cancer and other solid tumors*. Lab Invest, 2017. **97**(10): p. 1142-1151.
95. Vermeulen, L., et al., *Cancer stem cells--old concepts, new insights*. Cell Death Differ, 2008. **15**(6): p. 947-58.
96. Lin, R.Y., *Thyroid cancer stem cells*. Nat Rev Endocrinol, 2011. **7**(10): p. 609-16.
97. Iliopoulos, D., et al., *Inducible formation of breast cancer stem cells and their dynamic equilibrium with non-stem cancer cells via IL6 secretion*. Proc Natl Acad Sci U S A, 2011. **108**(4): p. 1397-402.
98. Hoek, K.S. and C.R. Goding, *Cancer stem cells versus phenotype-switching in melanoma*. Pigment Cell Melanoma Res, 2010. **23**(6): p. 746-59.
99. Veschi, V., et al., *Cancer Stem Cells in Thyroid Tumors: From the Origin to Metastasis*. Front Endocrinol (Lausanne), 2020. **11**: p. 566.
100. Seib, C.D. and J.A. Sosa, *Evolving Understanding of the Epidemiology of Thyroid Cancer*. Endocrinol Metab Clin North Am, 2019. **48**(1): p. 23-35.
101. Sung, H., et al., *Global Cancer Statistics 2020: GLOBOCAN Estimates of Incidence and Mortality Worldwide for 36 Cancers in 185 Countries*. CA Cancer J Clin, 2021. **71**(3): p. 209-249.
102. Vermeulen, L., et al., *The developing cancer stem-cell model: clinical challenges and opportunities*. Lancet Oncol, 2012. **13**(2): p. e83-9.
103. Battle, E. and H. Clevers, *Cancer stem cells revisited*. Nat Med, 2017. **23**(10): p. 1124-1134.
104. Colak, S. and J.P. Medema, *Cancer stem cells--important players in tumor therapy resistance*. FEBS J, 2014. **281**(21): p. 4779-91.

Publications

During my PhD program, I delved into the multifaceted nature of cancer stem cells (CSCs), exploring various biological characteristics that influence their behavior and impact their response to treatments. My reviews focused on studying the molecular mechanisms, the immunosuppressive role, the metabolic complexities, the interactions within the tumor microenvironment and the crucial role of epigenetic modifications in driving CSCs phenotype and behavior. Through in-depth study, I aimed to unravel the complexities these cells present in the context of cancer progression and treatment resistance. Particularly, the published original articles implemented innovative combinatorial approaches targeting CSCs in thyroid, colorectal, breast, and diffuse large B-cell lymphomas by inhibiting specific biomarkers and their molecular pathways, demonstrating promising alternative strategies for the treatment of these tumors.

Reviews:

- Turdo A, Porcelli G, D'Accardo C, Di Franco S, **Verona F**, Forte S, Giuffrida D, Memeo L, Todaro M, Stassi G. Metabolic Escape Routes of Cancer Stem Cells and Therapeutic Opportunities. *Cancers (Basel)*. 2020 May 31;12(6):1436. doi: 10.3390/cancers12061436. PMID: 32486505; PMCID: PMC7352619.
- Veschi V, **Verona F**, Lo Iacono M, D'Accardo C, Porcelli G, Turdo A, Gaggianesi M, Forte S, Giuffrida D, Memeo L, Todaro M. Cancer Stem Cells in Thyroid Tumors: From the Origin to Metastasis. *Front Endocrinol (Lausanne)*. 2020 Aug 25;11:566. doi: 10.3389/fendo.2020.00566. PMID: 32982967; PMCID: PMC7477072.
- Gaggianesi M, Di Franco S, Pantina VD, Porcelli G, D'Accardo C, **Verona F**, Veschi V, Colarossi L, Faldetta N, Pistone G, Bongiorno MR, Todaro M, Stassi G. Messing Up the Cancer Stem Cell Chemoresistance Mechanisms Supported by Tumor Microenvironment. *Front Oncol*. 2021 Jul 20;11:702642. doi:10.3389/fonc.2021.702642. PMID: 34354950; PMCID: PMC8330815.
- **Verona F**, Pantina V.D, Modica C, Lo Iacono M, D'Accardo C, Porcelli G, Cricchio D, Turdo A, Gaggianesi M, Di Franco S, Todaro M, Veschi V, Stassi G. Targeting epigenetic alterations in cancer stem cells. *Front. Mol. Med*, 20 September 2022 <https://doi.org/10.3389/fmmed.2022.1011882>.

Original articles:

- Gaggianesi M, Mangiapane LR, Modica C, Pantina VD, Porcelli G, Di Franco S, Lo Iacono M, D'Accardo C, **Verona F**, Pillitteri I, Turdo A, Veschi V, Brancato OR, Muratore G, Pistone G, Bongiorno MR, Todaro M, De Maria R, Stassi G. Dual Inhibition of Myc Transcription and PI3K Activity Effectively Targets Colorectal Cancer Stem Cells. *Cancers (Basel)*. 2022 Jan 28;14(3):673. doi: 10.3390/cancers14030673. PMID: 35158939; PMCID: PMC8833549.
- Turdo A, Gaggianesi M, Di Franco S, Veschi V, D'Accardo C, Porcelli G, Lo Iacono M, Pillitteri I, **Verona F**, Militello G, Zippo A, Poli V, Fagnocchi L, Beyes S, Stella S, Lattanzio R, Faldetta N, Lentini VL, Porcasi R, Pistone G, Bongiorno MR, Stassi G, De Maria R, Todaro M. Effective targeting of breast cancer stem cells by combined inhibition of Sam68 and Rad51. *Oncogene*. 2022 Apr;41(15):2196-2209. doi: 10.1038/s41388-022-02239-4. Epub 2022 Feb 25. PMID: 35217791; PMCID: PMC8993694.
- Veschi V, Turdo A, Modica C, **Verona F**, Di Franco S, Gaggianesi M, Tirrò E, Di Bella S, Iacono ML, Pantina VD, Porcelli G, Mangiapane LR, Bianca P, Rizzo A, Sciacca E, Pillitteri I, Vella V, Belfiore A, Bongiorno MR, Pistone G, Memeo L, Colarossi L, Giuffrida D, Colarossi C, Vigneri P, Todaro M, Stassi G. Recapitulating thyroid cancer histotypes through engineering embryonic stem cells. *Nat Commun*. 2023 Mar 11;14(1):1351. doi: 10.1038/s41467-023-36922-1. PMID: 36906579; PMCID: PMC10008571.
- Turdo A, Gaggianesi M, D'Accardo C, Porcelli G, Di Bella S, Cricchio D, Pillitteri I, Porcasi R, Lo Iacono M, **Verona F**, Modica C, Roozafzay N, Florena A.M, Stassi G, Mancuso S, Todaro M. EBF1, MYO6 and CALR expression levels predict therapeutic response in diffuse large B-cell lymphomas. *Front. Immunol*, 2023. doi: 10.3389/fimmu.2023.1266265.

Acknowledgements

“Study and in general the pursuit of truth and beauty is a sphere of activity in which we are permitted to remain children all our lives.”

Albert Einstein

I extend my heartfelt gratitude to Professors Giorgio Stassi and Matilde Todaro for warmly welcoming me into their cutting-edge Laboratory of Cellular and Molecular Pathophysiology and providing the invaluable opportunity to complete my doctoral project. Professor Veronica Veschi deserves my thanks for instilling in me a profound love for research and a strong work ethic. I am deeply grateful for the extensive scientific discussions, her enduring patience, and unwavering empathy.

I would like to express my gratitude to all my companions on this journey, who have provided unwavering assistance during the most challenging times and filled our shared experiences within and beyond the laboratory with laughter and meaning. My sincere thanks go to Sebastiano, Chiara, Davide, Caterina, Tania, Paola, Miriam, Alice, Laura, Simone, Ornella, Noemi, Kimiya, Narges, Melania, Irene, and Matteo.

To my parents, my father Elio and my mother Michela, I owe a debt of gratitude for their constant support, enabling me to pursue my passions and interests. They granted me the freedom to follow my own path. I am also thankful to my aunt Cleofe, uncle Mario and my cousin Gloria for their unwavering encouragement, ensuring me the necessary resources for my studies, day or night, without hesitation.

Carolina, a source of strength and positivity, deserves my appreciation for always standing by my side and finding beauty in even the most challenging situations, driving me to seek personal growth and new horizons.

Lastly, my deepest appreciation goes to my sister Chica to let me grow again.

Thank you all,

Ciccio.

Palermo, 21/02/2024.